Patrícia Isabel da Cruz Morgado Ferreira

Mestre em Ciências Biomédicas

Hydrogel-based asymmetrical membranes for wound dressing application: manufacture, drug delivery and wound-healing effects

Dissertação para obtenção do Grau de Doutor em Bioengenharia

Orientadora: Prof.ª Doutora Ana Isabel Nobre Martins Aguiar de Oliveira Ricardo, Professora Catedrática, Faculdade de Ciências e Tecnologia da Universidade NOVA de Lisboa

Orientador: Prof. Doutor Ilídio Joaquim Sobreira Correia, Professor Auxiliar com Agregação, Faculdade de Ciências da Saúde da Universidade da Beira Interior

FACULDADE DE CIÊNCIAS E TECNOLOGIA
UNIVERSIDADE NOVA DE LISBOA

Março 2016

Patrícia Isabel da Cruz Morgado Ferreira

Mestre em Ciências Biomédicas

Hydrogel-based asymmetrical membranes for wound dressing application: manufacture, drug delivery and wound-healing effects

Agradecimentos

Um doutoramento é uma longa viagem e aventura. Chega-se a um local novo e desconhecido, um pouco apreensiva com o que ali vem, mas ao mesmo tempo ansiosa por poder conhecer o desconhecido e aprender aquilo que ainda não foi aprendido. Um misto de momentos de euforia, tristeza, alegria, ansiedade e medos abraçaram esta aventura. Muitos percalços surgiram ao longo desta viagem, que só foram possíveis de ultrapassar porque as pessoas certas estavam ao meu lado, me apoiaram, me deram a mão, me disseram para não desistir e ser mais forte que os meus medos. São essas pessoas, que vou enunciar aqui numa das partes mais importantes desta dissertação, que ficaram no coração e que tornaram possível eu ter chegado ao fim e estar aqui hoje. Porque elas acreditaram em mim!

À minha orientadora Prof.ª Dr.ª Ana Aguiar-Ricardo, que me recebeu de braços abertos no seu laboratório quando decidi ficar por Lisboa. Obrigada pelo seu acolhimento durante estes quatro anos e conhecimento, para mim total desconhecido, sobre fluidos supercríticos, células de alta pressão e afins. Obrigada a si por ter contribuído a sair da minha zona de conforto e a alargar os meus conhecimentos em áreas completamente novas e tão úteis.
Ao meu orientador Prof. Dr. Ilídio J. Correia, que já me acompanha há bastantes anos. Um muito obrigado por todo o conhecimento sobre *Tissue Engineering* e afins, confiança e persistência que me transmitiu desde o mestrado.

À Fundação para a Ciência e Tecnologia e programa doutoral MIT-Portugal pela concessão da bolsa de investigação, sem o apoio dos quais este projeto de investigação não teria sido viável.

Ao meu amigo, confidente e irmão da Covilhã, Maximiano Ribeiro, um muito obrigado por todos os ensinamentos em culturas celulares, estudos *in vitro* e *in vivo* e desenvolvimento de hidrogéis. Contigo ri, chorei, desabafei e acredito que onde quer que estejamos a nossa amizade permanecerá. Obrigada à tua esposa Joana Tomás e vosso rebento Maria Inês por todo o carinho com que sempre me receberam.

Aos meus grandes amigos, confidentes e irmãos que arranjei em Lisboa, Vanessa Correia e Pedro Lisboa. Foram sem dúvida o meu suporte e sem o vosso apoio nada disto teria sido possível. Uma amizade cresceu, consolidou e desejo que permaneça assim para todo o sempre, estejam onde estiverem e dê a vida as voltas que tiver de dar. Obrigada pelos vossos conselhos, *brainstormings*, e partilha de conhecimentos. Desejo-vos o maior sucesso nas vossas vidas.

Às minhas *ladies* Anita Lourenço, Márcia Tavares, Vanessa Almeida, Gosia e Ana Paninho por me deixarem entrar nas vossas vidas e me proporcionarem momentos de pura felicidade. Obrigada por nunca se calarem sempre que queria silêncio naquele gabinete ☺. Um muito obrigado pela vossa amizade e apoio que sempre demonstraram.

À Rita Restani pela partilha de todas as nossas ansiedades e medos e apoio que demos uma à outra em momentos difíceis das nossas vidas.

À Sofia Silva, Mara Gonçalves e Diana Bicho, minhas companheiras desde a licenciatura. Obrigada pela vossa amizade e desejo-vos muito sucesso nas vossas vidas. Sejam felizes!

À Ritinha, Marta, Sara, Fabiana, Carmen, Rita Craveiro, Telma Barroso, Catarina Melo, Gonçalo Carrera, Ana Nunes, Teresa Casimiro e Vasco Bonifácio pelo carinho que sempre demonstraram e por terem feito parte deste percurso da minha vida.

À Sónia Miguel, minha companheira de investigação na Covilhã. Obrigada pelos testes de citotoxicidade e estudo *in vivo* e pela simpatia que sempre demonstraste.

À Dona Idalina, Conceição e Maria José, por todo o carinho e simpatia que sempre demonstraram.

À Cláudia Madeira um muito obrigado por todo o suporte e conselhos que me deu. Muito provavelmente sem a sua ajuda e profissionalismo, eu teria descambado e não teria tido forças psicológicas e mentais para prosseguir.

Aos primos Vi e Titi que me ajudaram muito enquanto estive sozinha. Obrigada pela vossa presença sempre que precisava, carinho, amizade e humildade.

Às minhas colegas de casa em Lisboa, Joana Paulo e Suzanna Hopffer. Tive muita sorte em vos ter encontrado.

Aos meus amigos de longa data, Sandrina Moura, Fernando Ribeiro, João Silva, Zé XT, Gonçalo Loureiro, Filipa Martins e o pequeno Migui. Obrigada pela vossa preocupação comigo e em saberem o que andava a fazer mesmo vocês sendo de áreas completamente diferentes. Obrigada por me deixarem fazer parte das vossas vidas, obrigada pela vossa amizade, carinho e que permaneçamos sempre juntinhos e amiguinhos para todo o sempre!

Aos meus sogros, Silvina e Diamantino Ferreira, cunhados, Nuno e Susana Ferreira, e sobrinhos, Nicole e Kevin, por me terem recebido sempre tão bem desde o primeiro dia em que fui apresentada à família e por se interessarem pela minha carreira. Por todo o amor que me dão. Muito obrigada por me permitirem fazer parte da vossa família.

À minha família por todo o suporte que sempre demonstraram nas minhas decisões. Aos meus queridos pais, João e Belinha, sem eles não teria chegado onde cheguei. Obrigada por todas as oportunidades que me deram para investir na minha carreira e não só! Ao meu querido irmão, Pedro, pelas suas maluqueiras e doidices, mas também pelo amor, carinho, amizade, proteção que sempre demonstrou. À minha querida avó Olinda que me criou com tanto amor e carinho e que eu adoro. À minha Titi, madrinha, confidente, amiga e segunda mãe por todo o amor que sempre me deu, por todo o carinho que sempre demonstrou, por sempre me tratar como uma verdadeira filha.

Finalmente, não poderia deixar de agradecer talvez à pessoa que mais me aturou em todo o sempre! O meu amigo, companheiro, confidente e querido esposo, Tiago Almeida Ferreira, por toda a paciência em me ouvir, por toda a sua preocupação em me acalmar em momentos mais difíceis, por me dar a mão sempre que precisei, por me dar o ombro sempre que uma lágrima caía. Por muitas vezes ter sido o meu saco de boxe, onde descarregava sempre que chegava a casa e vinha chateada com alguma coisa. Desculpa por esses momentos, mas obrigada pelo retorno carinhoso ☺. Obrigada por me fazeres feliz ontem, hoje e amanhã. Obrigada por estares sempre ao meu lado.

A todos vocês e a muitos outros que terão passado na minha vida e contribuído de alguma forma, mas que não estão aqui enunciados, um muito obrigado.

Resumo

O desenvolvimento de novos pensos para a regeneração de feridas cutâneas, capazes de mimetizar a estrutura nativa da pele e de permitir um processo de cicatrização mais rápido e menos doloroso, é uma necessidade urgente.

Utilizando a técnica de inversão de fases por dióxido de carbono supercrítico ($scCO_2$), produziram-se membranas assimétricas de álcool polivinílico/quitosano (PVA/CS) capazes de mimetizar a estrutura nativa da pele. As membranas (limpas, secas e prontas a usar) foram obtidas em apenas 4h, ao invés das 24h necessárias aquando a utilização dos métodos convencionais como sejam as técnicas de inversão de fases com precipitação por imersão ou por evaporação controlada. Apesar de recolhidas secas, as membranas formam rapidamente um hidrogel devido à sua elevada capacidade de absorção de água, constituindo uma propriedade crucial para a manutenção de um ambiente húmido favorável à cicatrização da ferida. Apresentam uma camada superior densa com cerca de 15 µm, que permite a troca de gases e evita a penetração de microrganismos, e uma camada interna porosa capaz de remover o excesso de exsudado.

Para avaliar a adequabilidade destas membranas como sistemas de libertação de fármacos, utilizou-se o ibuprofeno (IBP) como fármaco modelo. Devido às membranas terem propriedades semelhantes a um hidrogel, todo o IBP encapsulado nos pensos de PVA/CS foi libertado após 40 minutos, condicionando a sua aplicabilidade no tratamento de feridas. Para ultrapassar esta limitação, prepararam-se membranas contendo IBP encapsulado em complexos de IBP-β-ciclodextrinas (β-CDs) e microesferas de glicerol 1,3-dimetacrilato, a fim de susterem a libertação do fármaco de forma adequada para a aplicação dos pensos no tratamento de feridas cutâneas. Os resultados obtidos revelaram que as β-CDs permitiram uma libertação controlada do fármaco durante 3 dias, abrangendo o tempo da fase inflamatória. Além disso, os dados recolhidos a partir dos ensaios *in vivo* mostraram que a presença de um simples fármaco analgésico e com propriedades anti-inflamatórias foi fundamental para evitar uma fase inflamatória aguda e a formação de crosta, promovendo, assim, a regeneração da pele mais rapidamente.

Palavras-chave: membranas assimétricas, pensos para a cicatrização de feridas cutâneas, sistemas de libertação controlada de fármacos, procedimentos sustentáveis, dióxido de carbono supercrítico.

Abstract

The development of new wound dressings able to mimic the native structure of skin and to allow a faster and less-painful healing process is an urgent demand.

Dry, clean and ready-to-use poly(vinyl alcohol)/chitosan (PVA/CS) asymmetrical dressings were successfully developed through supercritical carbon dioxide ($scCO_2$)-phase inversion technique in just 4h instead of the 24h required when conventional methods, wet- and dry/wet-phase inversion, are used. The produced dressings were recovered in a dry state, but they can form a hydrogel due to their high water uptake ability, which is an important property for maintaining a moisturized environment for improving the wound healing process. They presented a dense skin top layer of about 15 µm, that allows gaseous exchange while avoiding microorganisms penetration, and a porous inner layer able to remove the excess of exudates.

To evaluate the suitability of these membranes for use as drug delivery systems, ibuprofen (IBP) was loaded in these membranes as drug model. However, due to the hydrogel-like properties, the IBP loaded into PVA/CS dressings was completely released after 40 minutes, which is not appropriate for wound healing purposes. To overcome such drawback, IBP-β-cyclodextrins (β-CDs) complexes and IBP-loaded poly(1,3-glycerol dimethacrylate) microbeads were used to customize the release profile of IBP and to allow the application of the dressings in the treatment of full-thickness wounds. The results obtained reveal that β-CDs allowed a sustained drug release during 3 days, which is compatible with the time frame of the inflammatory phase. Moreover, the data collected from *in vivo* assays showed that the presence of a simple anti-inflammatory and pain-relief drug within dressings was crucial to avoid an acute inflammatory phase and scab formation, thus promoting a faster skin renewal.

Keywords: asymmetrical membranes, wound dressings, drug delivery systems, sustainable procedures, supercritical carbon dioxide.

Table of contents

Agradecimentos v
Resumo vii
Abstract ix
Table of contents xi
Index of Figures xv
Index of Tables xvii
Abbreviations xix
CHAPTER 1. General Introduction 1
1.1. Motivation 3
1.2. Burn wound evaluation 4
1.3. Wound healing process 5
1.4. Tissue-engineered skin constructs 6
1.5. Asymmetric membranes as ideal wound dressings 10
1.6. Production methods of asymmetric membranes 13
1.6.1. Wet-phase inversion method 15
1.6.2. Dry/wet - phase inversion method 15
1.6.3. Supercritical fluids and supercritical CO_2 – assisted phase inversion technique 16
1.6.4. 3D self-assembled dressings produced by electrospinning technique 21
1.7. Required properties for asymmetric membranes to be applied as wound dressings 24
1.7.1. Morphology and porosity of the membranes 24
1.7.2. Water uptake ability (swelling) and contact angle analysis 24
1.7.3. Water vapor transmission rate and oxygen permeation analysis 25
1.7.4. Mechanical properties analysis 27
1.7.5. Antimicrobial activity of wound dressings 27
1.7.6. *In vitro* drug release studies 28
1.7.7. *In vitro* and *in vivo* cytotoxic studies 28
1.8. General aims and research plan of this thesis 30
CHAPTER 2. Poly(vinyl alcohol)/chitosan asymmetrical membranes: highly controlled morphology toward the ideal wound dressing 33
2.1. Abstract 35
2.2. Introduction 35
2.3. Experimental 37
2.3.1. Materials 37
2.3.2. Membrane preparation 37
2.3.3. Membrane characterization 38
2.3.4. Water vapor permeability 39
2.3.5. Water uptake and contact angle analysis 40

2.3.6. Membrane degradation studies 40
2.3.7. Contact-active antimicrobial agent 40
2.3.7.1. Membranes surface activation with plasma technology 40
2.3.7.2. Membranes grafting with ammonium quaternized oligo(2-methyl-2-oxazoline) 41
2.3.7.3. Determination of bacteria viability 41
2.3.7.4. Evaluation of biofilm deposition at PVA/CS membranes surface 41
2.3.8. Cytotoxicity assays 42
2.3.8.1. Proliferation of human fibroblast cells in the presence of membranes 42
2.3.8.2. Characterization of the cytotoxic profile of the membranes 42
2.3.9. Drug impregnation in $scCO_2$ environment 42
2.3.10. *In vitro* drug release experiments and mathematical modeling 43
2.4. Results and Discussion 45
2.4.1. $scCO_2$ phase inversion in the development of asymmetric membranes 45
2.4.2. Water uptake and contact angle analysis 47
2.4.3. Water vapor permeability 48
2.4.4. Membrane degradation studies and mechanical properties 50
2.4.5. Antimicrobial activity performed by oligo(2-methyl-2-oxazoline) quaternized with *N,N*-dimethyldodecylamine 53
2.4.6. *In vitro* drug release studies and mathematical modeling 55
2.4.7. *In vitro* cytotoxicity studies 56
2.5. Conclusions 57
CHAPTER 3. Ibuprofen loaded poly(vinyl alcohol)/chitosan membranes for wound healing: a highly efficient strategy towards faster skin regeneration 59
3.1. Abstract 61
3.2. Introduction 61
3.3. Experimental 63
3.3.1. Materials 63
3.3.2. PGDMA carriers development 63
3.3.3. (*S*)-Ibuprofen impregnation in carriers using $scCO_2$ 64
3.3.4. Preparation of membranes 64
3.3.5. Characterization of membranes and drug carriers 65
3.3.6. Water uptake analysis 65
3.3.7. Water vapor permeation studies 66
3.3.8. Oxygen permeability 66
3.3.9. Biodegradability assays 67
3.3.10. *In vitro* drug release experiments 67
3.3.11. *In vitro* biocompatibility studies 68
3.3.11.1. Human fibroblast cells growth in contact with microparticles-loaded membranes with/without *(S)*-Ibuprofen 68

3.3.11.2. Evaluation of the cytotoxic profile of the microparticles-loaded membranes with/without *(S)*-Ibuprofen 68
3.3.12. *In vivo* assays 69
3.3.13. Histological analysis 69
3.3.14. Statistical analysis 69
3.4. Results and Discussion 70
3.4.1. Development of hydrogel-based wound dressings by $scCO_2$ phase inversion technique 70
3.4.2. Water uptake analysis 71
3.4.3. Water vapor permeability 73
3.4.4. Oxygen permeability 74
3.4.5. Biodegradability and tensile properties 75
3.4.6. *In vitro* drug release studies 77
3.4.7. Dressings biocompatibility 81
3.4.8. Evaluation of membranes performance during the wound healing process 81
3.5. Conclusions 85
CHAPTER 4. Conclusions and future prospects 87
4.1. Conclusions 89
4.2. Future prospects 93
BIBLIOGRAPHY 95
References 97
SUPPLEMENTARY INFORMATION 113
Chapter 2. *Poly(vinyl alcohol)/chitosan asymmetrical membranes: highly controlled morphology toward the ideal wound dressing* 115
Chapter 3. *Ibuprofen loaded poly(vinyl alcohol)/chitosan membranes for wound healing: a highly efficient strategy towards faster skin regeneration* 117

Index of Figures

Figure 1.1. Schematic representation of skin structure in relation to burn wound depth terminology 5

Figure 1.2. Schematic representation of the three main stages of skin wound healing process. 6

Figure 1.3. Schematic representation of the possible roles of an asymmetric membrane in the wound healing process. 11

Figure 1.4. Schematic representation of the different methods used to develop asymmetric membranes. 14

Figure 1.5. Hypothetical ternary phase diagram for the system polymer/solvent/non-solvent. 19

Figure 2.1. Ideal characteristics of an asymmetrical membrane to be used as wound dressing 45

Figure 2.2. Scanning electron micrographs of 17.25 wt% (87% PVA / 13% CS) membranes. 46

Figure 2.3. Water uptake and contact angle analysis of PVA/CS membranes. 48

Figure 2.4. Evaluation of the structure stability of PVA/CS membranes at different pHs over 21 days 51

Figure 2.5. Young's modulus analysis of PVA/CS membranes at dry and wet states and over 21 days at different pHs 52

Figure 2.6. Evaluation of the antimicrobial activity of native and PVA/CS membranes grafted with OMetOx-DDA through disk diffusion tecnhique and rezasurin assay 54

Figure 2.7. Scanning electron micrographs of *S. aureus* in contact with native and PVA/CS membranes grafted with OMetOx-DDA. 54

Figure 2.8. Evaluation of PVA/CS membranes solvent uptake ability and its influence on ibuprofen release.. 55

Figure 2.9. Microscopic photographs of human fibroblast cells after being seeded in the presence of the membranes during 24 and 72h 56

Figure 2.10. Cellular activities measured by the resazurin assay after 24 and 72h. 57

Figure 3.1. Scanning electron micrographs of PVA/CS membranes containing the different drug delivery systems 71

Figure 3.2. Swelling behavior of PVA/CS membranes containing the different drug delivery systems at different pHs. 72

Figure 3.3. Evaluation of the structural stability of PVA/CS membranes containing the different drug delivery systems at different pHs, over 21 days 76

Figure 3.4. Young's modulus analysis of PVA/CS membranes containing the different carriers in dry and wet state. 77

Figure 3.5. *In vitro* drug release studies of IBP loaded into the several drug delivery systems and IBP release profile fitted through Korsmeyer-Peppas mathematical model. 79

Figure 3.6. Evaluation of cellular activity in contact with the different dressings with and without IBP through an MTS assay after 1, 3 and 7 days. 81

Figure 3.7. Characterization of the wound healing process under *in vivo* conditions by using the different developed membranes.. 83

Figure 3.8. Magnified images of H&E-stained histological sections of the test groups after 10 and 21 days post-injury 84

Figure 3.9. Representative images of Masson's Trichrome analysis of stained explants of the control and PVA/CS+β-CD_IBP groups.. 85

Figure 4.1. Schematic representation of the effect of a sustained IBP release on skin wound regeneration taking into account the healing phases. 92

Figure S2.1. Scanning electron micrographs of 17.25 wt% (77% PVA/23% CS) membranes. 115

Figure S2.2. Scanning electron micrographs of 13 wt% (67% PVA/33% CS) membranes. 116

Figure S2.3. Scanning electron micrographs of 9 wt% (50% PVA/50% CS) membranes 116

Figure S3.1. Maximal tensile strain (%) analysis of PVA/CS membranes with the different carriers at dry and wet state. 117

Figure S3.2. Tensile strength (MPa) analysis of PVA/CS membranes with the different carriers at dry and wet state. 117

Figure S3.3. Korsmeyer-Peppas Model for mechanism of IBP release from the different drug delivery systems 118

Figure S3.4. ATR-FTIR spectra of pure (*S*)-IBP and PF microbeads with/without IBP 118

Figure S3.5. ATR-FTIR spectra of pure (*S*)-IBP and PK microbeads with/without IBP 119

Figure S3.6. ATR-FTIR spectra of pure (*S*)-IBP and β-CD with/without IBP..... 119

Figure S3.7. ATR-FTIR spectra of PVA/CS+PK, PVA/CS+PF, PVA/CS+β-CD and PVA/CS membranes. 120

Figure S3.8. ATR-FTIR spectra of PVA/CS+PK, PVA/CS+PF, PVA/CS+β-CD membranes loaded with IBP and PVA/CS membranes without IBP..... 120

Figure S3.9. Microscopic photographs of human fibroblast cells after being seeded in the presence of the developed membranes with the different carriers during 1, 3 and 7 days.. 121

Figure S3.10. Microscopic photographs of human fibroblast cells after being seeded in the presence of the developed membranes with the different carriers loaded with IBP during 1, 3 and 7 days. 121

Figure S3.11. Characterization of the wound healing process under *in vivo* conditions. 122

Figure S3.12. Representative images of Masson's trichrome-stained histological sections of explants at day 10 and 21. 123

Index of Tables

Table 1.1. Tissue-engineered skin constructs commercially available. 9

Table 1.2. Comparison between the different CS and PU asymmetric membranes developed in the last two decades. 12

Table 1.3. Summary of the production methods of asymmetric membranes: advantages and disadvantages. 23

Table 1.4. Summary of methods used during the development of wound dressings 29

Table 2.1. Comparison of the water vapor transmission rate of different studied and commercially available wound dressings for burn treatment. 49

Table 2.2. Mechanical properties of various studied wound dressings. 52

Table 3.1. Average membranes' pore diameter and porosity determined by mercury intrusion porosimetry. 73

Table 3.2. Water vapor permeation of the different developed membranes. 74

Table 3.3. Comparison of the oxygen permeability of the different developed membranes. 75

Table 3.4. Modeling of IBP release from carriers using the Korsmeyer-Peppas equation. 80

Table 4.1. Comparison between conventional and $scCO_2$ – assisted phase inversion methods on asymmetrical membranes development 90

Table 4.2. Comparison of the properties of the different membranes developed taking into account the desired values of an ideal wound dressing. 93

Abbreviations

AgSD	silver sulfadiazine
AIBN	2,2-azo-isobutyronitrile
ATR-FTIR	Attenuated Total Reflection-Fourier Transform Infrared spectroscopy
β-CDs	β-cyclodextrins
$BF_3.OEt_2$	boron trifluoride diethyl etherate
CFCs	chlorofluorcarbons
CH_3COOK	potassium acetate
CO_2	carbon dioxide
COX	cyclooxygenase
CS	chitosan
DMEM-F12	Dulbecco's modified Eagle's medium
DMF	dimethylformamide
DMSO	dimethylsulfoxide
E. coli	*Escherichia coli*
ECM	extracellular matrix
FBS	fetal bovine serum
GDMA	glycerol dimethacrylate
H&E	hematoxylin & eosin
HICs	high-income countries
IBP	(*S*)-ibuprofen
IsoOx	2-isopropenyl-2-oxazoline
K^-	negative control
K^+	positive control
KGF	keratinocyte growth factor
LMICs	low and middle-income countries
MAFs	micro-assembled fibers
MetOx	2-methyl-2-oxazoline
MF	micro-filtration
miRNA	microRNA
MSC	mesenchymal stem cells
MTS	3-(4,5-dimethylthiazol-2-yl)-5-(3-carboxymethoxyphenyl)-2-(4-sulfophenyl)-2H-tetrazolium inner salt
$NaOH\text{-}Na_2CO_3$	sodium hydroxide-sodium carbonate
NF	nano-filtration
NHDF	normal human dermal fibroblasts adult
$(NH_4)_2SO_4$	ammonium sulfate
NSAID	non-steroidal anti-inflammatory drug
OMetOx-DDA	oligo(2-methyl-2-oxazoline) quaternized with *N,N*-dimethyldodecylamine

O_2	oxygen
P. aeruginosa	*Pseudomonas aeruginosa*
PAN	polyacrylonitrile
PBS	phosphate buffered saline
p_c	critical pressure
PCL	polycaprolactone
pCO_2	pressure of CO_2
PEG	polyethylene glycol
PEO	poly(ethylene oxide)
PF	poly(1,3-glycerol dimethacrylate) microparticles with 30 wt% of fluorolink
PFPE	perfluoropolyether
PGDMA	poly(1,3-glycerol dimethacrylate)
PK	poly(1,3-glycerol dimethacrylate) microparticles with 10 wt% of krytox
PLA	poly(*L*-lactide)
PLLA	poly(*L*-lactic acid)
PMO	peptide-morpholino oligomer
PS	polystyrene
PU	polyurethane
PVA	poly(vinyl alcohol)
RH	relative humidity
ROS	reactive oxygen species
S. aureus	*Staphylococcus aureus*
$scCO_2$	supercritical carbon dioxide
SCF	supercritical fluids
SEM	scanning electron microscopy
TBSA%	total percent surface area injured
T_c	critical temperature
THF	tetrahydrofuran
TRIS	tris(hydroxymethyl)aminomethane
UF	ultra-filtration
VOCs	volatile organic solvents
WHO	World Health Organization
WS	wound size
WVP	water vapor permeability
WVTR	water vapor transmission rate

CHAPTER 1. *General Introduction*

The major part of this chapter corresponds to the manuscript published in:

2015, Journal of Membrane Science, 490:139-151.
Patrícia I. Morgado, Ana Aguiar-Ricardo and Ilídio J. Correia.
Asymmetric membranes as ideal wound dressings: an overview on production methods, structure, properties and performance relationship.
(http://www.sciencedirect.com/science/article/pii/S0376738815003956)

Personal contribution:

Patrícia I. Morgado did a thorough bibliographic research about asymmetric membranes to be used as wound dressings (methods, structure and properties) and, with the help of all the authors, wrote the manuscript.

1. General Introduction

1.1. Motivation

Skin is the biggest organ in vertebrates and occupies an area of about 2 m^2, representing approximately one-tenth of the body mass [1, 2]. It has a complex three-layered structure (epidermis, dermis and hypodermis), which under normal physiological conditions, is intrinsically self-renewable [3]. This complex organ is the outermost barrier of the body that protects inner organs from microbial pathogens, mechanical and chemical insults, regulates the body temperature, gives support to blood vessels and nerves, and prevents dehydration [4]. Furthermore, it is also involved in the immune surveillance and sensory detection processes [5, 6].

As the largest external organ in the body, human skin is daily exposed to several toxic substances and pathogens, which makes it an easy target to be damaged. Indeed, skin wounds are a major social and financial burden and their healing process is extremely complex consisting of a cascade of biological responses with different cell types and growth factors involved. The loss of skin integrity can occur due to genetic disorders, acute trauma, chronic wounds (*e.g.* venous, diabetic and pressure ulcers) or even surgical interventions [7]. However, thermal traumas like burns are one of the most common causes of major skin loss where different skin layers can be damaged and depending on the type of burn, the possibility of skin regeneration is unlikely [8]. Additionally, they can result in extensive and deep wounds that compromise immunity and body image, induce fluid losses and scarring, and ultimately significant disability or even patient death, causing not only physical but also emotional and mental consequences [5, 9].

Based on the World Health Organization (WHO) data over 300 000 deaths are annually attributable to fire-related burn injuries, with high incidence in low and middle-income countries (LMICs), where resources to treat and manage injuries are scarce or unavailable [10-12]. Fortunately, the mortality rate due to burns has been reduced over recent decades especially in high-income countries (HICs) where improved data gathering systems, new and more stringent legislation (*e.g.* use of smoke detectors, installation of sprinkle systems, development of safer buildings), social marketing and advocacy have been implemented. Moreover, advances in the treatment and care of burn patients have also had a huge contribution for lowering the burn mortality rates. These good results have been achieved due to the intensive and helpful work of worldwide scientists in the research of new and better dressings with suitable properties that allow to cover the vast types of burned wounds and also make the healing process less painful and faster [13-15].

Despite there are several commercial available wound dressings, scientists continue to search for new or improve the currently available systems. Herein, our focus was to develop hydrogel-based asymmetrical dressings and drug delivery systems with highly controlled morphology toward the ideal wound dressing and able to mimic the native structure of skin, by taking advantage of the unique properties of supercritical fluid (SCF) technologies. We believe that our research could contribute for the continued reduction of mortality rate associated with burns. Furthermore, due to the low economic status of LMICs, the use of sustainable, low-cost and greener methods on the development of well-designed drug-loaded dressings could be extremely helpful for patients with low economic resources.

1.2. Burn wound evaluation

According to the US Wound Healing Society, a wound can be described as a result of a "disruption of normal anatomic structure and function" of the skin [16, 17]. The evaluation of skin burned wounds is mainly done taking into account two aspects: the depth and the total percent surface area injured (TBSA %). Along with the extent of burn and patient's age, burn depth is a primary determinant of mortality following thermal injury. Burn depth is also the primary determinant of the patient's long term appearance and function [18, 19].

Burn wound depth (Figure 1.1) has traditionally been divided into three levels according to skin anatomy: first degree burns or epidermal injuries, second degree burns or dermal injuries and third degree burns or sub dermal injuries. Nowadays, a two level nomenclature is used giving more importance on treatment strategies: partial thickness burns (including epidermal and superficial dermal injuries) and full thickness burns (including deep second degree and sub dermal burns) [20, 21]. In the case of epidermal injuries only the epidermis is affected, it is not required specific surgical treatment and skin regenerates rapidly, within 2-3 days, without any scarring. Superficial partial-thickness wounds affect the epidermis and superficial parts of the dermis, with epidermal blistering and severe pain accompanying this type of injury, especially in the case of thermal trauma. These wounds heal within 2 weeks. On the other hand, deep-dermal injuries involve damage of a larger area of dermis that results in the destruction of skin appendages, like hair follicles and sweat glands and, usually, take more than 3 weeks to heal. Finally, in full-thickness injuries all epithelial-regenerative elements are completely destroyed, making the wound healing process more difficult. This type of wounds cannot regenerate by their own and may lead to extensive scarring, resulting in limitations in joint mobility and severe cosmetic deformities [22].

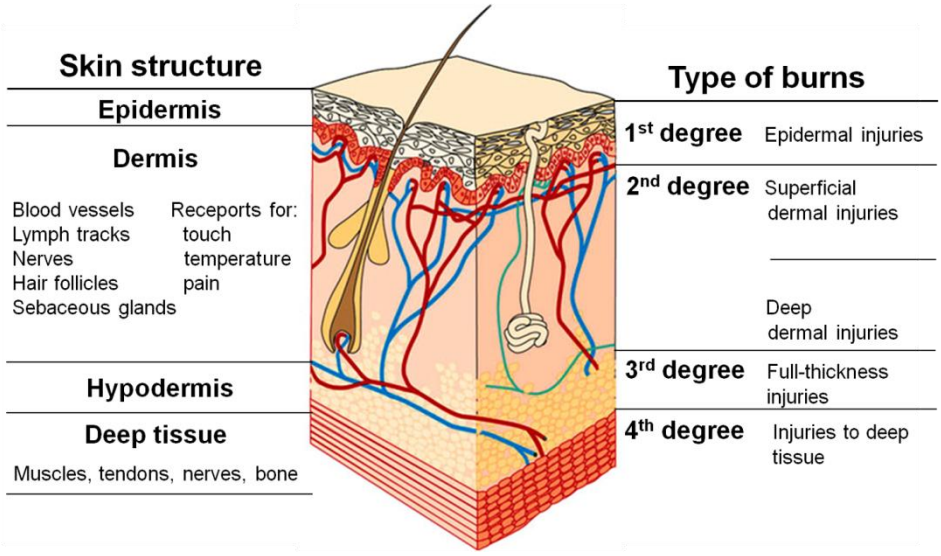

Figure 1.1. Schematic representation of skin structure in relation to burn wound depth terminology (adapted from [20, 23, 24]).

1.3. Wound healing process

The repair of epidermal, superficial partial-thickness, deep partial-thickness and full-thickness wounds are one of the most dynamic, interactive and difficult processes that occur during human life [16, 25, 26]. It involves complex interactions between extracellular matrix (ECM) molecules, soluble mediators, various resident cells (fibroblasts and keratinocytes) and infiltrating leukocyte subtypes. They act together to reestablish the integrity of the damaged tissue and replace the lost one [16, 27, 28]. To achieve this goal, the wound healing comprises five overlapping stages: hemostasis, inflammation, migration, proliferation and maturation [16]. These can be summarized in three main phases, *i.e.*, hemostasis and inflammation (typically are classified together, being regarded as just one phase), new tissue formation (or proliferation) and tissue remodeling [25, 27]. A time dependent schematic representation of the wound healing process stages is shown in Figure 1.2. Unless there is a severe arterial hemorrhage, hemostasis is achieved, initially, by the formation of a platelet plug, followed by a fibrin matrix deposition that becomes a scaffold for infiltrating skin cells (platelets and neutrophils) [25, 29-31]. The inflammatory phase begins almost simultaneously with hemostasis, sometimes from within a few minutes of injury to 24 h and lasts for up to 3 days. It plays a central role in wound healing, not only by protecting the wound from invading microbes, but also by participating in the tissue repairing processes [16, 32, 33]. In this phase, components of the coagulation cascade, inflammatory pathways and immune system are needed to prevent ongoing blood and fluid losses, to remove dead and dying tissues and also to avoid infection [25]. The second stage of wound healing, which occurs between 2-10 days after injury, is characterized by fibroblast migration, deposition of the ECM and formation of granulation tissue [25, 34]. Remodeling is the last step of normal acute wound healing, also called maturation, during which all processes that were activated after injury cease. It begins 2-

3 weeks after injury happened and lasts for a year or more [25, 28, 30]. Despite the importance of all the wound healing stages, the inflammatory phase is the most important one, since in burn wounds there is an expansion of the initial necrosis deeper into the tissue. After the initial injury, that leads to a progressive delay of wound re-epithelization and excessive formation of exudate, responsible for edema, it is imperative to use burn dressings to avoid progressive necrosis and exuberant inflammation [35]. Additionally, early wound closure decreases the severity of hypertrophic scarring, joint contractures and stiffness, and promotes quicker rehabilitation. Consequently, early healing is also a paramount for good aesthetic and functional recovery. For a suitable wound closure, the dressing used should present healing-based properties able to promote the restoration of the integrity of the damaged tissue as soon as possible [36].

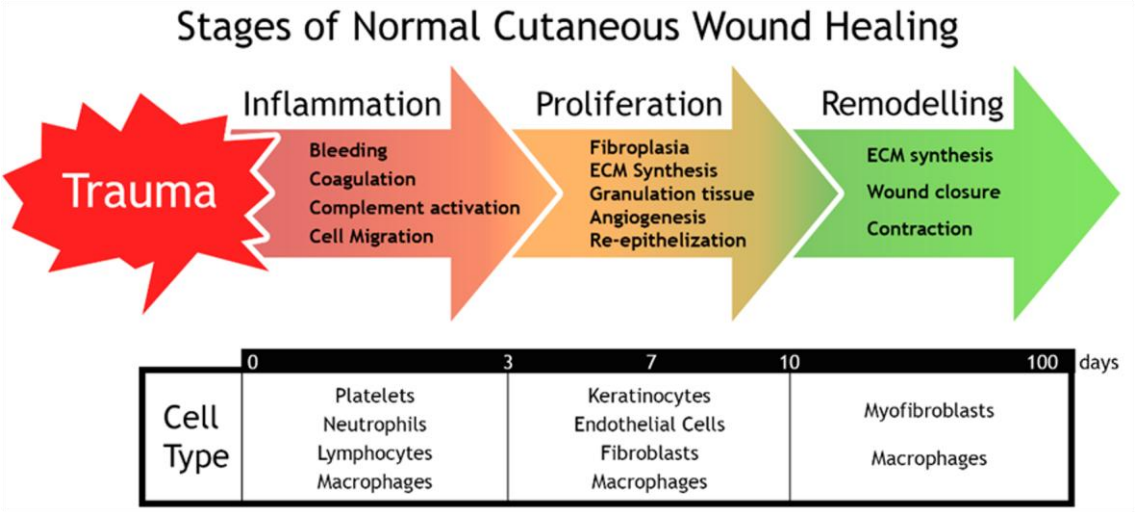

Figure 1.2. Schematic representation of the three main stages of skin wound healing process: inflammation, proliferation and remodeling.

1.4. Tissue-engineered skin constructs

Extensive skin loss is still a significant challenge to clinicians. Nowadays, the clinical “gold standard” in full-thickness injuries treatment is autologous skin graft. However, healthy tissue donor sites are extremely limited. Allografts arise as possible therapeutic alternatives, but their use depends on availability at the skin banks, religious grounds, viral diseases screening and standardized sterilization in order to reduce risks for patients [37]. This highlights the critical need for better technologies for wound care [38]. During the last decades a huge effort has been made to make the wound healing process less painful and faster. To do so, patient safety, clinical efficiency and convenience to be handled and applied and the ability to mimic the native properties of skin have been regarded during the development of new wound dressings [16, 22]. Today, as a result of such intense research, a myriad of skin substitutes exists and some of them are already available to be used in the clinic. These bioengineered cell-free as well as cell-containing skin substitutes offer protection from fluid loss and contamination, while delivering ECM components, cytokines, and growth factors to the wound bed, enhancing natural host

wound healing. Furthermore, wound dressings can be used as temporary coverings, until an autograft is available, or remain in the wound during healing or even thereafter [37, 39-41].

Depending on wound severity, epidermal, dermal and epidermal/dermal substitutes are available to clinicians (please see Table 1.1 for further details). Epidermal substitutes (*e.g.* CellSpray®, Epicel®, Myskin®) seek to restore the epidermal layer of skin. In general, the available epidermal substitutes are expensive, difficult to handle due to their thin and fragile nature, are unable to treat third degree burn wounds and their production is time consuming [39]. Dermal substitutes (*e.g.* Alloderm®, Dermagraft®, Matriderm®) are biomatrices that fulfill all the requirements of the dermal layer, being able to repair full-thickness skin defects, affecting both epidermis and dermis, and improve scar quality. These substitutes are also capable of preventing wound contraction, conferring mechanical support, and are available with different thickness and compositions. However, they cannot efficiently replace the dermal and epidermal layer and for some of them, further research is warranted to fully characterize side effects. Epidermal/dermal substitutes (*e.g.,* Apligraf®, Integra®, OrCel®) are the most advanced skin constructs available for clinic use. They contain keratinocytes and fibroblasts within their 3D matrix, gathering the potential to regenerate both the epidermal and dermal layers of skin. However, they have high production costs and some cases of immune rejection have been reported for this type of skin substitutes [41, 42].

Nowadays, advanced skin regeneration strategies combine biomaterials, cells, growth factors and modern biomanufacturing techniques to produce constructs that mimic skin anatomy and promote the regeneration of healthy and vascularized tissues. Despite the great advances attained in the area of skin tissue engineering, even the cutting-edge skin substitutes developed so far, do not incorporate many of the innate features of native skin, such as glands, dermal microvascularization, pilosity and other specialized cells that are responsible for the perception of heat, cold, pressure, vibration, pain and pigmentation. Moreover, the elasticity and strength of the native skin have not been attained until now [30, 43]. Recent studies in skin tissue engineering combined stem cells with gene recombination [44]. Due to their intrinsic characteristics, genetically modified stem cells can be used to produce and deliver cytokines and growth factors to the wound bed overcoming drawbacks such as physical inhibition and biological degradation of bioactive molecules that occur when they are administered topically.

In addition, other 3D matrices aimed at wound healing were also used as vehicles for nucleic acids. Kobsa *et al.*, produced electrospun polymeric meshes, composed by poly(*L*-lactide) (PLA) and polycaprolactone (PCL), that were loaded with plasmids encoding for keratinocyte growth factor (KGF). Such types of meshes allowed an improvement in the wound re-epithelization, keratinocyte proliferation and production of granulation tissue [45].

More recently, efforts have been made to develop asymmetric membranes trying to mimic full-thickness skin wounds since those types of dressings present a morphology similar to the native

skin and suitable properties for a better wound healing process as it will be described in the next section. Regarding the available skin substitutes presented on Table 1.1, just the epidermal/dermal substitutes present an asymmetric geometry. The epidermal and dermal layers correspond to the dense skin and sponge-like inner layers of the asymmetric membranes, respectively. Usually the porous matrix of the epidermal/dermal substitutes is composed by collagen, hyaluronic acid, fibronectin or other ECM proteins. A bandage made of silicone is normally used to form the thin upper layer to protect the wound from moisture loss and infection. However, it is possible to produce epidermal/dermal substitutes with an integral structure, *i.e.*, without the need to use a bandage to perform the dense skin layer. To improve the device properties according to the aimed biomedical application, several healing-trigger polymers can be used and different and more sustainable production methods may be applied [46-49]. This Chapter comprises a comprehensive analysis of proposed solutions to develop asymmetric and topologically controlled membranes highlighting the main achievements of these constructs for wound healing.

Table 1.1. Tissue-engineered skin constructs commercially available.

Commercial Product	Description	Application	References
Epidermal substitutes			
Epicel®	Cultured epidermal autograft (autologous keratinocytes grown in the presence of murine fibroblasts)	Full- and partial-thickness burns and chronic ulcers treatment	[50]
Epidex®	Cultured epidermal autograft (autologous outer root sheet hair follicle cells)	Full- and partial-thickness burns and chronic ulcers treatment	[51]
Laserskin®	Sub-confluent autologous keratinocytes seeded on esterified laser-perforated hyaluronic acid matrix	Full- and partial-thickness burns and chronic ulcers treatment	[52]
BioSeed-S®	Autologous oral mucosal cells on a fibrin matrix	Partial-thickness burns and chronic ulcers treatment	[53, 54]
Myskin®	Cultured epidermal autograft (autologous keratinocytes grown in the presence of irradiated murine fibroblasts)	Partial-thickness burns and chronic ulcers treatment	[55]
CellSpray®	Pre-confluent autologous keratinocytes delivered into a suspension for spray	Partial-thickness burns and chronic ulcers treatment	[56, 57]
Transcyte®	Human fibroblast derived skin substitute composed by a nylon mesh coated with porcine dermal collagen and bonded to a silicone membrane	Full- and partial-thickness burns	[58]
Dermal substitutes			
Dermagraft®	Bioabsorbable polyglactin mesh scaffold seeded with human allogeneic nenonatal fibroblasts	Full-thickness diabetic foot ulcers treatment	[59]
Alloderm®	Acellular allograft human dermis	Full- and partial-thickness wounds treatment	[60]
EZ-Derm®	Aldehyde-crosslinked porcine dermal collagen	Full- and partial-thickness wounds treatment	[61, 62]
Cymetra®	Micronized particulate acellular cadaveric dermal matrix	Wound filler in plastic surgery	[63, 64]
Biobrane®	Porcine collagen chemically bound to silicone/nylon membrane	Temporary covering of partial-thickness burns and wounds	[65]
Hyalograft 3D®	Esterified hyaluronic acid matrix seeded with autologous fibroblasts	Full- and partial-thickness wounds treatment	[66]
Matriderm®	Bovine dermal collagen type I, III, V and elastin	Full- or partial-thickness wounds treatment	[67]
Epidermal/dermal substitutes			
Integra®	Thin silicone layer; cross-linked bovine tendon collagen type I and shark glycosaminoglycan (chondroitin-6-sulfate)	Full- or partial-thickness wounds treatment	[68]
OrCel®	Human allogeneic neonatal keratinocytes on gel-coated non-porous side of sponge; bovine collagen sponge containing human allogeneic neonatal fibroblasts	Treat skin graft donor sites and mitten-hand surgery for epidermolysis bullosa	[69]
Apligraf®	Human allogeneic neonatal keratinocytes; bovine collagen type I containing human allogeneic neonatal fibroblasts	Venous and diabetic foot ulcers treatment	[70]
TissueTech®	Combination of Hyalograft 3D® and Laserskin®	Full- and partial-thickness burns and chronic ulcers treatment	[71]

1.5. Asymmetric membranes as ideal wound dressings

The first asymmetric membrane was produced with cellulose acetate using the phase inversion method, in the late 1950s by Loeb and Sourirajan, and was used in reverse osmosis [72, 73]. Since then, asymmetric membranes found applications in almost every industrial field, namely: micro/nano/ultra-filtration (MF, NF, UF), dialysis, gas separation, per-evaporation, waste water treatment, and more recently as wound dressings for skin injuries treatment [74-87].

Researchers involved in regenerative medicine started by developing occlusive wound dressings like Opsite®, Omiderm® or Spandre®, which were impermeable and, consequently, did not allow exudate absorption, resulting in a delayed healing process. Subsequently, macroporous constructs (*e.g.* Coldex® and Surfasoft®) appeared and allowed an effective drainage of wound exudate. However, these dressings were unable to avoid penetration of microorganisms and wound dehydration. Later, researchers came to the conclusion that the combination of both systems (occlusive and macroporous structures) would be the ideal as it could prevent the bacteria penetration, and at the same time, allow the exudate absorption and gaseous exchange. Thus, dressings consisting of a macroporous sub-layer or a hydrogel linked to a dense or hydrophobic microporous top layer were developed. Lyofoam®, Epigard®, and Duoderm® belong to such type of dressings. Nevertheless, they also presented some drawbacks: limited drainage capacity, exudate accumulation, and the need for frequent substitution which leads to an increased risk of wound infection. To overcome these handicaps, around 1990s, Hinrichs *et al.*, based on the work developed by Loeb and Sourirajan, designed for the first time an asymmetric membrane made of polyurethane (PU) [47]. The asymmetric PU membrane presented an interconnected microporous top layer (pore size < 0.7 µm), able to prevent rapid dehydration of the wound surface and bacterial penetration, as demonstrated through *in vitro* bacteriologic test using *Pseudomonas (P.) aeruginosa*. Furthermore, the sub-layer had a highly porous sponge-like structure containing micropores (pore size < 10 µm) and macropores (pore-size: 50-100 µm) that conferred high absorption capacity and enhance the tissue regeneration. Both layers acted also as drug release reservoirs while allowing controlled gaseous exchange, surpassing the limitations observed with Lyofoam®, Epigard®, and Duoderm®, as described before [49, 88]. On Figure 1.3, a schematic representation of an asymmetric membrane is presented highlighting the properties that make them good candidates for being used as ideal wound dressings.

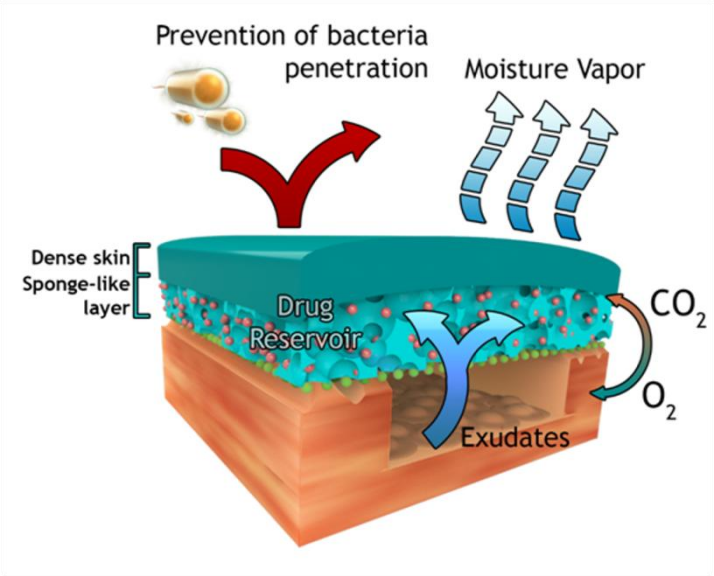

Figure 1.3. Schematic representation of the possible roles of an asymmetric membrane in the wound healing process.

As previously stated, the first asymmetric membrane was made of PU, which is a fully synthetic biodegradable material with uniform hard segments composed of butanediol and 1,4-butanediisocyanate and soft segments of $_{DL}$-lactide, ε-caprolactone and polyethylene glycol (PEG). It has been used in wound healing due to its biocompatibility, mechanical (*e.g.* flexibility) and hemostatic properties. The hydrophilic character of this material is responsible for attracting platelets and subsequently trigger the coagulation cascade [89]. In addition, asymmetrical membranes made of chitosan (CS) have also been produced. CS, a natural polymer that is obtained from the deacetylation of chitin, has been extensively used for wound dressing production, due to its intrinsic properties, *e.g.*, antimicrobial activity, biocompatibility, biodegradability and hemostatic properties. CS surface is recognized by platelets, and in a few seconds the coagulation cascade starts with the protonated amine groups of CS attracting the negatively-charged residues on red blood cell membranes, resulting on a strong agglutination, thrombin generation and fibrin mesh synthesis within the microenvironment created by this polysaccharide [49, 88, 90-94]. Table 1.2 presents the different CS and PU asymmetric wound dressings developed so far.

Table 1.2. Comparison between the different CS and PU asymmetric membranes developed in the last two decades.

Dressing / Characteristics	Bilayer CS with sustainable antibiotic delivery	Sponge-like asymmetric CS membrane	Asymmetric CS membrane	Asymmetric PU membrane with *in-situ* generated Nano-TiO_2	PU-based asymmetric membranes with acetic starch and PEG as fillers
Production Method	Dry/wet-phase inversion	Dry/wet-phase inversion	Dry/wet-phase inversion	Dry/wet-phase inversion	Wet-phase inversion
WVTR (g/m^2 per day)	1187 – 1230	2109 – 2792	2100 – 2800	1258 – 2689	2830 – 4939
O_2 permeability (L/m^2 per day)	456 – 1840	287 – 8278	0.5 – 12	n.a.	n.a.
Water uptake ability (%)	440 – 960	138 – 760	125 – 890	490 – 653	33 – 129 for PU/ASt and 25 – 109 for PU/PEG.
Antibacterial agent	Silver ion and sulfadiazine	n.a.	Silver ion and sulfadiazine	Nano-TiO_2 particles	n.a.
Antibacterial effect	Against *P. aeruginosa* and *Staphylococcus* (*S.*) *aureus*	Impermeable to *P. aeruginosa* and *S. aureus*	Against *P. aeruginosa* and *S. aureus*	Against *P. aeruginosa, S. aureus* and *Escherichia* (*E.*) *coli* by increasing nano-TiO_2 concentration	*E. coli* and *S. aureus* did not penetrate the membrane due to the difference between skin layer pore size and the minimal size of bacteria
Wound healing effect	Not available (n.a.)	After 21 days post-treatment higher than 70% of the wound were healed	n.a.	Better than gauze and commercial PU membrane dressing (Tegaderm®)	n.a.
References	[94]	[49]	[88]	[46]	[48]

Although PU and CS asymmetric membranes present several properties (antimicrobial activity, biocompatibility, hemostatic properties, gas and water permeation) that satisfy the common requirements of an ideal wound dressing, only 8 articles have been published in the last twenty years [74, 76, 78-82, 88]. This can be explained by the disadvantages of the most common methods used (wet- and dry/wet - phase inversion techniques) to prepare asymmetric membranes. These relatively simple methods usually require the use of toxic solvents which can only be removed by additional purification steps during the production process. In addition, the number of polymers used on skin wound regeneration that can be processed through the wet- and dry/wet - phase inversion techniques is limited by their solubility on the solvents used – always sodium hydroxide-sodium carbonate ($NaOH\text{-}Na_2CO_3$). This may be the reason why up to 1991, only CS and PU asymmetric membranes were reported for wound healing, as shown on Table 1.2. More recently, other methods such as supercritical carbon dioxide ($scCO_2$)-induced phase inversion technique and electrospinning started being used for the production of asymmetric membranes proving to be feasible alternatives to the conventional methods used hitherto as it will be discussed on the next sections of this Chapter and thesis. In the first technique, it is important that $scCO_2$ do not dissolve the polymers used but remove the solvents where the polymers were dissolved while in the electrospinning technique the solvent used is the more suitable to dissolve the polymers. Thus, CS and PU polymers can also be processed with these two techniques being the most used solvents acidified solutions and organic solvents as dimethylformamide (DMF) and tetrahydrofuran (THF), respectively [95-100]. Furthermore, with these new methods other healing-based polymers for the production of asymmetric membranes have arisen as poly(vinyl alcohol) (PVA), polyacrylonitrile (PAN), polyethylene oxide (PEO), and polystyrene (PS) [101-103].

1.6. Production methods of asymmetric membranes

The phase separation process required to yield an asymmetric membrane can be induced by different techniques as shown in Figure 1.4: i) by directly immersing a polymer solution into a non-solvent bath, the wet method or immersion precipitation; ii) by evaporating a polymer solution for a time period and then immersing it in a non-solvent, the dry/wet method; iii) more recently, by using $scCO_2$ to induce the phase separation, the $scCO_2$-induced phase inversion technique; iv) and by using electrospinning to form self-assembled 3D electrospun constructs [76, 80, 84, 103, 104]. The first two methods have been the most used so far (the so called conventional methods) and the last two appeared as easy, green and less time-consuming techniques, thus presenting several advantages over the conventional ones as stated in Table 1.3.

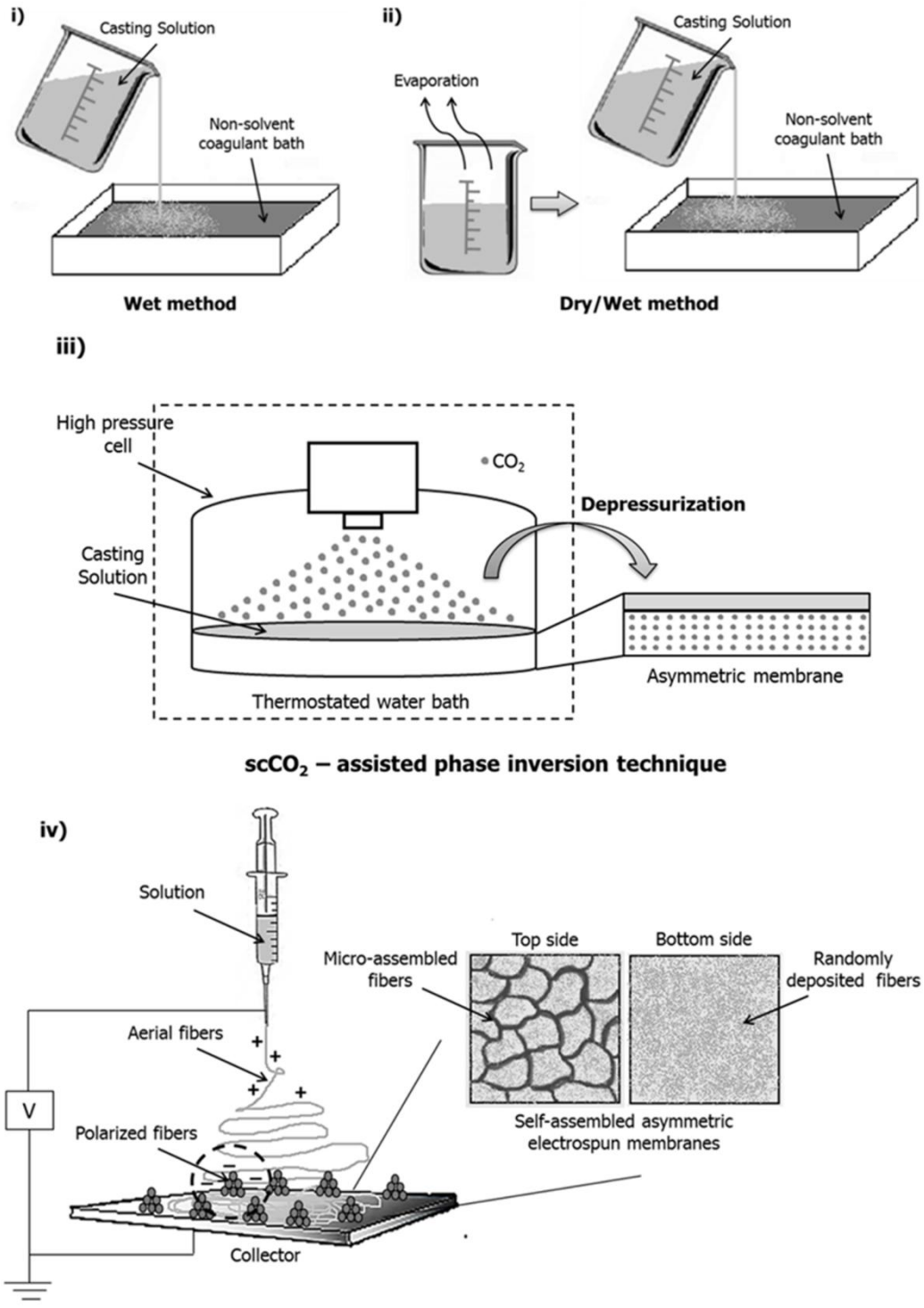

Figure 1.4. Schematic representation of the different methods used to develop asymmetric membranes: i) wet phase inversion method, ii) dry/wet phase inversion method iii) $scCO_2$ – induced phase inversion technique and iv) electrospinning technique.

1.6.1. Wet-phase inversion method

The wet-phase inversion method was the first technique developed to produce asymmetric membranes. This simple method involves the immersion of a casting polymer solution in a non-solvent coagulant bath, to promote membrane precipitation. The formation of a compact top cover with a porous sub-layer can be obtained through the delay of phase separation that takes place at the outmost interface region of the casting solution. When the membranes produced by wet-phase inversion, are to be used as wound dressings they present some limitations: the top layer formed is quite thin (less than 1 μm) and may present defects which limit the capacity to prevent excessive water vapor evaporation from the wound bed and compromise its barrier function against outside contaminants [46]. Lee *et al* [48] reported the use of wet-phase inversion method to produce PU-based asymmetric membranes which were tested as wound dressings, as shown in Table 1.2. However, to obtain a more compact and dense top layer, the authors have combined polymer-filler hybridization, by using acetic starch and PEG, with the immersion precipitation phase inversion. The water vapor transmission rate (WVTR) and the water uptake ability are directly proportional to the filler content.

1.6.2. Dry/wet - phase inversion method

The dry/wet-phase inversion method was adopted to overcome the defects observed on the top layer of the membranes produced by the wet-phase inversion method. To do so, researchers started to per-evaporate the casting solution before its immersion into the coagulation bath. With this per-evaporation process, the non-solvent diffuses to the outermost region of the polymeric casting solution allowing the formation of an integral and dense top layer able to protect the wound against outside contamination. However, this method requires at least one volatile solvent for the membrane forming polymer. Usually, the casting solution is heated in an oven for dry phase separation at 50 ºC for 10-60 min. After that, the underlying polymer solution with formed skin layer is immersed into a coagulation bath for 24 h (usually containing NaOH-Na_2CO_3), inducing the wet-phase inversion by the diffusion of non-solvent into and solvent out of the polymer solution. Afterwards, the solidified membrane is soaked in distilled water and finally frieze-dried [46, 88, 94, 104].

The dry/wet–phase inversion technique has been the most used method to produce asymmetric membranes composed of CS or PU. In some studies, the incorporation of antibacterial agents as silver sulfadiazine [88, 94] and nano-TiO_2 particles [46], was reported (please refer to Table 1.2). In some cases the pore size of the top layer is not sufficient to avoid bacteria penetration in addition to biofilms formation. The introduction of antibacterial agents was a suitable achievement to fight such drawback. In this process, the thickness of the skin layer increases with the increase of the evaporation time. This is explained by the re-dissolution of the solvent, which is evaporated from the underlying homogeneous solution [88]. The porosity of the sub-

layer with a sponge-like structure also decreases with longer evaporation periods, since the polymer solution becomes more concentrated [66]. The type of non-solvent used on the coagulation bath also influences the asymmetry of the membranes. It is known that a polar non-solvent with low molar mass (*e.g.* methanol) tends to give a high overall porosity, and reduce the membrane thickness, while a less polar non-solvent (*e.g.* butanol) allows the formation of a very thick film and a more open porous sub-layer. This is due to the higher miscibility of polar non-solvents which promote an instantaneous demixing upon immersion of the casting solution in the coagulation bath. Furthermore, higher polymer concentrations reduce the porosity and finally induce the formation of a dense structure [105-107]. The possibility to form membranes with suitable porosity and thickness using this method allow for a faster and less painful wound healing process. Nevertheless, the dry/wet method often requires the use of additional post-treatments to remove any cytotoxic residues that might remain in the membranes.

1.6.3. Supercritical fluids and supercritical CO_2 – assisted phase inversion technique

After its discovery in 1922 by Hermann Staudinger, polymers have become part of our lives [108]. In view of their importance in numerous applications, increasing attention is being given, not only to the synthesis, but also to polymer processing. As stated before, the traditional methods normally use environmentally hazardous volatile organic solvents (VOCs) and chlorofluorcarbons (CFCs). Due to the huge increment of VOCs and CFCs emissions and generation of aqueous waste streams, there is a growing interest in the development of alternative technological processes with minimized environmental impact, such as reduction energy consumption, less toxic residues, better use of by-products and also better quality and safety of final products. SCF technology is one of such methods used as processing solvents or plasticizers [109, 110].

A fluid is termed supercritical when it is above the critical temperature (T_c) and pressure (p_c) but below the pressure needed for condensation [111]. In general terms, SCF show liquid-like densities with gas-like transport properties and solvent power for several applications that can be continuously adjusted by changes in pressure and temperature [112].

Several substances can be used as SCF as water, ethane, ethylene, propane, carbon dioxide (CO_2), methanol and acetone [113]. However, in SCF technology, CO_2 is the most common used solvent for a variety of chemical and industrial processes. It is a clean and versatile solvent and a promising alternative to VOCs and CFCs. It is non-toxic, non-flammable, chemically inert and inexpensive. Though it is abundant in the atmosphere, a large amount is also available in high-purity as a by-product from many processes including the fermentation of biomass (NH_3, H_2 and ethanol production). Its supercritical conditions are easily achieved (T_c = 31.3 ºC and p_c = 7.38 MPa) and it can be removed from a system by simple depressurization. In addition, the use of $scCO_2$ does not create a problem with respect to the greenhouse effect as it can be recovered during processing [109, 114-116].

$scCO_2$ have found applications in a broad range of areas [117, 118] being the most popular the decaffeination of tea [119] and coffee [120] and the extraction of flavours [121], spices [122], and essentials oils [123, 124] from plants. More recently, this unique solvent has found considerable commercial interest in applications as diverse as dry cleaning [125], metal degreasing [126], polymer modification and polymerization [127-129] and pharmaceutical processing including drug impregnation [130-132].

Nowadays, $scCO_2$-assisted processes have been proposed in tissue engineering field overcoming several limitations of the conventional biomaterials fabrication techniques (fiber bonding, solvent casting, particulate leaching, melt molding, gas foaming, freeze-drying, wet- and dry/wet-phase inversion) [133, 134]. Through the conventional techniques it is difficult to achieve: i) large porosity together with a control of the pore diameter, connectivity and mechanical resistance; ii) large porosity together with the nanometric surface that enhances cells adhesion and growth; iii) complex 3D symmetric or asymmetrical structures; iv) the removal of toxic solvents that are retained deep inside the structure [135]. By using SCF technologies as $scCO_2$-assisted phase inversion technique, supercritical gel processing and $scCO_2$-assisted electrospinning, biomaterials with the aimed morphology can be obtained thanks to the modulability of CO_2 mass transfer properties, characteristic of dense gases and the specific thermodynamic behavior of gas mixtures at high pressure. Additionally, an efficient solvent elimination can be obtained due to the high affinity of $scCO_2$ with almost all the organic solvents. Furthermore, short processing times are possible, taking advantage of the enhanced mass transfer rates [135].

When $scCO_2$-induces the demixing of a polymeric solution forming a porous membrane the method is often denominated as $scCO_2$-assisted phase inversion method. Herein, CO_2 acts as a solvent, extracting the solvents used for preparing the casting solution, and as a non-solvent, for the polymers. The $scCO_2$ solubilizes in the casting solution promoting the removal of solvent from the polymer solution and, subsequently, the membrane formation through the polymer precipitation, as it is observed in Figure 1.4 (iii). The properties of the membranes can be modified by changing the concentration of the casting solution, the ratio of non-solvent/solvent, the pressure, the temperature and the depressurization rate. The relative affinity of a polymer and solvent can be assessed by comparing the solubility parameters [136]. It allows the production of porous matrices by the induction of nucleation and growth of bubbles inside the polymer stimulating the porous growth. Furthermore, it can allow the production of materials with high degree of swelling and transparent membranes in a wet state, which is useful to be used as wound dressings. It overcomes the several disadvantages of chemically crosslinking gels since it does not need the use of organic solvents that are difficult to be removed [137-139].

Furthermore, it allows the production of dry, clean, ready-to-use and stable membranes with short processing times, unlike those produced by wet and dry/wet-phase inversion methods that demanded additional post-production treatments [140-142].

For instance, Temtem and co-workers [99] have explored this technique for the production of CS devices using moderate temperatures and three environmentally acceptable solvents (water, ethanol and CO_2). They also have demonstrated that the $scCO_2$-induced phase inversion technique allowed a single-step strategy in the preparation of an implantable antibiotic system by co-dissolving gentamicin with CS and the solvent. These membranes were also biocompatible allowing the adhesion and proliferation of human mesenchymal stem cells (MSC). The obtained results provided a starting point for the "green" design and production of CS-based materials with potential applications in tissue engineering and regenerative medicine, as well as drug delivery. In a similar study [143] it was investigated the feasibility on the fabrication of porous crosslinked CS hydrogels in an aqueous phase using dense gas CO_2 as foaming agent. Glutaraldehyde and genipin were used as crosslinkers and CS hydrogels were obtained with a highly porous biocompatible skeleton with an average pore diameter of 30-40 µm. Furthermore, the produced hydrogels exhibited a comparable mechanical strength and swelling ratio compatible with its application for soft tissue (skin and cartilage) engineering regeneration.

The preparation of membranes using supercritical-fluid-assisted methods, implies the use of specialized and robust high-pressure apparatus as the one designed by Temtem *et al.* (2008) [144]. The heart of the apparatus is a stainless steel high-pressure cell which can stand pressures up to 60 MPa. The cell includes a porous structure that supports a bed of Rasching rings inside to allow the homogeneous dispersion of CO_2 through the casting solution as it is schematically represented in Figure 1.4 (iii).
Taking advantage of the additional parameters that the $scCO_2$-assisted phase inversion method offers for controlling the morphological properties of the polymeric membrane, asymmetrical PVA/CS membranes were recently developed and their performance as skin wound dressing was evaluated, one the of the main achievements attained in this thesis project and well discussed on the following Chapters [103]. The concentration of the casting solution and the depressurization rate (fast or slow) were the key factors to obtain the desired membrane structure. Nevertheless, when all the parameters described before are well established, an asymmetrical membrane is easily and directly formed in just 4 h instead of the 24 h needed when using conventional methods. To the best of our knowledge it was the first time that asymmetric membranes for skin wound regeneration were developed using supercritical fluids. The technique can be also extended for the production of other polymeric membranes using different polymers and incorporating different bioactive agents on the top and bottom surfaces.

The events that lead to the membranes' formation, *i.e.* thermodynamic interactions between polymer/solvent/non-solvent and the concentration/phase changes that occur during phase inversion (the ratio of the solvent outflow to non-solvent inflow) are often visualized using the ternary phase diagram (Figure 1.5) developed in the late 1950s by Tompa and used in the early 1970s by Strathmann *et al.* and Michaels [49, 77, 145, 146]. Each corner of the diagram

represents each pure component (the polymer – PVA/CS, the solvent – acidified water, the non-solvent – $scCO_2$ + ethanol), the axes represent the three pseudo-binary systems and any point located inside the diagram represents a mixture of the three components. In the liquid + fluid region a primary (binodal curve) and a secondary envelope (spinodal curve) enclose demixing boundary. Both curves coincide at the critical point and the region between them corresponds to a metastable state. Two different mechanisms have to be considered as far as liquid-liquid (L-L) demixing is concerned: nucleation/growth and spinodal decomposition. The structures obtained and pore dimension are dependent on the path followed through the ternary diagram. The arrows numbered from 1 to 4, in Figure 1.5, report the different composition paths that can occur during membranes formation [99, 147]:

1 Increasing of polymer concentration since the outflow of the solvent from the solution is faster than the inflow of the non-solvent. The phase inversion does not occur and the polymer solidifies by gelation into a dense structure.
2 The ternary polymer solution becomes metastable. Cellular structure by nucleation and growth of droplets of the polymer-rich phase.
3 The ternary polymer solution becomes unstable. Bicontinuous structure due to spinodal phase separation.
4 Beads-like structure due to nucleation and growth of droplets of the polymer-poor phase.

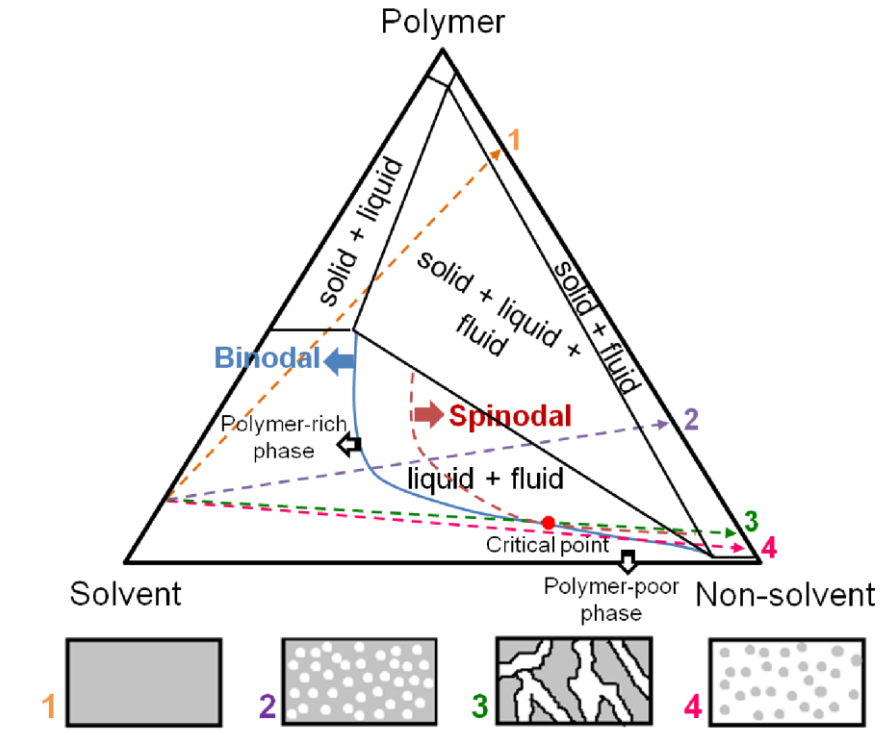

Figure 1.5. Hypothetical ternary phase diagram for the system polymer / solvent / non-solvent with the various composition paths indicated by arrows and numbers and the typical membrane structures obtained in the different paths (adapted from [99]).

Considering the formation of asymmetric membranes through $scCO_2$-assisted phase inversion technique the simultaneous presence of a dense top layer and porous (cellular) inner layer indicates that the competition between two different mass transport mechanisms occurs during membrane formation process. A hypothetical mechanism that may describe the asymmetry formation in the PVA/CS membranes is the following one: in a first step, the solvent (acidified water) outflows from the solution before the $scCO_2$ can cause the phase separation leading to polymer accumulation and the formation of the dense skin layer. Subsequently, the solvent outflow is stopped by the dense layer formation, and $scCO_2$ with ethanol (co-solvent) diffuses inside the remaining solution extraction the solvent and causing the L-L phase separation above the critical point leading to the cellular structure in the inner layer (path 2 schematically represented in Figure 1.5) [99, 147].

However, and as stated previously, the asymmetry and the inner morphology of the membranes can be easily changed taking into account the several process parameters. Matsuyama *et al.* [148, 149] used $scCO_2$-assisted phase inversion process to produce and analyze the effect of several process parameters (temperature, pressure and polymer concentration) on the asymmetry of PS membranes [148] and the influence of a kind of solvents used in the formation of asymmetrical cellulose acetate membranes [149]. They observed that as the pressure increased from 8 to 16 MPa (maintaining the temperature (35 ºC) and casting solution concentration (20 wt%)), both the pore size (in the upper and bottom layers of the membrane) and the membrane thickness increased. The increase of CO_2 incorporation leads to the decrease of the solution viscosity due to polymer concentration decrease, resulting in higher membrane porosity. As the polymer concentration increased, the overall membrane thickness increased because of the higher amount of polymer. Finally, as the temperature increased, the asymmetry becomes more pronounced. As general, the pores are more isolated at the top surface because the polymer concentration becomes higher due to the evaporation of solvent before CO_2 introduction and the dissolution of the solvent in the $scCO_2$ phase. More recently, Reverchon *et al.* [147] have performed a similar study by testing the versatility of the $scCO_2$-assisted phase inversion process on the formation of PVA/dimethylsulfoxide (DMSO) asymmetrical membranes. Polymer concentration, temperature, pressure and the affinity between $scCO_2$ and solvent continued to be the key parameters to obtain an asymmetrical structure. Regarding the affinity between $scCO_2$ and solvent, they observed that when acetone (with higher affinity to $scCO_2$ than DMSO) is added to the procedure, the skin layer thickness decreased since the phase-separation process is faster, limiting the outflow of the solvent. In addition to the processing conditions previously described, in our work it was found that the depressurization rate is also a key parameter to obtain the PVA/CS membranes with the desired structure, in addition to casting solution concentration [103]. As already observed by Temtem *et al.* [136] higher rates of depressurization produce larger pores, *i.e.* in a slow depressurization the CO_2 diffuses slowly out of the polymer phase (not affecting the polymer structure), while for a fast depressurization a large amount of CO_2, dissolved in the polymer, shrinks the pores and consequently increase their mean diameter.

1.6.4. 3D self-assembled dressings produced by electrospinning technique

Electrospinning is a very well-established method for preparing structures for tissue engineering purposes. The technique allows the production of electrospun nanofibrous membranes with a similar structure to that of native ECM [150], as a result of charging and ejecting a solution through a spinneret under a high voltage electric field (up to 30 kV). Different natural and synthetic materials have already been used in the development of nanofiber wound dressings such as alginate, cellulose, chitin, collagen, CS, dextran, gelatin, hyaluronic acid, PCL, PLA and poly(*L*-lactic acid) (PLLA), PVA, among others [151-153]. This reveals that this technique allows the use of a huge variety of polymers when compared to the other techniques presented above.

However, the electrospun materials are usually obtained as 2D flat non-woven meshes with dense fiber packing limiting the cells penetration into the materials and compromising in some degree the tissue regeneration. In fact, cells adhesion, proliferation and differentiation in a 3D scaffold behave differently from 2D flat surfaces. The third dimension improves cell-cell interactions, cell migration and morphogenesis, and supports a cell density higher than 2D structures. The interconnectivity within the 3D construct allows a controlled exchange of nutrients and metabolites [154, 155]. Generally, there are four main strategies for the production of 3D electrospun fibrous macrostructures: (a) increasing spinning time; (b) assembly by post-processing of 2D electrospun structures (*e.g.*, folding, layer-by-layer electrospinning, sintering, mechanical expansion); (c) direct assembly by an auxiliary factor (*e.g.*, a 3D template, liquid collector) and (d) by self-assembly [156-159]. Nevertheless, the strategies (a), (b) and (c) are time-consuming (normally takes from 20 min to 24 h to form a well-defined 3D structure) and require additional support. Self-assembly allows a rapid growth of 3D constructs, by controlling some parameters during the electrospinning process as solution concentration/viscosity, electrostatic field and ambient humidity, without human intervention, which otherwise will be expensive, slow and complex.

Recently, T. Reis *et al.* [160] developed and described the production process of 3D PCL electrospun constructs by self-assembled with asymmetric geometry as can be seen in Figure 1.4 (iv). The self-assembled process, which results from the electrostatic forces between polarized and aerial fibers, leads to a compact arrangement of micro-assembled fibers (MAFs) on the top side of the membrane that can improve the contact with the wound and absorbs the wound exudate allowing the new tissue growth, and an extremely smooth surface with random deposited fibers on the bottom side that with further modifications can protect the wound against outside contamination [160, 161]. Furthermore, the electrospun membranes are produced in a dry, clean and ready-to-use state, similarly to the ones obtained by $scCO_2$-assisted phase inversion method. PCL allows good adhesion, growth, viability, morphology and mitochondrial activity of cells [162]. The development of 3D electrospun constructs has been previously

investigated using other polymers such as PAN, PVA, PEO, and PS, but none of them were developed envisaging the application as wound dressing [101, 102].

The main advantages and disadvantages of the methods described above and that were used so far for producing asymmetrical membranes are summarized in Table 1.3.

Table 1.3. Summary of the production methods of asymmetric membranes: advantages and disadvantages.

Production Method	Advantages	Disadvantages
Wet-phase inversion	Simple method	Formation of a too thin top layer, which leads to an excessive water vapor loss and limits the protection against microorganisms penetration Applies only to a limited number of polymers
Dry/wet-phase inversion	Formation of an integral and dense top layer allowing the protection of the wound	It requires a volatile solvent Additional post-treatments are required to remove potential cytotoxic residues Time consuming (the full process takes, usually, more than 24 h) Applies only to a limited number of polymers
scCO_2-phase inversion	Easy, fast (about 4 h) and green technology It can form dry, clean (solvent-free) and ready-to-use membranes It can produce a dense top layer (~15 µm) and a homogeneous inner layer Applies to a large number of polymers Different operating parameters can be used to tune and control the membrane morphology	Specialized high-pressure apparatus and people with know-how in high-pressure techniques
Electrospinning	Easy, fast and green technology It can form dry, clean (solvent-free) and ready-to-use membranes It can produce self-assembled membranes with well-defined shape on one side and flat surface on the other side Applies to a large number of polymers Different operating parameters, such as solution concentration, voltage, humidity, temperature and distance between the tip and the collector, can be optimized enabling the production of 3D electrospun constructs	Precise control of working atmosphere, temperature and humidity is required Specialized equipments: DC power supplier and syringe pump are required

1.7. Required properties for asymmetric membranes to be applied as wound dressings

When an asymmetrical membrane is intended to be used as a wound dressing, its intrinsic properties have to be evaluated [48, 49, 88]. These properties include i) morphology; ii) water uptake ability (swelling) and hydrophilicity (contact angle analysis); iii) WVTR and O_2 permeation; iv) elasticity and tension at brake; v) bacterial activity; vi) *in vitro* drug release profiles (when a biologic active agent is intended to be loaded in the dressing); and vii) *in vitro* and *in vivo* cytotoxicity studies. Table 1.4 comprises a summary of all the techniques usually applied in the development of wound dressings.

1.7.1. Morphology and porosity of the membranes

The study of cell behavior (adhesion and proliferation) in the presence of biomaterials is crucial to know whether tissue regeneration will be enhanced or not [163]. The materials surface morphology and porosity are usually characterized using scanning electron microscopy (SEM) and mercury intrusion porosimetry, two of the most important physical properties controlling cell behavior. Pores interconnectivity, evaluated through water flux permeability studies, is also an important factor as it enables cells to penetrate through the porous membrane and the diffusion of nutrients [99, 144, 164-166].

1.7.2. Water uptake ability (swelling) and contact angle analysis

An ideal dressing must also have the ability to absorb excessive exudates from the wound beds. Materials with a high water uptake capacity and consequently hydrophilic character, allow the diffusion of nutrients, cells, bioactive molecules and waste [167]. In general, commercially available PU membrane dressings and others, such as Tegaderm®, Bioclusive® and OpSite®, exhibit low fluid absorption ability *i.e.* in the range of 31-46% (weight gained), due to their dense structure, which limits their applications to wounds with low exudate production. In fact, an ideal dressing normally present water absorption in the range of 100-900% and high wettability (materials usually display a contact angle lower than 90º) [46, 168]. For asymmetric membranes such characteristics rely on the porosity presented by the membrane's sub-layer which usually ranges from 60% to 90%. Mi *et al.*, on a study that reported the production of asymmetrical CS membranes by dry/wet-phase inversion technique, revealed that these membranes presented lower water uptake capacity due to the decreased porosity of the sponge-like porous layer. The reported studies also showed that the water uptake capacity of the membranes produced through the dry/wet-phase separation method falls with the increase of evaporation time, in the "dry" phase separation process [88]. When the $scCO_2$-assisted phase inversion technique is used, membranes' swelling is dependent on the depressurization rate. For electrospun

membranes, the water uptake ability depends essentially on the materials used, *i.e.* on the hydrophilic or hydrophobic character of materials. Electrospinning methods, by allowing the random deposition of fibers, originate membranes with a high surface "open" area, that present an extremely porous structure [169, 170].

1.7.3. Water vapor transmission rate and oxygen permeation analysis

The WVTR across the top surface of the membrane, determines the wound moist environment which is crucial to the healing process [46, 48, 49, 171]. In fact, an excessive WVTR results in a rapid water loss, leading to dehydration of the wound and to the possible dressing attachment to the injured skin. On the other hand, a low WVTR might cause the exudate retention and the buildup of a back pressure, that leads to maceration of the healthy tissue surrounding the wound, inducing pain to the patient [46, 171]. Considering that the WVTRs for normal skin, first degree burns, and granulating wounds are (20 ± 1) x 10, (28 ± 3) x 10, and (51 ± 2) x 10^2 g/m^2 day, respectively, it is recommended that wound dressings having WVTRs values in the range of (20-25) x 10^2 g/m^2 day, which is half of the value presented by granulating wounds, provide an adequate moisture and prevent exudate accumulation [46]. However, in practice, some of the commercially available wound dressings are not in conformity with this demand. For example, Comfeel®, Dermiflex®, Tegaderm® and OpSite® present WVTR of about 285, 76, 491 and 792 g/m^2 day [46, 172-174].
It is important to notice that the WVTR depends on the structural properties (thickness and porosity) of the dressing as well as on the chemical properties of the material from which it is made [103]. The WVTR of asymmetrical membranes rises with the increasing porosity of the sponge-like inner layer and the diffusion of water molecules slows down with increasing thickness of the dense skin layer [49]. WVTR can also be influenced by external conditions like the environmental relative humidity (RH) and temperature [175].

The permeability of oxygen (O_2) across the membrane is another important property for the wound healing process. O_2 is an essential nutrient for cell metabolism, especially for energy production and for reparative processes like cell proliferation and collagen synthesis. In addition, recent discoveries highlighted a new role of O_2 in wound healing via the production of reactive oxygen species (ROS) (such as free radicals and H_2O_2) by wound-cells specialized enzymes. These ROS contribute as cellular messengers to promote processes that support wound healing including cytokine action, angiogenesis, cell motility, and ECM formation. Low O_2 concentration at the wound compromises the function of the enzymes in the oxygen conversion and, consequently, leads to an impaired healing. As previously described in several studies, wound dressings which allow a suitable gas microcirculation are clinically preferred, since CO_2 accumulation leads to a localized pH decrease that leads to wound irritation, while an hypoxic environment decelerates the regeneration of peripheral tissues, or even allow anaerobic bacteria growth. An excellent wound healing is attained for O_2 permeation ranging from 456 –

1840 L/m^2 day [94, 176-179]. Although most of the authors de-prioritize CO_2 permeation through the dressings, since no recommendation is available for this parameter, others consider that the permeability of dressings to carbon dioxide may also be clinically important. CO_2 has a critical role in the maintenane of body's pH buffer system, which is maintained at 7.35-7.45 in the blood and tissues. The respiratory system regulates the pressure of CO_2 in the body at about 40 mmHg at 37ºC and the skin being relatively impermeable to CO_2 helps on the maitainance of the pCO_2 constant in the body. However, when a wound occurs the skin barrier is compromised and the CO_2 pressure decreases. On the other hand, once a dressing is in place, the flow of CO_2 from tissues will begin to accumulate under the dressing, and the pCO_2 will begin to increase. If a dressing permeable to O_2 is used (one of the main requirements to have a suitable gas permeation), it will also be permeable to CO_2 (since the kinetic diameter of CO_2 (~0.330 nm) is lower than the kinetic diameter of O_2 (~0.343 nm)), and consequently the CO_2 pressure in blood and tissues will not remain constant (~40 mmHg). In order to maintain a beneficial pressure of CO_2, some studies proposed the use of carbon dioxide as an aerosol propellant or co-propellant applied to the wound dressings [180-182].

As previously stated WVTR depends on the porosity of the sponge-like inner layer and on the thickness of the top dense skin layer, while the O_2 flux is significantly controlled by the top dense skin layer since the size of the pores available on the sublayer are usually fully permeable to O_2. Therefore increasing the thickness of the top dense skin layer significantly decreases the gas flux [49, 88]. The optimization of these two parameters (thickness and porosity) is thus a key factor to allow a suitable gas flux permeation and also to prevent wound dehydration and exudate accumulation.

The asymmetric membranes produced through conventional methods (namely, wet- and dry/wet-phase inversion), present skin layers, in the range 5-10 µm of thickness, that allow a suitable balance between WVTR and gas permeabilty. The asymmetric CS membranes produced by Mi *et al.* (2001) had a dense skin layer of about 6.5 µm and a sponge-like inner layer with 74% of porosity. These membranes presented a WVTR, O_2 permeablity and water uptake ability of 2376 g/m^2 per day, 644 L/m^2 per day and 320 %, respectively, which are in the range of the desired values of an ideal wound dressing. Furthermore, the sub-layer of the studied membranes presented pores that had the adequate size (about 10-100 µm) to transport O_2 molecules into the wound [46, 49, 88, 94, 183].
Other asymmetrial dressings present the so called finger-like voids, that allow oxygen transportation across the membrane, without demanding gas exchange between or through the pores available in the membrane [184]. On the other hand, in order to avoid bacteria penetration (as it will be discussed on section 1.7.5.), the top dense skin layer could have pores with a mean diameter smaller than bacteria (< 0.5 µm). Nevertheless, a membrane with an integral and dense structure is preferred in order to better control the vapor and gas permeation.

1.7.4. Mechanical properties analysis

The design of a wound dressing with specific mechanical properties must consider its final application: whether they will be used topically (to protect cutaneous wounds) or for internal wound support. In addition, the wound dressing should be flexible but, simultaneously, stable and strong enough to cover the wound surface along the healing period. It must present an easy handling during wound's coverage, maximizing patient comfort and convenience [48, 171]. In the literature, it is described that the Young's modulus or elastic modulus (the substance's resistance to being deformed elastically) of the skin varies between 0.42 and 0.85 MPa for torsion tests, 4.6 and 20 MPa for the extension tests and between 0.05 and 0.15 MPa for the suction tests. However, these values can vary with several factors like age, skin colour, previous lesions and genetic heritage [185]. The Young's modulus showed by wound dressings is dependent on materials thickness and porosity and also on the processing techniques used in their production.

1.7.5. Antimicrobial activity of wound dressings

The capacity of wound dressings to protect the wound from infection, acting as a barrier against microorganism penetration, is another property that has to be fully screened during wound dressing development. The asymmetric morphology of membranes is essential to avoid microorganism penetration, since the size of the pores available at the dense skin layer is usually smaller than bacteria. Despite the fact that asymmetrical membranes act as a barrier for microorganisms, some bacteria may colonize upon the dressing and the surrounding healthy tissue, and then migrate into the wound, triggering infection after injury. To avoid such drawback, antibacterial agents can be added to the membranes, to further improve the intrinsic antimicrobial properties of some polymers, like CS [46]. Silver sulfadiazine (AgSD) has been incorporated in wound dressings to prevent wound infection [88, 186-188], although, concerns about the potential silver toxicity have been raised. Other antimicrobial agents have also been investigated like: Nano-TiO_2 [46]; different Southern Thailand medicinal plant formulas as well as their medicinal plant components [189]; peptide-morpholino oligomer (PMO) conjugates targeted to *S. aureus* gyrase A mRNA [190] and some antibiotics (vancomycin, daptomycin, linezolid, clindamycin and doxycycline) [191].

Recently, biocompatible antimicrobial agents oligo(2-methyl-2-oxazoline) and oligo(2-bisoxazoline) quaternized with *N,N*-dimethyldodecylamine have been used against *S. aureus* and *E. coli*, the most common and dangerous pathogens in burn injuries [192, 193]. The results obtained revealed that they are good candidates to prevent wound infection.

1.7.6. *In vitro* drug release studies

In addition to antimicrobial agents and drugs, future research and development in the area of bioengineered skin constructs will most likely be focused on the delivery of growth factors, DNA and microRNA (miRNA) to prevent and mitigate inflammation, and to improve tissue regeneration by stimulating healthy healing responses with the minimum final scar formation. Indeed, gene therapy has been suggested as ideal for chronic wound treatment where limited duration of target gene expression is required. Usually, in these cases, growth factors encoded in DNA plasmids are entrapped into the biomaterial to be topically applied on the wound. However, these active agents, which are expensive, have not been included so far in asymmetric dressings being a thematic that must be further considered, to improve the performance of these wound dressings [164, 175, 194-197]. On the other hand, anti-inflammatory agents have been incorporated to minimize the inflammatory phase during the wound healing process. For example, ibuprofen was successfully loaded into PVA/CS asymmetrical membranes herein produced [103]. For wound healing purposes the anti-inflammatory drugs should be at least released during the first twelve hours after injury, which corresponds to the peak of inflammatory phase. Nevertheless, the pharmacokinetic behavior of the drug is dependent on its interaction with the polymer, structure and swelling behavior of the wound dressing and, sometimes, the release medium used.

1.7.7. *In vitro* and *in vivo* cytotoxic studies

Finally, to assess the applicability of the wound dressing for the envisioned biomedical application, the cytocompatibility should first be evaluated through *in vitro* studies, using appropriate cell line models. In this context, the *in vitro* studies enable the pre-screening of the hazard effect of various chemical compounds that are aimed at skin regeneration, before animal models are used [40]. *In vitro* studies were initially performed using two-dimensional monolayer cultures of human cells, although, they were unable to reproduce cell-cell and cell-ECM interactions. To overcome such handicap, new three dimensional cell culture techniques have been developed to allow the interaction of different types of cells and between them and the surrounding matrix [198, 199]. Conversely, *in vivo* assays are used to fully monitor the wound healing process and to evaluate local and systemic immune response through histological analysis [200, 201]. Nevertheless, results gained from experiments conducted with animal models are often limited due to the metabolic variances and anatomical architecture structure of the human skin. Additionally, these studies are expensive when compared to *in vitro* studies [202].

Table 1.4. Summary of methods used during the development of wound dressings [46, 49, 88, 94, 103, 168].

Methods	Allows to characterize	Desired values
SEM	The inner structure of the membranes Monitoring the different steps of wound dressing development	Dense top layer, with a thickness in the range 5-10µm Homogeneous porous inner layer
Mercury intrusion porosimetry	Materials pore size and porosity	High porosities (60-90%) independently of the pore size to obtain suitable water uptake ability
Water uptake ability and Contact angle analysis	The hydrophilic character of the membranes	Suitable to promote exudate drainage and to assure a moisturized environment of the wound (100-900%) It depends on the porosity of the membrane's inner layer
WVTR and O_2 permeation	Essential to confirm if the dressing can maintain the moisturized environment of the wound	The desired values are in the range of (20 - 25) x 10^2 g/m^2 day for WVTR The desired values are in the range of 456 – 1840 L/m^2 day for O_2 permeability
Young's modulus	Essential to determine the elasticity of the dressing	For extension tests the Young's modulus of the skin varies between 4.6 to 20 MPa The dressing should be flexible but strong enough to be handling during wound's coverage
Bacteria penetration tests	Essential method to determine the penetration and/or survival of bacteria through the membrane	Provided by the dense top layer Some antibacterial agents could be loaded into membranes
Loading and *in vitro* drug release studies	Drug loading to avoid and mitigate inflammation and accelerate tissue regeneration	For wound healing purposes the drug release should be controlled and at least during the inflammatory phase
***In vitro* and *in vivo* studies**	Essential to determine the biocompatibility and biodegradability of the dressings and them performance to heal a wound	The dressing should be biocompatible and accelerate the wound healing process.

1.8. General aims and research plan of this thesis

As reported along this Chapter and based on the works already reported in the literature, it is possible to conclude that asymmetrical membranes composed by different types of polymers can be developed using $scCO_2$ technologies, despite the old conventional methods. However, few studies related with the development of asymmetrical membranes through $scCO_2$-assisted phase inversion technique have been thoroughly reported thus far and even less described the use of this technique to produce asymmetrical membranes for skin wound regeneration. Probably, this can be due to the need of specialized and robust high-pressure apparatus, qualified people with know-how in high-pressure techniques and the small amount of information on the scientific media concerning the production of membranes with a highly controlled morphology using a faster and non-residue method.
In order to stress the potential of SCF technologies on the development of asymmetrical membranes to be used as wound dressings, following the good practices of wound-management for a faster and less painful healing process, the present doctoral project had three main goals:

1. Development of hydrogel-based asymmetrical wound dressings, able to mimic the native structure of skin, through a non-residue, green, fast, non-expensive and non-labor intensive method: $scCO_2$-assisted phase inversion;
2. Design and production of drug-loaded carriers with sustained ibuprofen (IBP) release profile;
3. Evaluation of the drug-loaded asymmetrical membranes and the effect of IBP in the wound healing process.

In order to pursue the general objectives of the Ph.D. work, different research studies were carried out and presented as individual Chapters for a better understanding from the reader. Four Chapters (1-4) constitute the main body of this Ph.D dissertation. Chapter 1 and 4 present a general introduction and the conclusions and future prospects of the research work developed, respectively. Chapters 1 and 2 have already been published in peer reviewed international journals and Chapter 3 was submitted for publication at the time this thesis was completed. The Chapter presentation order does not perfectly reflect the chronological order of the manuscripts' publication. Each Chapter is preceded by a title page describing the reference of the publication, the poster and/or oral communications related with the developed work (if applicable) and the personal contribution of the author of this thesis in each work. Additionally, besides the Ph.D dissertation includes a general introduction and conclusions, each Chapter presents extensive and specific introduction, discussion and conclusion sections. Supplementary information is also present at the final of this dissertation.

Below is a brief description of the contents of each of the Chapters, in order to answer to the general aims of this Ph.D. dissertation:

Chapter 1. This Chapter highlights the motivation of this work and intends to provide the reader information about the incidence of burn-related wounds in the world and the importance of continuing to search for better systems that are able to mimic the skin native structure and enable the complete restoration of skin integrity. It also reviews the state of the art about the production of asymmetrical membranes, highlighting the several advantages of $scCO_2$-assisted phase inversion and electrospinning techniques in comparison with the conventional wet- and dry/wet-phase inversion methodologies. Moreover, the required properties that an asymmetrical membrane should present to be applied as wound dressings, is extensively described.

Chapter 2. This Chapter describes the development and characterization of asymmetrical PVA/CS hydrogel-based membranes to be used as wound dressings through $scCO_2$-assisted phase inversion technique.

Chapter 3. This Chapter describes the incorporation of drug-loaded carriers in order to obtain a sustained drug release from the hydrogel-based PVA/CS asymmetrical membranes (described on Chapter 2). Additionally, it demonstrates the performance of the developed systems and the effect of a simple non-steroidal anti-inflammatory drug (IBP) in the wound healing process, by the induction of transcutaneous full-thickness wounds in Wistar rats.

Chapter 4. This Chapter provides a global overview of the subjects addressed throughout all the other Chapters, highlighting the main results and conclusions achieved. New research questions are proposed based on the current limitations of the available materials and future prospects of work are addressed.

Acknowledgements

The authors are grateful to S.A. Ricardo for her advice.
The authors would like to thank the financial support from Fundação para a Ciência e Tecnologia (FCT - Lisbon) and FEDER funds through POCI-COMPETE 2020 contracts UID/Multi/00709/2013, UID/QUI/50006/2013, POCI-01-0145-FEDER-007265, POCI-01-0145-FEDER-007491 and SFRH/BD/80648/2011 (P.M.).

CHAPTER 2. *Poly(vinyl alcohol)/chitosan asymmetrical membranes: highly controlled morphology toward the ideal wound dressing*

This chapter corresponds to the manuscript published in:

2014, Journal of Membrane Science, 469:262-271.
Patrícia I. Morgado, Pedro F. Lisboa, Maximiano P. Ribeiro, Sónia P. Miguel, Pedro C. Simões, Ilídio J. Correia and Ana Aguiar-Ricardo.
Poly(vinyl alcohol)/chitosan asymmetrical membranes: Highly controlled morphology toward the ideal wound dressing.
(http://www.sciencedirect.com/science/article/pii/S0376738814004864)

These results were presented as a poster in: 11º Encontro Nacional de Química-Física, Faculdade de Ciências da Universidade do Porto, Portugal, May 9-10th 2013; 4th MIT Portugal Program Conference: New Frontiers for a Sustainable Prosperity, Coimbra, Portugal, June 27th 2014; Gordon Research Seminar and Conference on Green Chemistry, The Chinese University of Hong Kong, Hong Kong, China, July 26th-August 1st 2014; XX Encontro Luso-Galego de Química – XXLGQ, Complexo FFUP/ICBAS, Oporto, Portugal, November 26-28th 2014.

Personal contribution:

Patrícia I. Morgado contributed to the design of the study, performed most of the experimental work (with exception of mathematical modeling performed by Pedro F. Lisboa, and biocompatibility assays and antimicrobial testing performed by Maximiano P. Ribeiro and Sónia P. Miguel), interpreted data and wrote the manuscript.

2. Poly(vinyl alcohol)/chitosan asymmetrical membranes: highly controlled morphology toward the ideal wound dressing

2.1. Abstract

Asymmetrical membranes have been reported as ideal wound dressings for skin regeneration. The usual methods (dry/wet-phase inversion) to produce those specific membranes are time consuming, and in the majority of the cases demand the use of harmful organic solvents. In this study, $scCO_2$-assisted phase inversion method was applied to prepare PVA/CS asymmetrical membranes. This technique can tailor the final structure of the dressing by tuning the processing conditions allowing the development of high porous materials with optimized morphology, mechanical properties and hydrophilicity. The PVA/CS dressings produced are recovered in a dry state but can form a hydrogel due to their high water uptake ability maintaining the moisturized environment needed for wound healing. The dressing presents a top thin layer of about 15 μm that allows gaseous exchange while barriers the penetration of microorganisms, and a sponge bottom layer able to remove excess exudates. A mathematical model based on Fick's second law of diffusion was developed to describe the pharmacokinetic release profile of a small drug (ibuprofen) from the swollen membrane in physiological conditions that mimic the wound. *In vitro* studies revealed that the dressings had excellent biocompatibility and biodegradation properties adequate for skin wound healing.

Keywords: $scCO_2$, phase inversion, asymmetrical membranes, mathematical modeling, wound dressings.

2.2. Introduction

Human skin is the first line of defense against all sorts of environmental assaults. This complex organ plays highly specialized functions, such as protection of the organism against toxins and microorganisms, body temperature regulation, support to blood vessels and nerves, and prevents the dehydration of all non-aquatic animals [4, 5, 9, 88]. Furthermore, it is also involved in the immune surveillance and sensory detection processes [5, 6]. If the skin is damaged, a complex and painful wound healing process, comprising three main steps (wound edges contraction, epithelialized scar formation and tissue regeneration) begins [164].

To minimize the damage and the risk of infection during the healing process and to promote the restoration of the integrity of the damaged tissue the wound should be coated [165]. Currently there are several commercially available wound dressings made from a wide range of synthetic and natural materials including PU (*e.g.* PolyMem®) or polysaccharides such as starch (*e.g.* Iodosorb®), respectively. This abundance of wound dressings is related not only with the management of different types of wounds but also with the complexity of wound healing process

[203, 204]. Furthermore, the ideal dressing is the one that must protect the wound from physical damage and micro-organisms, be comfortable, compliant and durable, be non-toxic, non-adherent, and non-irritant, allow gaseous exchange, allow high humidity at the wound, be compatible with topical therapeutic agents and be able to allow maximum activity for the wound to heal without retarding or inhibiting any stage of the process [86].

Asymmetrical polymeric membranes have demonstrated to be promising wound dressings for the treatment of skin wounds since they present the most required characteristics of the ideal ones [88]. This type of membranes contain a dense surface skin layer and interconnected micropores designed to protect the wound and dehydration of the wound surface but allows the drainage of wound exudate. On the other hand, the sponge-like sublayer is designed to achieve high adsorption capacity for fluids, drainage of the wound by capillary and enhancement of tissue regeneration [49]. During these years several asymmetrical membranes have been developed to be used as wound dressings. CS [90] and PU [46, 48] have been the most used polymers to produce those types of membranes. Until now, the dry/wet-phase inversion method was the most used to produce asymmetrical membranes [142]. However this technique presents some disadvantages: it requires high levels of organic solvents and sometimes high temperatures. The presence of residual organic solvents is being rigorously controlled by international safety regulations, so it is required to warrant the complete removal and absence of these substances. Furthermore, a long drying process (12-48h) has to be performed, which can lead to the collapse of the porous structure as well discussed on Chapter 1 [205].

In this work, $scCO_2$-assisted phase inversion method is proposed for the first time as an alternative technique to produce asymmetrical membranes for skin wound healing. Besides being a green technology, it can form solvent-free membranes with short processing times and no collapse of the structure. Furthermore, $scCO_2$-assisted phase inversion allows the production of dry, clean and ready-to-use membranes with highly controlled morphology (by changing the pressure, temperature and/or depressurization rate) and reduces the solvent recovery costs. The process does not require additional post-treatments and any potential organic solvent used can easily be removed [99, 140, 141].

PVA and CS were the polymers chosen to produce the wound dressings for different reasons: PVA is a water-soluble synthetic material very attractive for producing membranes due to its good chemical and thermal stability, biocompatibility, biodegradability and adequate resistance, on the other hand CS is a natural polysaccharide readily available from the deacetylation of chitin and due to its demonstrated hemostat and antimicrobial properties has been commonly indicated in the treatment of skin wounds. The use of these two polymers has also been reported as suitable drug delivery systems [147, 165, 206-208].

In this work, a wound dressing system prepared from PVA/CS asymmetrical membrane was developed using a non-residue technology. A detailed characterization in terms of morphology, water uptake ability, water vapor permeability, mechanical properties and biocompatibility was performed. Additionally, oligo(2-methyl-2-oxazoline) quaternized with *N,N*-

dimethyldodecylamine (OMetOx-DDA) was used as a contact-active antimicrobial agent, synthesized and grafted on PVA/CS asymmetrical membranes' surface combining plasma surface activation and SCF technology. This antimicrobial agent was thoroughly studied and synthesized for the first time by Correia *et al.* (2015) for water purification [209]. OMetOx-DDA efficiently killed *S. aureus* cells upon direct contact, preventing biofilm formation. Moreover the *in vitro* pharmacokinetic release profile of IBP was studied in order to evaluate the mass transfer properties of the loaded matrix in conditions that mimic the wound physiological media [175]. To better understand mass transfer mechanism of the drug release from the membrane, the experimental data was modeled using a realistic mathematical model based on the Fick's second law of diffusion which has been broadly and successfully applied in the literature [210] for controlled drug release for thin slabs.

2.3. Experimental

2.3.1. Materials

CS (75-85% deacetylated, medium molecular weight: 190-310 kDa), PVA (Mw = 89-98 kDa, 99% hydrolyzed), (*S*)-(+)-Ibuprofen (Mw = 206.28, 99%), absolute ethanol, glacial acetic acid (purity ≥99%), phosphate buffered saline (PBS), tris(hydroxymethyl)aminomethane (Tris), sodium acetate, ammonium sulfate ($(NH_4)_2SO_4$), potassium acetate (CH_3COOK), monomer 2-methyl-2-oxazoline (MetOx, purity>98%), 2-isopropenyl-2-oxazoline (IsoOx, purity>99%), initiator boron trifluoride diethyl etherate ($BF_3.OEt_2$), LB Broth, kanamycin, Dulbecco's modified Eagle's medium (DMEM-F12) and resazurin based *in vitro* toxicology assay kit were purchased from Sigma-Aldrich (Sintra, Portugal). Agarose (low melting point-ultrapure grade) was acquired from Nzytech (Lisboa, Portugal). *N,N*-dimethyldodecylamine was purchased from Fluka (Sintra, Portugal). Human fibroblast cells (Normal human dermal fibroblasts adult (NHDF), cryopreserved cells) were purchased from PromoCell (Labclinics, S.A.; Barcelona, Spain). Fetal bovine serum (FBS) was purchased from Biochrom AG (Berlin, Germany). Carbon dioxide was obtained from Air Liquide with 99.998% purity. All materials and solvents were used as received without any further purification.

2.3.2. Membrane preparation

Membranes were produced following a procedure already described in detail elsewhere [136, 144]. Different casting solutions of PVA and CS were prepared: 17.25 wt% (87% PVA / 13% CS and 77% PVA / 23% CS), 13 wt% (67% PVA / 33% CS) and 9 wt% (50% PVA / 50% CS). Both polymers were dissolved in acidified water (1% acetic acid) and loaded into a stainless steel cap (with a diameter of 68mm and 1.5mm height) and placed inside the high pressure vessel. The vessel was closed and immersed in a visual thermostated water bath, heated by means of a

controller (Hart Scientific, Model 2200) that maintains the temperature within ±0.01 ºC. A non-solvent flow was added using two Gilson piston pumps (models 305 and 306) until the desired pressure was reached and the operation was performed in a continuous mode with a flow rate of 5 mL/min. The non-solvent was a binary mixture of 90% CO_2 and 10% ethanol (co-solvent) with a constant composition. After reaching the normal operational pressure (20 MPa), the supercritical solution passes through a back pressure regulator (Jasco 880-81) which separates the CO_2 from the acidified water used in the casting solution. The pressure inside the system was monitored with a pressure transducer (Setra Systems Inc., Model 204) with a precision of ±100 Pa.

All the experiments were performed at 20 MPa and 45 ºC with a non-solvent (CO_2 + ethanol) flow of 5 mL/min during 120 min. After this time period, a pure CO_2 flow of 10 mL/min was passed through the high pressure cell to wash the structures and remove the excess of ethanol. At the end, the system was depressurized at three different rates: fast (4min), medium (10 min) and slow (30 min) and thin homogeneous membranes were obtained.

2.3.3. Membrane characterization

The morphological properties of the membranes were characterized using SEM in a Hitachi S-2400, with an accelerating voltage set of 15 kV. The membrane samples were frozen and fractured in liquid nitrogen for cross-section analysis. All samples were coated with gold before analysis. The tensile properties of the membranes were tested with a tensile testing machine (MINIMAT firm-ware v.3.1) at room temperature. The samples (n = 5) were cut into strips with 15mm × 5mm. The length between the clamps was set as 5 mm and the speed of testing set to 0.1 mm/min A full scale load of 20 N and maximum extension of 20 mm were used. Measurements were performed with dried membranes, membranes soaked in PBS solution overnight before testing, as well as membranes soaked in three different solutions at different pHs during 21 days changing the pH as each seven days (1-7 days: Tris 0.1 M, pH 8; 7-14 days: PBS 0.1 M, pH 7.4; 14-21 days: sodium acetate 0.1 M, pH 5). Load extension graphs were obtained during testing and converted to stress and strain curves applying the following equations:

$$\text{Stress} = \sigma = \frac{F}{A} \qquad \textbf{Equation 2.1}$$

$$\text{Strain} = \varepsilon = \frac{\Delta l}{L} \qquad \textbf{Equation 2.2}$$

where F is the applied force; A the cross-sectional area; Δl the change in length; and L is the length between clamps.

The porosity of the membranes was determined by mercury intrusion porosimetry (micromeritics, autopore IV).

2.3.4. Water vapor permeability

Water vapor permeability (WVP) studies were done following a procedure already described in detail elsewhere [211] with slight modifications. The WVP was measured gravimetrically at 30 ºC. The membranes were placed in a glass dish with a diameter of 5 cm and placed in a desiccator containing a saturated salt solution and equipped with a fan to promote air circulation. Room temperature and RH inside the desiccator were monitored over time using a thermohygrometer (Vaisala, Finland). Two different driving forces were imposed. In the first one, a saturated $(NH_4)_2SO_4$ solution was used inside the glass dish (RH = 81%), placed in a desiccator containing a saturated CH_3COOK solution (RH = 22%). The WVP was measured using membranes conditioned previously at a relative humidity of 81%. The second driving force tested was imposed using a saturated $NaNO_2$ (RH = 65%). The water vapor flux was determined by weighing the glass dish in regular time intervals for 8 h. Three independent runs were performed. Mann-Whitney U Test and Factorial ANOVA were used to perform the statistical analysis between the values obtained. Computations were performed using a MYSTAT 12 statistical package (Systat Software, a subsidiary of Cranes Software International Ltd.) [165, 171].

The WVP was calculated using the following equation:

$$WVP = \frac{N_w \times \delta}{\Delta P_{w,eff}} \qquad \textbf{Equation 2.3}$$

in which, N_w is the water vapor mass flux, δ is the film thickness and $\Delta P_{w,\,eff}$ is the effective driving force, expressed as the water vapor pressure difference between both sides of the membrane. Other equations used are described in detail by Alves *et al* (2011).

The WVTR was calculated using the following equation:

$$WVTR = \text{mass} / (\text{area})(\text{time}) = (P/L)(P_w) \triangle(RH), \qquad \textbf{Equation 2.4}$$

were, P is the water vapor permeability, L is the membrane thickness, (P/L) is the water vapor transfer rate (or permeance), P_w is the saturated water vapor pressure at the experimental temperature and $\triangle(RH)$ is the difference of relative humidity between inside atmosphere and outside atmosphere of the membrane glass dishes [49, 175].

2.3.5. Water uptake and contact angle analysis

The swelling tests were performed in order to determine the membrane's water uptake ability. Dry membranes samples were weighted and immersed in 15 mL Tris solution at pH 8 and 35 ºC. Periodically, the samples were removed from the swelling medium, wiped to remove excessive water of the surface and weighted. After 24 h, when the mass of membranes reached a plateau value, the samples were transferred to a pH 5 medium (sodium acetate solution) at 35 ºC. After another 24 h, a new plateau was reached, and the samples were transferred to the pH 8 medium. Thus dynamic swelling and shrinking was studied during 1 week. Equilibrium hydration or swelling degree *W* (%) of the samples was determined as defined by Equation 2.5:

$$W\,(\%) = \left(\frac{W_w - W_d}{W_d}\right) \times 100 \qquad \textbf{Equation 2.5}$$

where W_d is the weight of the dried sample and W_w is the weight after immersion.

As a complementary study, membranes hydrophilicity was evaluated through the measurement of the contact angle of glycerol droplets in a KSV Goniometer Model CAM 100.

2.3.6. Membrane degradation studies

The biodegradability of PVA/CS membranes were studied *in vitro* over 21 days by changing the pH at each seven days: (1-7 days: Tris 0.1 M, pH 8; 7-14 days: PBS 0.1 M, pH 7.4; 14-21 days: Sodium acetate 0.1 M, pH 5). After the specific time intervals, the samples were taken out from the solutions, washed with distilled water, freeze-dried and placed in the solution at different pH. The weight was measured before and after each freeze-drying step.

2.3.7. Contact-active antimicrobial agent

2.3.7.1. Membranes surface activation with plasma technology

Membrane surface activation was performed following a procedure already described in detail elsewhere [209] with slight modifications. PVA/CS asymmetrical membranes were activated by argon plasma treatment, in a radio frequency plasma reactor (Plasma system FEMTO, version 5), for further grafting with OMetOx-DDA in $scCO_2$. Membrane samples were introduced in the plasma chamber which was purged with a continuous flow of argon to reduce trace amounts of air and moisture. Samples were placed on top of a porous network in order to assure a homogeneous activation of all superficial area, top and bottom. During the treatment, the argon flow was adjusted in order to keep a constant pressure of 0.1 MPa inside the chamber. A power

of 60 W was applied during 30 min. Afterwards, the plasma chamber was ventilated and the samples were immediately introduced in 33 mL high-pressure cell to be coated.

2.3.7.2. Membranes grafting with ammonium quaternized oligo(2-methyl-2-oxazoline)

Ammonium quaternized oligo(2-methyl-2-oxazoline) was grafted onto membranes surface according to the method described by Correia *et al.* (2015). Briefly, the previous weighted membranes and the monomer IsoOx were loaded into a 33 mL high-pressure cell, sealed and immersed in a thermostated water bath at 65 ºC and then CO_2 was pumped into the system until the desired pressure, 28 MPa, was attained. The high-pressure cell was divided in two compartments by using a macroporous structure in order to avoid any contact between membrane samples (in the top compartment) and monomer (placed in the bottom compartment). $scCO_2$ was used as a solvent to carry the monomer to the activated polymeric substrates. The reaction was allowed to proceed for 24 h. After that period of time, membrane samples were thoroughly washed with fresh CO_2 to remove unreacted monomer.
After the initial grafting step, the monomer MetOx was added to the high pressure reactor together with the initiator $BF_3.OEt_2$. The reaction took place at 23 MPa, 65 ºC during 20 h. In the end, a tertiary amine was added to the reactor and the reaction occurred at 25 MPa, 65 ºC during 20 h. To finalize all the procedure, fresh CO_2 passed through the high-pressure cell in order to wash the membrane samples and to remove all unreacted components. In all the reactions, it was assumed that the yield was 100% and monomer was added in excess to assure that there was not any limiting step.

2.3.7.3. Determination of bacteria viability

S. aureus ATCC 25923 bacterial strain was used to evaluate the antimicrobial properties of OMetOx-DDA grafted onto PVA/CS membranes. *S. aureus* ($1x10^6$ colony-forming units (CFU)/mL) were inoculated in culture medium (LB Broth) in presence of PVA/CS-OMetOx-DDA membrane samples (n=5), in 96-well plate, and incubated for 24 h, at 37 ºC. A negative (without membranes) and a positive control (containing kanamycin antibiotic (30 mg/mL)) were also prepared. For monitoring bacterial growth, 10 µL of resazurin 0.1% (w/v) was added to each well and, after 24 h, the fluorescence was measured using a fluorescence plate reader with filler set Ex545/Em590 [167].

2.3.7.4. Evaluation of biofilm deposition at PVA/CS membranes surface

S. aureus proliferation at membranes surface was also evaluated by SEM analysis [167, 212]. PVA/CS and PVA/CS-OMetOx-DDA membrane samples with approximately 1 cm^2 of superficial area were placed on the surface of a plate of LB agar, in contact with *S. aureus* ($1x10^8$

CFU/mL), without any other antimicrobial agent. Then, the Petri plate was incubated for 24 h, at 37 ºC. After, the morphologies of PVA/CS membranes with/without the bacteria strains were analyzed by acquiring SEM images.

2.3.8. Cytotoxicity assays

2.3.8.1. Proliferation of human fibroblast cells in the presence of membranes

To evaluate NHDF growth in the presence of PVA/CS membranes, cells were initially seeded in contact with the dressings in 96-well plates, at a density of 4 x 10^4 cells/cm^2 per well and using as culture medium DMEM-F12 supplemented with FBS, for 3 days, at 37 °C under a 5% CO_2 humidified atmosphere. Samples were previously sterilized using UV irradiation during 30 min. The cell growth was monitored using an Olympus CX41 inverted light microscope (Tokyo, Japan) equipped with an Olympus SP-500 UZ digital camera [164, 165].

2.3.8.2. Characterization of the cytotoxic profile of the membranes

NHDF cell viability in the presence of sterilized dressings (4 mg/mL) was evaluated by resazurin assay (n=5). Firstly, 4 x 10^4 cells per well were seeded in contact with the materials and then, after 1 and 3 days of incubation at 37º C under a 5% CO_2 humidified atmosphere, the culture medium was removed and replaced by a mixture of 100 µL of fresh culture medium and 10 µL of resazurin 0.1% (w/v) in 5% CO_2 humidified incubator, for 24h, at 37ºC. Fluorescence of metabolized resazurin was measured using a Gemini EM spectrophotometer at an excitation/emission wavelength of λ=545/590nm, respectively [213]. Wells containing cells in the culture medium without materials were used as negative control (K^-). Ethanol (96%) was added to wells that were used as a positive control (K^+) [165, 214].

2.3.9. Drug impregnation in $scCO_2$ environment

PVA/CS membranes were impregnated with IBP using $scCO_2$ in batch mode following reported conditions [132, 215]. Drug impregnation experiments were performed at 40 ± 0.1 ºC and 25 MPa within 20 h, in a 33 mL high-pressure cell with a macroporous support that divides the cell in two compartments to avoid the physical contact between the drug and the samples. IBP was placed in the bottom compartment, under the porous support with a magnetic stirrer bar, and with a concentration that was enough to obtain medium saturation, at the pressure and temperature favorable for impregnation of the drug. The membrane samples were put on the top compartment of the cell. At the end of the impregnation period, the system was quickly depressurized.

2.3.10. *In vitro* drug release experiments and mathematical modeling

Drug release studies from PVA/CS membranes were performed using a permeation cell that maintains the top surface of the dressing exposed to environmental conditions and the bottom exposed to the release solution in order to simulate local *in vivo* release within a burn-wound environment [88]. To do so, the membranes were suspended in 65 mL of Tris 0.1 M solution (pH 8) and 1 mL aliquots were withdrawn periodically and the same volume of fresh medium was added to the suspension. The studies were performed at 35 ºC in a shaking water bath. The amount of IBP present in each sample was quantified by UV spectroscopy at its maximum absorbance (λ = 264 nm) by external standard calibration. The total mass of released drug in each moment of the experiment was calculated taking into account the aliquots taken and the dilution produced by addition of fresh buffer.

The IBP release was modeled using a mathematical model based on the Fick's second law of diffusion for thin slabs. The diffusion of a drug from a thin film with negligible edge effects (high surface area : thickness ratio) is given by Equation 2.6 [210].

$$\frac{\partial \mathrm{C_i}}{\partial \mathrm{t}}(\mathrm{t},\mathrm{z}) = \frac{\partial}{\partial \mathrm{z}}\left[\mathrm{D_i}(\mathrm{C_{1,}t},\mathrm{z})\frac{\partial \mathrm{C_i}}{\partial \mathrm{z}}(\mathrm{t},\mathrm{z})\right] \qquad \textbf{Equation 2.6}$$

where C_i and D_i are the concentration and the diffusion coefficient of the migrating species (i =1 for the penetrant solvent, i=2 for the drug) at a time *t* and spatial position *z*, respectively. At the beginning of the experiment, it is assumed that the membrane is solvent free and the drug is homogenously dispersed in the initial spatial coordinate x_0 with an initial concentration C_0. At the membrane-solution interface, *z* = *x*(t), the penetrant concentration is considered to be at equilibrium C_{eq}, and the drug concentration is equal to 0. For simplicity we only have modeled half thickness of the membrane, thus assuming an ideal and isotropic diffusion.

The initial and boundary conditions are given by:

Initial conditions:

$t = 0 \qquad C_1(\mathrm{t},\mathrm{z}) = 0, C_2(\mathrm{t},\mathrm{z}) = C_0 \qquad 0 < z < x_0$ **Equation 2.7**

Boundary conditions:

$t > 0 \qquad C_1(\mathrm{t},\mathrm{z}) = C_{\mathrm{eq}},\ C_2(t,z) = 0 \qquad z = x(t)$ **Equation 2.8**

$t > 0 \qquad \frac{\partial C_\mathrm{i}}{\partial z}(t,z) = 0 \qquad z = 0$ **Equation 2.9**

The solution of the equation Equation 2.6 is not straightforward due to the movement of the membrane thickness caused by the swelling process. It is important to take into account the membrane volume changing since it results in the increasing of the drug diffusing path and the sudden decreasing of the local drug concentration in the membrane. Hence the solution of the Equations 2.6-2.9 can be solved by using the "fronting-fixing method" where the position of the interface is fixed by applying the transformation of $\xi = z/x(t)$ [216]. With these new space variables the diffusion domain $z \in [0, x(t)]$ is transformed into a fixed domain, $\xi \in [0,1]$. Using the chain rule for the partial differential equations for the new function $C_i(t, z) = C_i(\tau, \xi), \tau \equiv t$ we have:

$$\frac{\partial C_i}{\partial z}(t, z) = \frac{1}{x(t)} \frac{\partial C_i}{\partial z}(t, \xi) \qquad \textbf{Equation 2.10}$$

$$\frac{\partial^2 C_i}{\partial z^2}(t, z) = \frac{1}{x(t)^2} \frac{\partial^2 C_i}{\partial z^2}(t, \xi) \qquad \textbf{Equation 2.11}$$

$$\frac{\partial C_i}{\partial t}(t, z) = -\frac{\xi}{x(t)^2} \frac{dx}{dt}(t) \frac{\partial C_i}{\partial \xi}(\tau, \xi) + \frac{\partial C_i}{\partial t}(t, \xi) \qquad \textbf{Equation 2.12}$$

Introducing the above equations into equation diffusion (Equation 2.6), we now have the following convection-diffusion equation:

$$\frac{\partial C_i}{\partial t}(t, \xi) = \frac{1}{x(t)^2} \frac{\partial}{\partial \xi} \left[D_i(C_1, t, \xi) \frac{\partial C_i}{\partial \xi}(t, \xi) \right] + \frac{\xi}{x(t)} \frac{\partial C_i}{\partial \xi}(t, \xi) \frac{dx}{dt}(t) \qquad \textbf{Equation 2.13}$$

The dependence of the diffusivity with the penetrant concentration was introduced by the following relationship [217]:

$$D_i(t, \xi) = D_{i,eq} e^{-\beta_i \left[1 - \frac{C_1(t,\xi)}{C_{eq}}\right]} \qquad \textbf{Equation 2.14}$$

In Equation 2.14, β_i is a dimensionless constant that describes the diffusivity dependency of the penetrant solvent and drug upon the degree of membrane swelling and $D_{i,eq}$ are the diffusion coefficients of solvent and drug in the fully swollen membrane.
The variation of the membrane thickness $x(t)$ was monitored experimentally during the swelling studies using a micrometer and it was correlated with the following equation.

$$x(t) = x_0(1 + \gamma(1 - e^{-\omega t}) \qquad \textbf{Equation 2.15}$$

The values of β_1 and $D_{1,eq}$ were determined by adjusting Equations 2.13-2.15 to the experimental data obtained in the solvent uptake swelling studies while the values β_2 and $D_{2,eq}$ were obtained later by fitting the same set of equations to the drug release experimental data.

The partial differential equations were converted on a set of algebraic differential equations (DAE´s) using Finite Differences Method implemented in gPROMS (general PROcess Modeling System). A fourth order central finite difference method is used to discretize the spatial domain and the set of DAE's are integrated over time using the implicit DASOLV [218] solver which is based in the backward-difference formula. The process of fitting parameters was also performed using gPROMS software using the built-in formulation centered in the maximum likelihood parameter estimation [219].

2.4. Results and Discussion

2.4.1. $scCO_2$ phase inversion technique in the development of asymmetric membranes

As described previously, the main goal of this study was to prepare asymmetrical PVA/CS membranes which can fit the basic requirements of an ideal wound dressing using $scCO_2$ technologies, despite the old conventional methods. Indeed, a membrane with a dense skin top layer that can protect the wound from physical damage and infection, can act as a drug release reservoir and control the gaseous exchange in addition to presenting a sponge-like inner layer useful to absorb the wound exudate and promote space for tissue regeneration is the suitable structure to be used in skin regeneration (Figure 2.1).

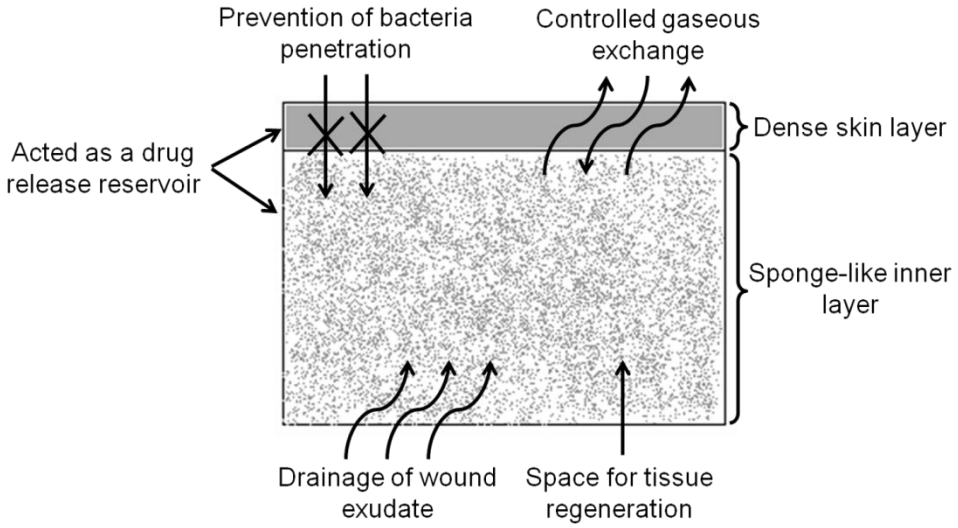

Figure 2.1. Ideal characteristics of an asymmetrical membrane to be used as wound dressing.

Meanwhile, the dry/wet-phase separation process is time-consuming requiring the evaporation of the volatile solvent for dry phase separation and the solvent-non solvent exchange for wet-phase separation. The evaporation of the volatile solvent allows the rate for solvent loss and polymer coagulation that forms the asymmetrical structure which turns this process very thorough [88]. In this study we showed that it is possible to produce PVA/CS asymmetrical

membranes using a more sustainable technology as $scCO_2$-phase inversion technique. $ScCO_2$ and ethanol are used as anti-solvents for the polymers used and for the acidified water, respectively. For membranes production several parameters must be controlled to obtain the desired structural characteristics, in particular the polymers used, the concentration of the casting solution, the composition of the co-solvent and the pressure, temperature and depressurization rate [99, 136]. In this work, most of the above parameters were fixed except the depressurization rate (4, 10 and 30 min) and the composition of initial casting solution that varied from 17.25 wt% (87% PVA / 13% CS and 77% PVA / 23% CS) to 13 wt% (67% PVA / 33% CS) and 9 wt% (50% PVA / 50% CS) .

It was observed by SEM images that from the different compositions studied a well-defined asymmetry is obtained for a polymer solution composed by 17.25 wt% (87% PVA / 13% CS) with a depressurization rate of 10 min (Figure 2.2). The morphology of the others solutions studied is shown on images presented in Supplementary Information (Figures S2.1 – S2.3).

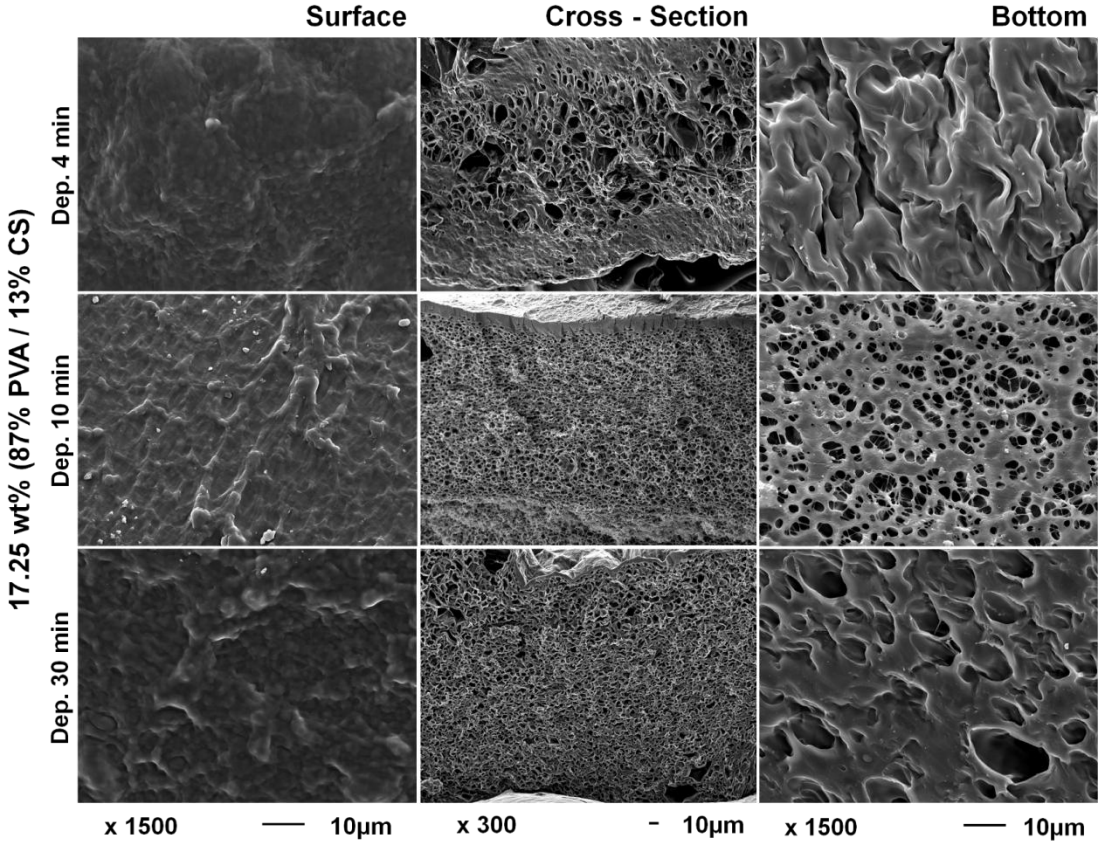

Figure 2.2. Scanning electron micrographs of 17.25 wt% (87% PVA / 13% CS) membranes surface, cross-section and bottom obtained with depressurization rates of 4, 10 and 30 min.

Observing Figure 2.2, it is possible to see that with a fast depressurization rate (4 min) different pore sizes can be obtained and a dense skin top layer is not visible as it can be seen in the membranes produced with depressurizations of 10 and 30 min. In these membranes a

homogeneous inner layer and a porous bottom layer can be obtained. Nevertheless, the dense skin layer is larger using a depressurization of 10 min than 30 min, being the 17.25 wt% (87% PVA / 13% CS) with a depressurization of 10 min the elected membranes to be used as wound dressings. From this conclusion, all the subsequent studies presented are focused on the different properties between the membranes composed by 17.25 wt% (87% PVA / 13% CS) with depressurizations of 4 and 10 min.

2.4.2. Water uptake and contact angle analysis

The water uptake ability of the membranes was assessed at 35 ºC and at two different pHs, 5 and 8, during 4 days in order to visualize if there is any influence of the pH on membranes' swelling degree. These two pHs were chosen taking into account the protocol followed on a clinical trial that studied the skin pH variations from the acute phase to re-epithelization in burn patients treated with new materials during 22 days (the normal time for a wound to heal) [220]. The study revealed that, independently of the therapy administered, the skin pH was found to be around 8, 30 minutes post-burn, continuing to rise until day 4 reaching a peak of 10. Afterwards, it progressively decreases as the burn zone gradually re-epithelializes returning to the normal skin pH around 5 by day 22. The membranes herein developed present shape-memory behavior with highest swelling degree at pH 5 due to the protonation of CS amino groups which occurs predominantly at pH lower than pKa (pKa (CS) = 6.5 [221]) of chitosan (Figure 2.3A). This swelling behavior is an advantage when considering the pH profile of the skin: i) by wetting the membrane at pH 5 (when the swelling is higher) some soluble bioactive agents can be entrapped; ii) then, when the membrane is put onto the wound (which has a basic pH in the first stages of the healing) the bioactive agents can be delivered over time due to the shrinking of the material simultaneously expelling water maintaining a suitable moisturized environment; afterwards, the pH of the skin becomes acidic and the swelling degree of the membranes will allow the removal of the exudates of the wound, one of the required characteristics of the ideal dressings.

Regarding the membranes' morphology, the PVA/CS membranes depressurized in 10 min (PVA/CS_10min) present higher swelling degree than the ones depressurized in 4 min (PVA/CS_4min). This can be explained by the internal structure of those membranes. The evaluation of pores size and porosity by mercury porosimetry revealed that both membranes present similar porosities, around 40%, however different average pore diameter as shown in SEM images (Figure 2.1). The PVA/CS_10min have lower pore diameter (0.0995 μm) than the membranes depressurized in 4 min (0.2516 μm). Nevertheless, the PVA/CS_10min, present pores homogeneously distributed and also a porous bottom layer while the PVA/CS_4min, although having higher pore diameter, they present similar porosity and large dense sections which reduces their ability to absorb water.

The contact angle analysis was assessed using glycerol in order to mimic the viscosity of the wound exudate [160]. In Figure 2.3B it is possible to confirm the high hydrophilicity of the membranes since the contact angles were smaller than 90º, reaching around 20º, 2 min after weeping with the glycerol droplet. Furthermore, the asymmetry of the PVA/CS_10min membranes is now evidenced due to the slightly difference on the contact angles of both membranes. The dense skin layer of PVA/CS_10min membranes hampers the crossing-over of the glycerol drop justifying the higher contact angle. This high hydrophilicity allows the formation of hydrogel-like membranes when in contact with the wound exudate allowing a high humidity at the wound, other requirement of an ideal wound dressing.

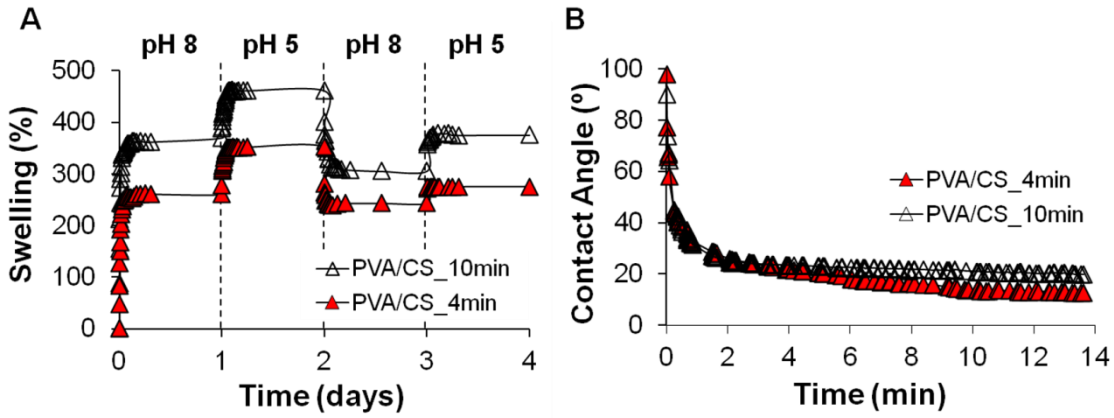

Figure 2.3. (**A**) Swelling behavior of PVA/CS_4min (▲) and PVA/CS_10min (Δ) membranes at different pHs; (**B**) Static contact angle assessment of PVA/CS_4min (▲) and PVA/CS_10min (Δ) membranes.

2.4.3. Water vapor permeability

As described previously, one of the most important requirements of an ideal wound dressing is to perform a moist environment at the wound which must therefore be determined by the water uptake ability of the dressing and the WVTR through the dressing [171]. It is described that an excessive WVTR may lead to wound dehydration and adherence of the dressing to the wound bed caused by rapid water loss, whereas a low WVTR might lead to maceration of healthy surrounding tissue due to exudate retention and buildup of a back pressure and pain to the patient [46, 171]. In this study the measurement of WVTR for PVA/CS asymmetrical membranes was performed at two different gradient of RH, 81 – 22% and 65 – 22% at T = 30 ± 0.5 ºC in order to evaluate if there is any influence on membranes' vapor permeability mimicking what happens in a real situation. As shown in Table 2.1, by decreasing the RH, a 2-fold decrease of WVTR occurs for both membranes. Indeed, there is a significant difference between the two RH% studied on WVTR, WVP and permeance ($p < 0.05$) for all membranes studied. Nevertheless, comparing the data obtained for each membrane in the same range of RH%, there is not a significant difference between PVA/CS_4min and PVA/CS_10min

membranes. These results show that the difference on the membranes' morphology does not have any effect on the water vapor ability of the dressings. It is explained by V. Alves *et al*., that there is a higher water vapor sorption coefficient at high RH, as it was observed in the results obtained. Furthermore, water diffusivity depends on the interactions between water molecules and the polymeric matrix. The water adsorbed acts as a plasticizer and loosens the matrix facilitating water diffusion. Consequently, it could be expected an increase of water diffusivity as the amount of adsorbed water increased.

It was reported that the WVTRs for normal skin, first degree burns, and granulating wounds are (20 ± 1) x 10, (28 ± 3) x 10, and (51 ± 2) x 10^2 g/m^2 day, respectively. Furthermore it was recommended that wound dressings with WVTRs in the range of (20-25) x 10^2 g/m^2 day, half the loss of granulating wounds, would be sufficient to give adequate moisture and prevent exudate accumulation, as already explained on Chapter 1 [46]. However, in practice, the available commercial wound dressings, for example Comfeel®, Dermiflex®, Duoderm CGF®, Vigilon®, Tegaderm®, Bioclusive® and Op Site® **(**Table 2.1) do not necessarily conform to this range. It is important to notice that the WVTR depends on the structural properties (thickness, porosity) of the dressing as well as the chemical properties of the material from which it is made [171]. Indeed, in the case of asymmetrical membranes, the water vapor adsorption increases with increasing porosity of the sponge-like inner layer and the diffusion of water molecule slows down with increasing thickness of the dense skin layer resulting in lower WVTR [49]. Not least, required WVTR can be influenced by external conditions like the environmental RH and temperature which determine the water vapor partial pressure driving force across the dressing [175]. Despite the produced membranes present low WVTR their high water uptake ability contrabalance these results allowing the absortion of wound exudate while maitaining a moisturized enviroment due to the hydrogel-like properties of the membranes at wet state.

Table 2.1. Comparison of the water vapor transmission rate of different studied and commercially available wound dressings for burn treatment.

Wound Dressing	RH (%)	WVTR (g/m^2 day)	WVP (x10^{-13} g/m s Pa)	Permeance (x10^{-10} g/m^2 s Pa)
PVA/CS_4min	81 – 22	201 ± 17	5.3 ± 0.9	9.4 ± 0.8
Asymmetrical PVA/CS_10min	81 – 22	214 ± 16	5.6 ± 0.8	9.9 ± 0.8
PVA/CS_4min	65 – 22	105 ± 13	3.7 ± 0.3	6.6 ± 0.8
Asymmetrical PVA/CS_10min	65 – 22	115 ± 28	4.9 ± 0.9	7 ± 2
Asymmetrical chitosan membrane [49]	40	2792.8	41.5	93.6

Table 2.1. Comparison of the water vapor transmission rate of different studied and commercially available wound dressings for burn treatment (continuation).

Wound Dressing	RH (%)	WVTR (g/m^2 day)	WVP ($x10^{-13}$ g/m s Pa)	Permeance ($x10^{-10}$ g/m^2 s Pa)
Comfeel (Coloplast A/S) [172-174, 222]	22 - 49	285 ± 8	-	-
Dermiflex (Johnson-Johnson) [172-174, 222]	22 - 49	76 ± 5	-	-
Duoderm CGF (ConvaTec Ltd) [172-174, 222]	22 - 49	120 ± 19	-	-
Vigilon (+1 film) (Bard) [172-174, 222]	22 - 49	50 ± 19	-	-
Polyurethane membranes with Nano – TiO_2 [46]	22 - 49	1258 – 2689	-	-
Tegaderm (3M) [46, 172-174]	22 - 49	491 ± 44	-	-
Bioclusive (Johnson-Johnson) [46, 172-174]	22 - 49	394 ± 12	-	-
Op Site (Smith & Nephew) [46, 172-174]	22 - 49	792 ± 32	-	-

2.4.4. Membrane degradation studies and mechanical properties

The biodegradability of the membranes was studied over 21 days and using three different pHs (8, 7.4 and 5) that were changed at each seven days in order to mimic what happens in a real wound healing situation as explained before. As seen in Figure 2.4, there is a higher weight loss in the first seven days at pH 8 although it is not significant since the maximum weight loss is around 5% and 10% for PVA/CS_10min and PVA/CS_4min membranes, respectively. After those seven days, a stabilization on membranes' weight is observed. The slightly difference on membranes' weight loss that is more pronounced for PVA/CS_4min membranes can be due to the higher polymer weight loss per surface area of the dense sections present on the top and bottom of the membrane. Based on the results obtained so far (swelling studies, membranes' morphology, biodegradability, and texture of the membranes) it is possible to obtain comfortable, compliant and durable wound dressings that need to be replaced less often during the treatment, contributing to decrease the suffering of the patient.

The mechanical properties of a wound dressing are a crucial factor in its performance, whether it is to be used topically to protect cutaneous wounds or as internal wound support. Furthermore, the wound dressing should be flexible but strong enough to be handled during wound's coverage [171].

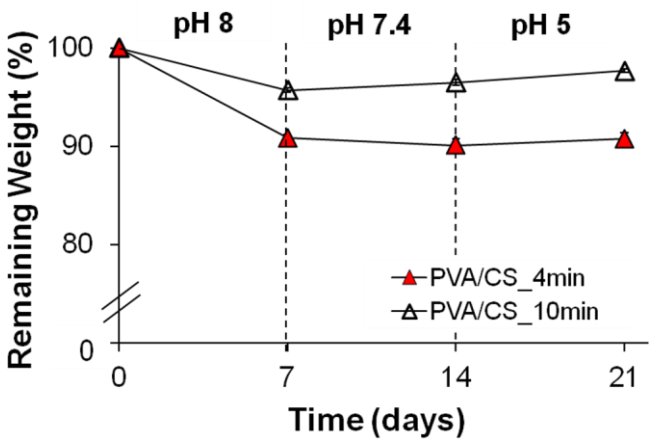

Figure 2.4. Structure stability of PVA/CS_4min (▲) and PVA/CS_10min (Δ) membranes at different pHs over 21 days.

In the literature, the Young's modulus of the skin varies between 0.42 and 0.85 MPa for torsion tests, 4.6 and 20 MPa for the extension tests and between 0.05 and 0.15 MPa for the suction tests. However, these values can vary with several factors like age, skin color, previous lesions and genetic factors [185]. The mechanical properties of PVA/CS membranes were assessed at dry and wet state (sample membranes were placed overnight in PBS at room temperature) in order to visualize the difference on membranes' elasticity on both states and during 21 days by changing the pH at each seven days following the same procedure previously described for biodegradability studies.

Observing Figure 2.5A, as it was expected, wet membranes showed higher elasticity (lower Youngs' modulus) than dry ones since the latest are more fragile and slightly brittle. It is important to notice that the elongation at break for both dry membranes is around 20% while for wet PVA/CS_4min is around 200% and for PVA/CS_10min membranes the elongation at break is higher than the maximum displacement of the equipment. This difference on wet membranes is due to their inner morphology. As discussed before and though PVA/CS_4min present higher pore size they present more dense sections and lower water uptake ability which turns those membranes weaker than PVA/CS_10min membranes. Despite the Young's modulus of dry membranes (around 7 MPa) being in the range of skin values for extension tests, the wet membranes revealed to be more promising due to their higher maximum tensile strength and elongation at break which would be advantageous on dressing changes allowing at the same time humidity control on the wound.

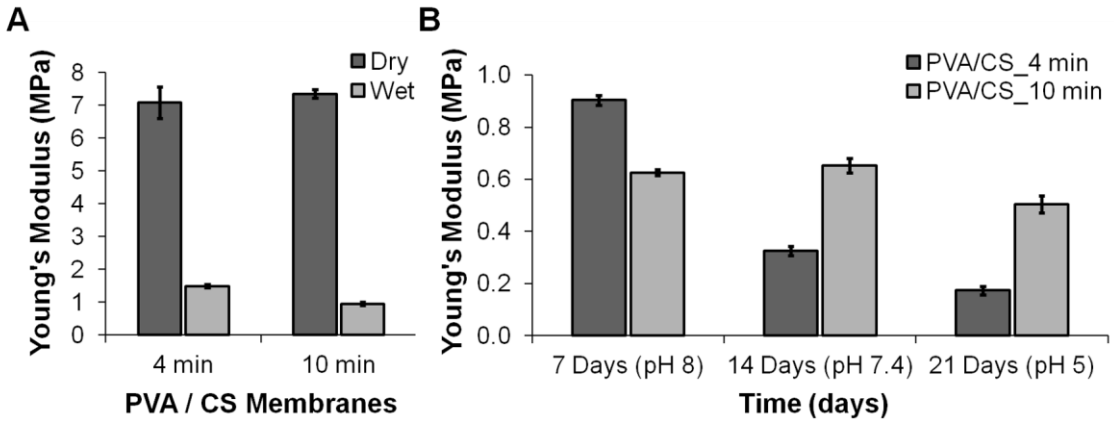

Figure 2.5. (**A**) Young's modulus (MPa) analysis of PVA/CS_4min and PVA/CS_10min membranes at dry and wet states; (**B**) Young's modulus (MPa) analysis of PVA/CS_4min and PVA/CS_10min membranes over 21 days at different pHs.

Table 2.2. Mechanical properties of various studied wound dressings.

Wound Dressing		Young's Modulus (MPa)	Tensile Strength (MPa)	Elongation at break (%)
PVA/CS_4min	Dry	7.1 ± 0.5	1.7 ± 0.4	20 ± 5
	Wet	1.5 ± 0.1	2 ± 1	211 ± 4
Asymmetrical PVA/CS_10min	Dry	7.4 ± 0.1	0.7 ± 1.1	21 ± 2
	Wet	0.96 ± 0.05	> max. disp. equip.*	> max. disp. equip.*
Electrospun poly-(*L*-lactide-*co*-ϵ-caprolactone) (50:50) mat [223]		8.4 ± 0.9	5 ± 2	(10 ± 2) x 10^2
Electrospun gelatin mat [223]		(49 ± 5) x 10	2 ± 1	17 ± 4
BSA1 (composite polyglyconate mesh, coated with PDLGA porous matrix) [171]		(13 ±3) x 10	24 ± 4	55 ± 5
PU/ASt composite membranes [48]		11 ± 1	5.1 ± 0.1	(4.8 ± 0.4) x 10^2
PU/PEG composite membranes [48]		11 ± 1	8 ± 1	(4.5 ± 0.3) x 10^2

* A full scale load of 20 N and maximum extension of 20 mm were used.

Comparing with other studied wound dressings (at dry state) the membranes herein developed are more elastic, which is the result not only of the materials used but the further processing techniques (Table 2.2). In Figure 2.5B it is possible to see the pH influence on membranes Young's modulus. Over the days the membranes turn more elastic due to their higher swelling ability at acidic pH as seen in Figure 2.3A. The Young's modulus of PVA/CS_4min decreases more at each seven days than on PVA/CS_10min membranes. As observed in the

biodegradation studies (Figure 2.4) PVA/CS_4min membranes lose more weight on the first seven days, reflecting on their mechanical properties. Once more, PVA/CS_10min membranes revealed to be the more promising wound dressings.

2.4.5. Antimicrobial activity performed by oligo(2-methyl-2-oxazoline) quaternized with *N,N*-dimethyldodecylamine

As well described on Chapter 1, the ability of wound dressings to protect the wound from infection is a property that has to be fully screened during wound dressings' development. Despite, an asymmetrical membrane presents a dense skin top layer that can avoid microorganism penetration (considering that the size of the pores available at the dense skin layer is smaller than bacteria), some bacteria may colonize upon the dressing and the surrounding healthy tissue, and then migrate into the wound, triggering infection after injury [224]. Some polymers, such as CS present intrinsic antimicrobial properties. It was shown by Miguel *et al.* (2014) that the antimicrobial activity of a CS/Agarose-hydrogel like dressing is dependent on CS concentration. Concentrations higher than 188 µg/mL exhibited antimicrobial activity, providing a defense barrier against *S. aureus* [46, 167]. However, many wound dressings developed do not contain any polymers with antimicrobial activity or in other cases the concentration of antimicrobial polymers used is insufficient to kill bacteria and avoid biofilm formation. To overcome such drawbacks, antimicrobial agents can be added to the membranes, being AgSD the most used to prevent wound infection, despite the potential silver toxicity [225-228].

In this study, a contact-active antimicrobial agent (OMetOx-DDA) was grafted upon PVA/CS membranes' surface by using eco-friendly procedures as plasma and supercritical fluids technologies. As stated before, Correia *et al.* grafted and synthesized for the first time oligo(2-oxazoline)s and studied the best monomer and amine quaternization to have a broad spectrum activity against different microorganisms comprising fungi and bacteria, while being biocompatible [192, 193, 209]. PVA/CS-OMetOx-DDA antimicrobial properties were firstly evaluated by disc diffusion technique and by determining the bacteria viability using *S. aureus*. The bacterial strain was deemed appropriate for performing this assay, since it is reported in the literature as the most common gram-positive pathogen found in skin infections, when biomaterials are used for wound treatments [229]. Figure 2.6A revealed the lack of a visible inhibition zone for both native and grafted PVA/CS membranes. Furthermore, the viability of bacterial cells after incubation with OMetOx-DDA-grafted membranes remained higher than 80% (Figure 2.6B), independently of the depressurization rate of the membranes, which could be indicative of lack antimicrobial property of the oligomer used.

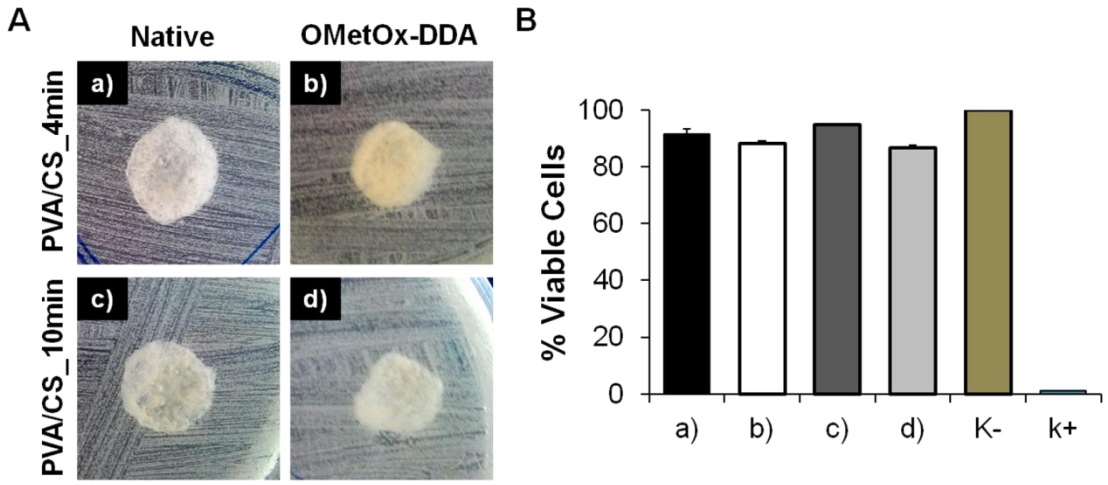

Figure 2.6. (**A**) Disk diffusion tecnhique with the aim to observe the zone of growth inhibition for *S. aureus* for native and gafted PVA/CS membranes (**B**) Determination of bacteria viability though rezasurin assay: a) Native PVA/CS_4min membranes, b) PVA/CS_4min membranes grafted with OMetOx-DDA, c) native PVA/CS_10min membranes and d) PVA/CS_10min membranes grafted with OMetOx-DDA.

However, as observed through SEM images (Figure 2.7), there is a visible inhibition of bacterial growth when OMetOx-DDA is present. These results are indicative of a contact-active killing mechanism, *i.e.* kill only upon contact with bacteria, as observed by Correia *et al.* (2015) [209]. Such fact can be considered an advantage since the antimicrobial agent remains grafted to the dressing, maintaining the materials' antimicrobial activity over time.

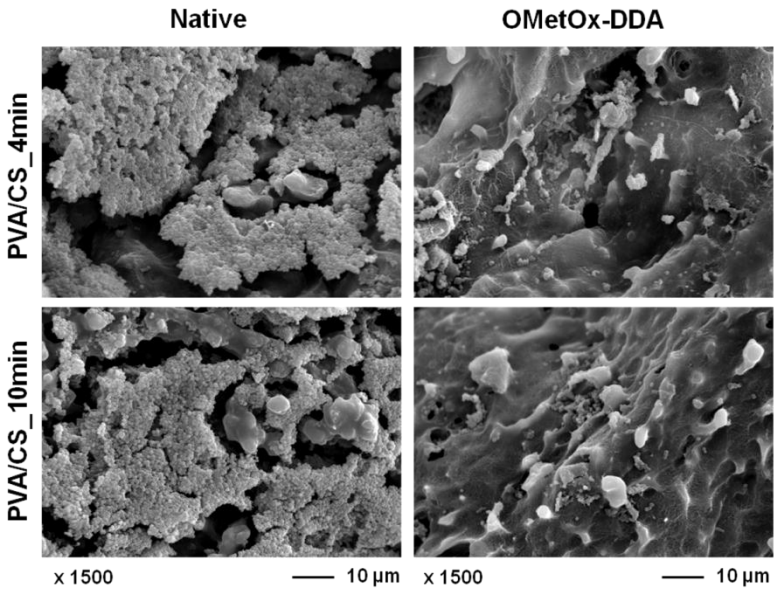

Figure 2.7. SEM images of *S. aureus* in contact with native and PVA/CS membranes grafted with OMetOx-DDA.

2.4.6. *In vitro* drug release studies and mathematical modeling

According to literature, controlled drug delivery of bioactive molecules continues to be an essential component of engineering strategies for tissue defect repair [230]. To do so, a non-steroidal anti-inflammatory drug (NSAID) was loaded into the membranes and the mass transfer mechanism of the drug was studied by combining the experimental data with mathematical modeling. As described previously, the mathematical model applied take first into account the water uptake ability of the membranes to further determine the diffusion coefficients of the drug from the two membranes studied.

As observed in Figure 2.8A, the solvent uptake into the membranes was similar with B_1 = 0 which means that it is not dependent upon the membranes' swelling degree. Indeed, the diffusion coefficients of the solvent to the membrane were similar, D_1 = 1.17x10^{-6} and D_1 = 1.55x10^{-6} cm^2/s for PVA/CS_4min and PVA/CS_10min membranes, respectively. However the drug diffusion constant in the swollen membrane was higher for PVA/CS_10min than for PVA/CS_4min membranes $D_{2,eq}$ = 2.76x10^{-6} and $D_{2,eq}$ = 1.60x10^{-6} cm^2/s, respectively (as observed by the faster drug release from PVA/CS_10min membranes showed on Figure 2.8B). Meanwhile, the PVA/CS_10min membrane exhibited an higher value of β (1.6 against to the 0.6 for PVA/CS_4min), meaning that although the greater diffusivities, the higher swelling degree observed for PVA/CS_10min membranes (Figure 2.3A) leads to a decrease of the drug concentration gradient between the membrane and the solution.

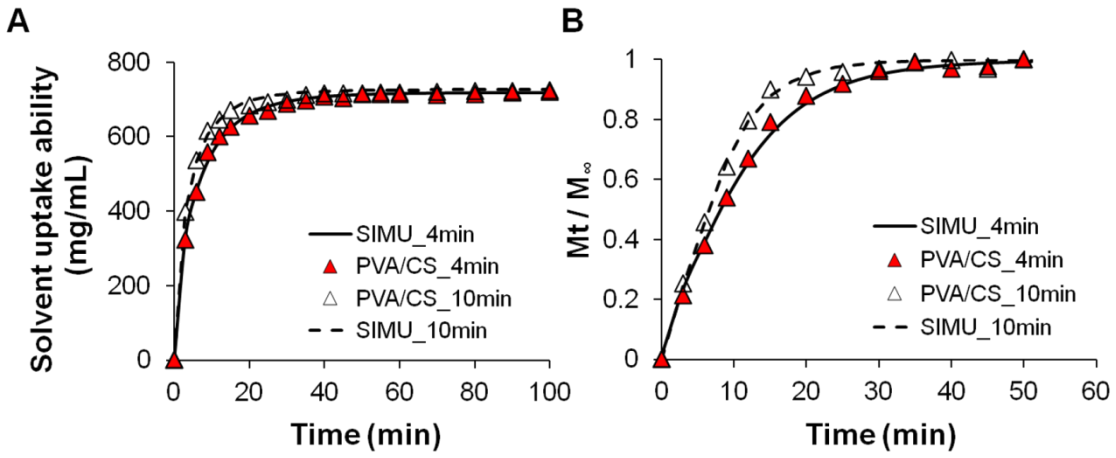

Figure 2.8. (**A**) Solvent uptake concentration (mg/mL) into the membranes: PVA/CS_4min (▲) and PVA/CS_10min (Δ) membranes, the respectively fittings are represented by ——SIMU_4min and - - - SIMU_10min; (**B**) *In vitro* drug release studies of IBP loaded into PVA/CS_4min (▲) and PVA/CS_10min (Δ) membranes at pH 8 and 35ºC, the respectively fittings are represented by —— SIMU_4min and - - - SIMU_10min.

The drug was released after 40 min which, by the wound healing process point of view, is really fast. The ideal drug release profile should occur over twelve hours which corresponds to the peak of the inflammatory phase [230]. The fast drug release observed could be due to the development of very thin slabs, the presence of high hydrophilic polymers and the use of a basic drug release solvent (pH 8) in which the dissolution of IBP is higher [231].

2.4.7. *In vitro* cytotoxicity studies

Finally, the applicability of membranes for the envisioned biomedical application should be assessed. To do so, the cytocompatibility of PVA/CS membranes was characterized through *in vitro* studies by seeded human fibroblast cells with wound dressings. Cell adhesion and proliferation was observed in wells where cells were in contact with PVA/CS_4 and 10min (Figure 2.9) and in the negative control (cells without materials), at the predetermined time points. The observation of cell adhesion and proliferation in the presence of the membranes showed that they are biocompatible. To further assess their biocompatibility, resazurin assay was performed. This assay showed that cells remained viable in contact with tested samples after 24 and 72 h of incubation (Figure 2.10). The relatively higher percentage of viable cells on both membranes after 72 h in comparison with the negative control can be justified by the growth of cells not only on the well but also on the membranes. These results clearly reveal that these membranes are biocompatible and can be used as wound dressings.

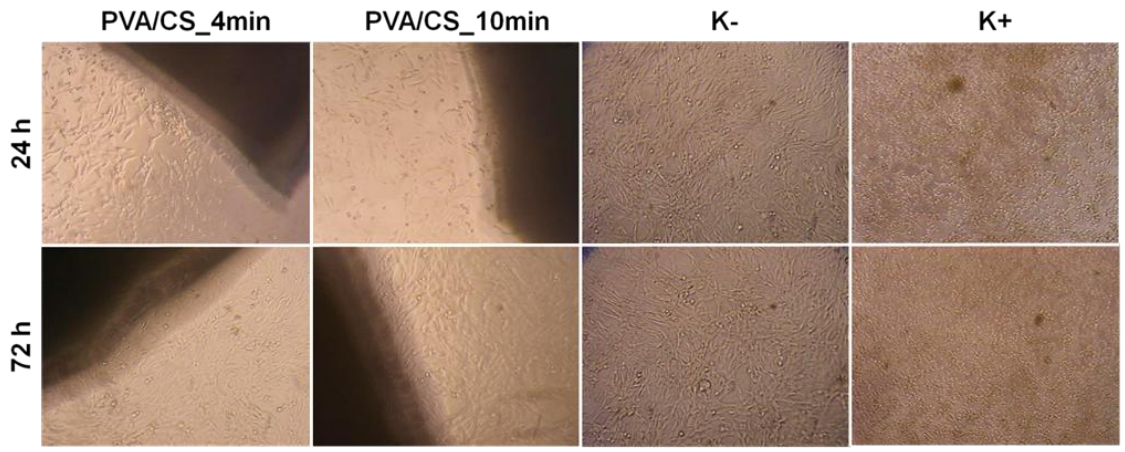

Figure 2.9. Microscopic photographs of human fibroblast cells after being seeded in the presence of the membranes during 24 and 72h. K^-: live cells; K^+: death cells. Original magnifications 100x.

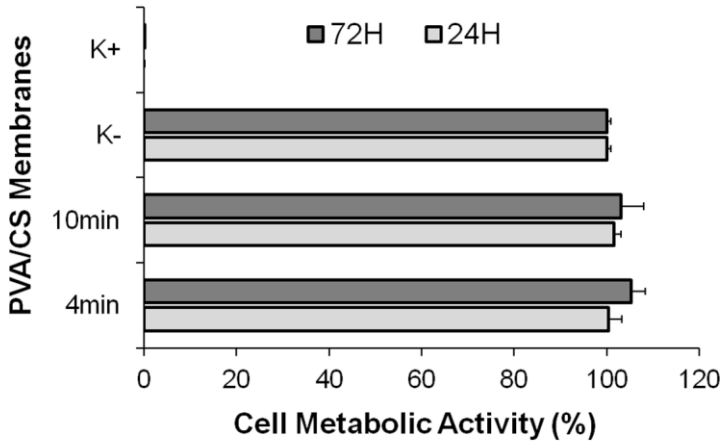

Figure 2.10. Cellular activities measured by the resazurin assay after 24 and 72h. PVA/CS_4min; PVA/CS_10min; K^- live cells; K^+ death cells.

2.5. Conclusions

This study reports the production of PVA/CS asymmetrical membranes using $scCO_2$-assisted phase inversion technique, despite the use of conventional methods as dry/wet-phase inversion methods. To the best of our knowledge, no investigation on the production of asymmetrical membranes using supercritical fluids has been reported yet with the main purpose to use the membranes as wound dressings for skin regeneration. It was demonstrated that using adequate parameters such as casting solution concentration, ratio between polymers and depressurization rate it is possible to obtain asymmetric membranes. The membranes obtained present the most required characteristics of an ideal wound dressing although the fast anti-inflammatory drug release observed. Moreover, the mass transfer mechanism of the drug across the hydrogel asymmetrical membrane was well correlated using a mathematical model based on Fick's second law of diffusion for thin slabs taking into account the swelling behavior of the membranes. The asymmetrical membranes produced revealed to be highly biocompatible, able to protect the wound from physical damage, to provide adequate moisture (minimizing the risk of wound dehydration) and were flexible and strong enough to be handled during wound coverage. In addition, oligo(2-methyl-2-oxazoline) quaternized with *N,N*-dimethyldodecylamine revealed to be an effective contact-active antimicrobial agent against *S. aureus*. Based on the overall results obtained, it can be concluded that PVA/CS asymmetrical membranes prepared by $scCO_2$–assisted phase inversion technique are promising dressing systems to be used for skin regeneration.

Acknowledgements

The authors would like to thank the financial support from Fundação para a Ciência e Tecnologia (FCT - Lisbon) and FEDER funds through POCI-COMPETE 2020 contracts UID/Multi/00709/2013, UID/QUI/50006/2013, POCI-01-0145-FEDER-007265, POCI-01-0145-FEDER-007491, SFRH/BD/80648/2011 (P.M.) and SFRH/BDE/51890/2012 (P.L.). We also thank Professor Isabel Coelhoso and her Ph.D. student A. Rita Ferreira (Biochemical and Process Engineering Group, FCT-NOVA) for the help and scientific advice with water vapor permeability measurements, and the Department of Material Sciences (FCT-NOVA) for providing the equipment for mechanical measurements.

CHAPTER 3. *Ibuprofen loaded poly(vinyl alcohol)/chitosan membranes for wound healing: a highly efficient strategy towards faster skin regeneration*

The contents of this chapter were submitted for publication to a peer reviewed international journal:

Patrícia I. Morgado, Sónia P. Miguel, Ilídio J. Correia and Ana Aguiar-Ricardo.
Ibuprofen loaded poly(vinyl alcohol)/chitosan membranes for wound healing: a highly efficient strategy towards faster skin regeneration.

These results were presented as an oral communication in: XXIV Encontro Nacional da Sociedade Portuguesa de Química, Coimbra, Portugal, July 1st-3rd 2015.
These results were presented as a poster in: 2nd EuCheMS Congress on Green and Sustainable Chemistry, NOVA University of Lisbon, Portugal, October 4th-7th 2015.

Personal contribution:

Patrícia I. Morgado contributed to the design of the study, performed most of the experimental work (with exception of the *in vitro* biocompatibility assays performed by Sónia P. Miguel), interpreted data and wrote the manuscript.

3. Ibuprofen loaded poly(vinyl alcohol)/chitosan membranes for wound healing: a highly efficient strategy towards faster skin regeneration

3.1. Abstract

During wound healing, an early inflammation can cause an increase of the wound size, and the healing process can be considerably belated if a disproportionate inflammatory response occurs. (S)-ibuprofen (IBP) has been used in muscle healing and to treat venous leg ulcers, however its effect in skin regeneration has not been thoroughly studied thus far. Herein, IBP-β-cyclodextrins and IBP-loaded poly(1,3-glycerol dimethacrylate) carriers were designed to customize the release profile of IBP from PVA/CS dressings in order to promote a faster skin regeneration. All the systems were produced using sustainable $scCO_2$-assisted techniques. *In vitro* IBP release studies show that due to poor water solubility and the formation of hydrophobic complexes, the carriers allow a controlled drug release from the hydrogels. Moreover, the *in vivo* rat skin wound model study revealed that the presence of IBP in the dressings is essential for skin wound renewal, preventing an excessive inflammation and enabling earlier reparation.

Keywords: drug delivery systems, composite membranes, hydrogels, ibuprofen, wound healing, $scCO_2$.

3.2. Introduction

Wound infection and inflammation after a surgical intervention or traumatic wounds, abrasions and skin burns are frequent and, if not appropriately treated, might lead to life-threatening sepsis and multi-organ failure which, ultimately, lead to patient dead [167, 232]. Moreover, wound infection can impair wound contraction and, consequently, retard the healing process. Such fact can be explained by the release of bacterial enzymes and metalloproteinases which can degrade the fibrin matrix and growth factors. The fibrin matrix is crucial for skin re-epithelization through the migration of fibroblasts, and is also needed to keep the phagocytic activity of macrophages [27, 233-235].

Different strategies have been adopted to prevent an acute inflammatory phase: the use of a suitable wound dressing able to prevent bacteria penetration while promoting the re-establishment of the integrity of the injured tissue, the use of antibacterial agents to improve the intrinsic antimicrobial properties of some polymers and/or simply the use of non-steroidal anti-inflammatory agents [103, 224, 226, 236, 237].

(S)-ibuprofen is a familiar NSAID, effective, safe and well-tolerated compound with anti-inflammatory, antipyretic and pain relief properties. IBP acts through the inhibition of two isoforms of cyclooxygenase (COX) enzymes responsible for prostaglandin biosynthesis: COX-1 and COX-2, responsible for physiological functions and involved in inflammation, respectively.

The anti-inflammatory behavior of IBP has been particularly tested in osteoarticular, venous leg ulcers and muscles wound healing through oral administration [238-246]. Müller-Decker *et al.* [239] have also studied the effect of two NSAIDs by oral administration (SC-560 and valdecoxib, responsible for COX-1 and COX-2 inhibition, respectively) and revealed that both drugs do not impair skin wound healing. Therefore, in the present study, we combine IBP with drug delivery systems and hydrogel-based dressings to control excessive inflammation in the first phases of the healing process and to protect the wound from physical damage and microorganism penetration.

Previously, our group developed polymeric membranes and drug delivery systems using a non-residue method: $scCO_2$ - assisted phase inversion technique for different purposes [99, 132, 247-250]. In particular, by using this technique, dry, clean, ready-to-use and highly porous IBP–loaded PVA/CS membranes with an asymmetrical geometry were obtained which gelled upon contact with biological fluids, as well reported on Chapter 2. Such intrinsic properties of hydrogel-based membranes enabled the total release of IBP after 40 minutes limiting the applicability of these systems during the full wound healing process. Ideally, a drug should be released during the time course of the peak of the inflammatory phase, which usually occurs 12 hours post-injury [103]. Among the several wound dressings available on the market, hydrogel-based ones are the most commonly used, characterized by having a porous 3D structure that mimics the ECM found by cells in skin tissue, able to absorb and retain wound exudate, promoting cell migration and proliferation and a moisturized environment, leading to pain reduction and consequently to a higher patient acceptability [251-257].

However, when hydrogels are intended to be used as drug delivery systems, they present some limitations related with their highly porous interconnected network. The amount of drug that can be loaded into them is restricted, mainly for hydrophobic drugs, and their significant water content and huge pore sizes often cause a fast drug release. These issues, not only confine the therapeutic efficacy of the loaded drug, but also increase the risk of harmful side-effects for patient (instigated by his exposure to high drug concentrations) [258, 259]. To overcome some of the hydrogel's handicaps related with unsuitable drug kinetic release profile, different approaches have been explored in order to promote a sustained and localized release of drug from these 3D structures, namely through the modification of the interactions between hydrogel and drug and/or by further tightening the mesh in order to restrict drug release from the hydrogel. These approaches are essential to reduce the number of therapeutic doses needed, increasing the drug therapeutic effectiveness. The incorporation of nano- and microparticles, liposomes, dendrimers, within the polymeric matrix of a hydrogel has been shown to be fundamental for long-term release of bioactive molecules [99, 131, 140, 164, 260-266]. In particular, taking into account our current concern in the development of controlled drug delivery systems we examined the use of β-cyclodextrins (β-CDs) and poly(1,3-glycerol dimethacrylate) (PGDMA) for the sustained release of small drugs. Thus, to address these challenges, we speculate that the administration of IBP incorporated into β-CDs forming hydrophobic complexes, or impregnated it in functional (with hydroxyl free groups) mesoporous PGDMA

microbeads, could efficiently protect the loaded cargo IBP from the environment and mediate its delivery *in situ* to reduce the inflammatory phase of the wound healing process. Cyclodextrins, due to their oligosaccharide-cyclical structure may hold drug molecules in their barrel-shaped cavity, creating inclusion complexes that are stabilized by intermolecular forces (host-guest) like hydrogen bonding, van der Waals forces and hydrophobic interactions [267-271]. PGDMA is a polyester-based polymer, well-attractive due to its biodegradable and biocompatible characteristics and can establish double H bonding interactions between their carbonyl and the hydroxyl groups with IBP. It should be also highlighted that functional PGDMA microbeads were produced from glycerol dimethacrylate (GDMA), a by-product from biodiesel production, through the use of a contaminant free, $scCO_2$ technology [215, 272]. Moreover, the selected nano β-CDs and PGDMA microbeads demonstrated to be efficiently loaded with IBP by supercritical CO_2 impregnation [140, 215]. The designed IBP delivery systems were then incorporated into the highly structured and porous PVA/CS membranes for active healing of dermal wounds.
The results herein obtained may cast some light on the use of IBP in skin regeneration by preventing an acute inflammatory phase and promoting faster healing.

3.3. Experimental

3.3.1. Materials

CS (75-85% deacetylated, medium molecular weight: 190-310 kDa), PVA (Mw = 89-98 kDa, hydrolysis degree 99%), IBP (Mw = 206.28, 99%), absolute ethanol, glacial acetic acid (purity ≥99%), PBS, Tris, sodium acetate, $(NH_4)_2SO_4$, CH_3COOK, GDMA, Krytox 157 FSL® (Dupont), Fluorolink C® (Ausimont), 2,2-azo-isobutyronitrile (AIBN), β-CD (minimum 98%) and DMEM-F12 were acquired from Sigma-Aldrich (Sintra, Portugal). 3-(4,5-dimethylthiazol-2-yl)-5-(3-carboxymethoxyphenyl)-2-(4-sulfophenyl)-2H-tetrazolium, inner salt (MTS) cell proliferation assay kit were purchased from Promega (Canada, USA). NHDF were purchased from PromoCell (Labclinics, S.A.; Barcelona, Spain). FBS was purchased from Biochrom AG (Berlin, Germany). Carbon dioxide was obtained from Air Liquide with 99.998% purity. All materials and solvents were used as received without any further purification.

3.3.2. PGDMA carriers development

The PGDMA-based carriers were prepared according to a method described in literature [215]. Briefly, initially the monomer (glycerol dimethacrylate), the stabilizer agent (krytox or fluorolink) and the initiator (AIBN) were loaded into a high-pressure reactor, which was then sealed and immersed in a thermostated water bath at 65º C. Afterwards, CO_2 was pumped into the system until the desired pressure, 24 MPa, was attained, and it was maintained for 24 h. 10wt% of krytox and 30wt% of fluorolink (percentage with respect to monomer) were added based on the

IBP release studies previously done by Restani *et al.* [215]. After those 24 h, fresh $scCO_2$ passed through the white and dried powder obtained to wash it and remove the possible unreacted monomer and the waste of stabilizer.

3.3.3. (*S*)-Ibuprofen impregnation in carriers using $scCO_2$

IBP was loaded, in supercritical conditions, into PGDMA with 10wt% of krytox and 30wt% of fluorolink microparticles (PK and PF, respectively), following the method previously used with slight modifications [215]. Drug loading were performed at 40 ± 0.1 ºC and 25 MPa, during 20 h, and with a concentration to attain the saturation of the medium, at the temperature and pressure favorable for IBP loading. A 33 mL reactor was used and it was divided in two compartments by using a macroporous support to avoid the contact between carriers and drug. IBP was put in the bottom compartment, under stirring, while the PGDMA microparticles were placed on the top of the cell inside a snake skin membrane. A fast depressurization of the system were performed after the loading period [215]. β-CDs were impregnated with IBP using the same procedure.

3.3.4. Preparation of membranes

The membranes were prepared following the method previously described in literature [103, 136, 144]. A 17.25wt% casting solution was prepared (87% PVA/ 13% CS), using acidified water (1% acetic acid) as a solvent, spread over a stainless steel cap (68 mm of diameter and 1.5 mm of height) and introduced into the reactor. Then the reactor was closed and placed in a visual thermostated water bath at 45 ± 0.01 ºC. The temperature was maintained constant using a Hart Scientific (Model 2200) controller. By the use of two Gilson piston pumps (models 305 and 306), a non-solvent flow (90% CO_2 and 10% ethanol (co-solvent)) was added until the desired pressure (20 MPa) was attained. During the assay, the operational pressure was maintained constant using a back pressure regulator (Jasco 880-81), while a Setra Systems Inc. (Model 204) transducer, with a precision of ±100 Pa, was used to monitor the pressure inside the reactor.

At the end, a pure CO_2 flow of 10 mL/min passed through the reactor to extract the ethanol that could be entrapped within the formed membranes. The system was then depressurized in 4 (fast) and 10 min (slow) and membranes with different inner morphologies were obtained.

β-CDs, PK and PF microparticles (approximately 100 mg) with and without IBP were previously added to the casting solution, before membranes preparation.

3.3.5. Characterization of membranes and drug carriers

Membranes' morphology was investigated by SEM data analysis. For cross-section observation, membrane samples were frozen in liquid nitrogen and cracked. The specimens were gold coated before SEM procedure. The images were obtained on a Hitachi S-2400 instrument, with an accelerating voltage set at 15 kV.

In addition, the mechanical properties of the carriers-loaded membranes were studied using a tensile testing machine (MINIMAT firm-ware v.3.1) at indoor temperature. The membranes (n = 5) were cut into 15 mm length and 5 mm width strips, the distance between the clamps was set as 5 mm and the test speed to 0.1 mm/min. 20 N of full scale load and 90 mm of maximum extension were previously fixed. The studies were done with dry and wet membranes. The tensile measurements performed with the wet membranes lasted 21 days, changing the pH every 7 days: i) first 7 days at pH 8 using Tris 0.1M; ii) second 7 days at pH 7.4 using PBS 0.1M and iii) the last seven days at pH 5 using sodium acetate 0.1M. Load/extension graphics were achieved and transformed to stress-strain curves using the following equations:

$$\text{Stress} = \sigma = \frac{F}{A} \qquad \textbf{Equation 3.1}$$

$$\text{Strain} = \varepsilon = \frac{\Delta l}{L} \qquad \textbf{Equation 3.2}$$

where F is the applied force; A the cross-sectional area; Δl the change in length; and L is the length between clamps.

The porosity of the membranes was determined by mercury intrusion porosimetry (micromeritics, autopore IV).

Attenuated Total Reflection-Fourier Transform Infrared spectroscopy (ATR-FTIR) was employed to evaluate the membranes' composition with or without carriers loaded with the drug.

3.3.6. Water uptake analysis

The swelling degree of membranes was determined at two different pHs (8 and 5), that were changed after 24 h, when the mass of the membranes reached a plateau value. Firstly, dry membrane specimens were weighted and introduced in 15 mL pH 8 Tris solution at 35 ºC. At specific time intervals, membrane specimens were taken out from the swelling medium, wiped to remove surface moisture and weighted. After 24 h, the specimens were transferred and introduced in 15 mL pH 5 sodium acetate solution at 35 ºC. Membranes' swelling and shrinking was examined for one week.

The swelling degree *W* (%) was determined as follows, see Equation 3.3:

$$W\,(\%) = \frac{W_w - W_d}{W_d} \times 100 \qquad \textbf{Equation 3.3}$$

where the W_d is the weight of the dried sample and W_w is the weight after immersion.

3.3.7. Water vapor permeation studies

WVP was measured gravimetrically at 30 ºC following a method previously reported [103, 211]. A glass dish with 5 cm of diameter was used to place the membranes with the different carriers. Then, the glass dish (n=3) was introduced into a desiccator containing a saturated CH_3COOK solution with a RH of 22%. A fan was used to promote air circulation and a thermohygrometer (Vaisala, Finland) to control the RH and temperature inside the desiccator. The water vapor flux through the membranes was studied at two different driving forces by using a saturated $(NH_4)_2SO_4$ solution (RH = 81%) and a saturated $NaNO_2$ (RH = 65%) inside the glass dish. The glass dishes were weighed over time for 8 h to determine the membranes' vapor permeability.
The WVP was calculated using the following equation:

$$WVP = \frac{N_w \times \delta}{\Delta P_{w,eff}} \qquad \textbf{Equation 3.4}$$

in which, N_w is the water vapor mass flux, δ is the film thickness and $\Delta P_{w,eff}$ is the effective driving force, expressed as the water vapor pressure difference between both sides of the membrane. Other equations used are described in detail by Alves *et al*. [211].
The WVTR was calculated using the following equation:

$$WVTR = \text{mass} / (\text{area})\,(\text{time}) = (P/L)\,(P_w)\,\triangle(RH), \qquad \textbf{Equation 3.5}$$

where, *P* is the water vapor permeability, *L* is the membrane thickness, (*P/L*) is the water vapor transfer rate (or permeance), P_w is the saturated water vapor pressure at the experimental temperature and △(RH) is the difference of relative humidity between inside atmosphere and outside atmosphere of the membrane glass dishes [49, 175].

3.3.8. Oxygen permeability

The pure gas permeability of the developed membranes loaded with the different carriers was determined in accordance with a procedure already described in detail elsewhere [273] with slight modifications. The membranes were placed in the middle of a stainless steel cell divided

into two identical compartments. O_2 permeability was evaluated by pressurizing both compartments (feed and permeate), and after opening the permeate outlet. A driving force of around 0.07 MPa between the feed and the permeate compartments was established. The pressure change in both compartments over time was followed using two pressure transducers (Druck, PDCR 910 models 99166 and 991675, England). All measurements were performed as a constant temperature, 30 ºC, using a thermostatic water bath (Julabo, Model EH, Germany).
When the plot of *Q* (cm^3, the amount of gas that permeated through the membrane) versus *t* (s, testing time) became linear, a steady-state gas permeability coefficient *P* (cm^3 cm / cm^2 s atm) could be calculated as follows:

$$P = \frac{dQ/dt}{S \times \Delta p/l} \qquad \textbf{Equation 3.6}$$

where *S* and *l* stand for the permeation area (cm^2) and the sample thickness (cm), respectively; Δ*p* is the pressure driving force (atm) [46].
Additionally, the diffusion flux *J* (L / m^2 day) can be calculated based on Equation 3.7:

$$J = \frac{P}{l} \times \Delta p \qquad \textbf{Equation 3.7}$$

where *P* is the gas permeability coefficient (m^3 m / m^2 s Pa), calculated previously; *l* the sample thickness (m) and Δ*p* the pressure driving force (Pa).

3.3.9. Biodegradability assays

The *in vitro* biodegradability of the several systems was carried out over 21 days by changing the pH every 7 days, following the same procedure already described on section 3.3.5 to study the tensile properties. In each seven days, the membrane specimens were taken out from the solutions, washed with distilled water, freeze-dried and introduced in the medium at a different pH. The samples were weighed before and after each freeze-drying step. All measurements were carried out in triplicate.

3.3.10. *In vitro* drug release experiments

The IBP release from PVA/CS membranes containing microparticles loaded with this drug was determined by using a permeation cell. The dressing top layer was exposed to environmental conditions, while the bottom layer was in contact with the release medium to mimic local *in vivo* release within a burn-wound environment [103]. 50 mL of Tris 0.1 M buffer solution (pH=8) at 35ºC was set as release medium (a shaking water bath was used). 1 mL aliquots were

withdrawn periodically and the same volume of fresh medium was added to the suspension. The IBP released was quantified by UV spectroscopy at 264 nm.

The drug release behavior from swelling-controlled membranes was modeled by the Korsmeyer-Peppas equation for the first 60% of release, as follows:

$$\frac{M_t}{M_\infty} = kt^n \qquad \textbf{Equation 3.8}$$

where Mt / M_∞ is the fractional drug release at time *t*, *k* is a constant which takes into account the geometric and structural characteristics of the drug release systems, and *n* is the diffusion exponent reporting the mechanism of drug release [274, 275].

3.3.11. *In vitro* biocompatibility studies

3.3.11.1. Human fibroblast cells growth in contact with microparticles-loaded membranes with/without *(S)*-Ibuprofen

To assess cell behavior in the presence of PVA/CS dressings loaded with microparticles with/without IBP, NHDF cells were initially seeded with the various dressings in 96-well plates, at a density of 2×10^4 cells per well and using DMEM-F12 as culture medium, supplemented with FBS. The studies were performed for 1, 3 and 7 days, at 37° C, under a 5% CO_2 humidified atmosphere. Membrane samples were previously sterilized using UV irradiation during 30 min. An Olympus CX41 inverted light microscope (Tokyo, Japan) equipped with an Olympus SP-500 UZ digital camera was used to control cell growth [165, 167].

3.3.11.2. Evaluation of the cytotoxic profile of the microparticles-loaded membranes with/without *(S)*-Ibuprofen

NHDF cell viability in contact with the sterilized dressings was evaluated by an MTS assay. Firstly, 2×10^4 cells per well were seeded in contact with the materials and then, after 1, 3 and 7 days of incubation at 37º C under a 5% CO_2 humidified atmosphere, the medium of each well was removed and replaced with a mixture of 100 µL of fresh DMEM-F12 and 20 µL of MTS/phenazine methosulfate (PMS) reagent solution. After 4 h of incubation, cells viability was determined by measuring the absorbance at 492 nm using a microplate reader (Sanofi, Diagnostics Pauster). Cells growth without dressings was set as negative control (K^-). Death cells (by the addition of ethanol (96%)) were used as positive control (K^+) [214, 276].

3.3.12. *In vivo* assays

36 Wistar rats (8-10 weeks) weighing between 150-200g were used to evaluate the suitability of the developed systems for improving the wound healing process. The animal studies were carried out according to the guidelines set forth in the National Institute of Health Guide for the care and use of laboratory animals, and following a procedure already used by Ribeiro *et al*. [164]. The animals were separated into nine groups and the wounds were covered as follows: 1) used as control, the wounds were covered with PBS; 2) PVA/CS membranes; 3) the wound was wetted with a solution of IBP (1mg/mL) dissolved in PBS; 4) PVA/CS membranes containing PF carriers without IBP (PVA/CS+PF); 5) PVA/CS membranes loaded with PF carriers containing IBP (PVA/CS+PF_IBP); 6) PVA/CS membranes containing PK carriers without IBP (PVA/CS+PK); 7) PVA/CS membranes loaded with PK carriers containing IBP (PVA/CS+PK_IBP); 8) PVA/CS membranes containing β-CD carriers without IBP (PVA/CS+β-CD); and 9) PVA/CS membranes loaded with β-CD carriers containing IBP (PVA/CS+β-CD_IBP). All over the study, the animals were maintained in separate cages and were fed with commercial rat food and water *ad libitum*.

The wounds were photographed over time with a digital camera (NikonD50) to follow the healing process, and the wound size (WS) was determined through image analysis software ImageJ (Scion Corp., Frederick, MD). 10 and 21 days post-injury, the animals were sacrificed.

3.3.13. Histological analysis

Tissue samples from the skin injuries and organs (heart, brain, lung, spleen, liver, and kidney) were obtained by necropsy 10 and 21 days post-injury, to examine the local and systemic immune response of the host to the membranes herein produced. Tissue samples were formalin fixed and paraffin embedded for routine histological processing. A cryostat microtome (Leica CM1900) was used to obtain 3 µm sections of each sample that were, subsequently, dyed with hematoxylin and eosin (H&E) and Masson's trichrome. The processed samples were then observed using a light microscope with specific image analysis software from Zeiss [164, 167, 277].

3.3.14. Statistical analysis

One-way ANOVA with Tukey's multiple comparisons test was used to evaluate the significant statistical differences between the obtained results for WVP and the surface area of the burn wounds. Computations were performed using a MYSTAT 12 statistical package (Systat Software, a subsidiary of Cranes Software International Ltd.).

3.4. Results and Discussion

3.4.1. Development of hydrogel-based wound dressings by $scCO_2$ phase inversion technique

Usually, the production of hydrogel-based systems involves the use of organic solvents which may have some degree of toxicity, and consequently cause harmful side effects for patient health, in addition to the long processing times to obtain the desired clean hydrogel matrix [278-281]. In order to overcome these drawbacks, $scCO_2$-induced phase inversion technique has been recently used as a solventless and very efficient method on the production of gelled systems. This process is fast, allows the production of porous matrices by the induction of nucleation and growth of bubbles inside the polymer and can be used to produce symmetric and asymmetric 3D structures [99, 103, 137, 143, 282].

Meanwhile, we have already demonstrated that PVA/CS asymmetrical membranes loaded with IBP could be developed using the $scCO_2$ phase inversion technique. However, due to structural constrains those membranes released the full drug cargo after 40 min of incubation at pH 8. To achieve a longer-lasting IBP release, drug-loaded microparticulated systems were incorporated within the matrix of the membranes. In addition, during the membranes production process, the depressurization rate was varied, *i.e.* periods of 4 and 10 min of depressurization were used in order to study their influence on the membranes' inner aspect and on the subsequent related properties.

SEM images (Figure 3.1) show that the fast depressurization rate (4 min) promote more dense sections, while a depressurization of 10 min enables the formation of membranes with a porous inner layer, a characteristic that allows the absorption of wound exudate, keep a moist environment in the wound and also facilitate cells penetration and nutrients diffusion [99, 144, 164-166]. The characteristic dense top surface obtained for all the membranes is fundamental for skin protection against harmful external agents. The bottom of the membranes presents some roughness that can allow the drainage of the wound exudate and also avoid dressing adherence to the wound bed. The comparison of the cross-section SEM images reveals the structural asymmetry of PVA/CS+PK membranes depressurized for 10 min, which present a more dense section on the top of the dressing and a porous inner layer. However, in general, the introduction of the carriers into the casting solution, somehow, avoided the formation of asymmetrical structures.

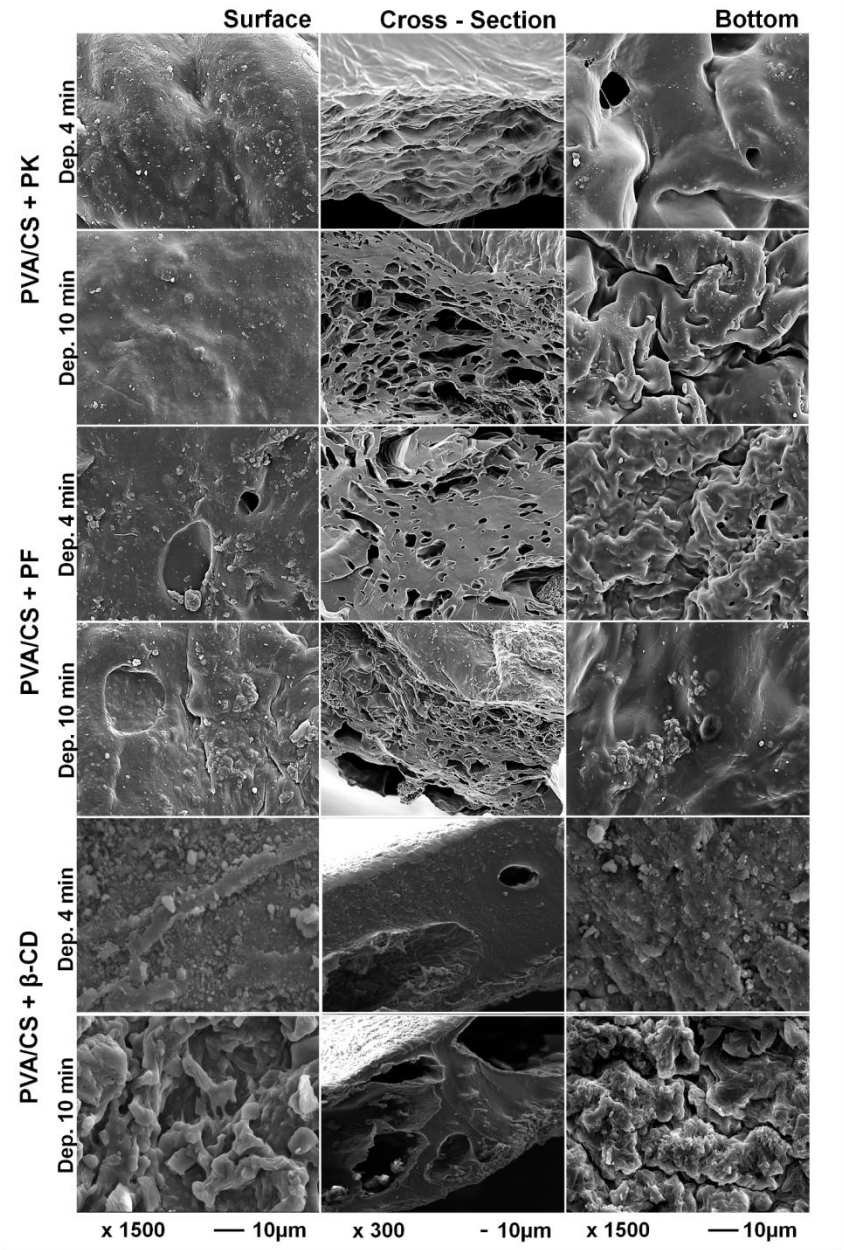

Figure 3.1. Scanning electron micrographs of the surface, cross-section and bottom of PVA/CS membranes containing the different drug delivery systems (PK, PF and β-CD) produced with two depressurization times, 4 and 10 min.

3.4.2. Water uptake analysis

The swelling behavior of the hydrogel-based wound dressings was studied at 35º C (the normal skin temperature [283]), using two different buffers with pH 5 and 8, for a period of 4 days, taking into account the skin pH variation during the wound healing process (from basic to normal skin pH around 5), as already well described in Chapter 2 [103, 220]. Once more, as it is possible to see on Figure 3.2, the membranes herein developed, independently of the carriers used, continued to present a shape-memory behavior displaying the highest swelling degree at

pH 5 (250-350%), which results from the CS amino groups protonation that happens at pH values lower than CS pKa (pKa (CS) = 6.5 [221]). This swelling behavior could be considered an advantage, when a wound dressing containing impregnated IBP-microparticles is used. The initial basic pH promotes a sustained release of the drug and then, the decrease of skin pH allows the increase of water uptake capacity of membranes, allowing the removal of wound exudates, a major requirement of an ideal dressing. Furthermore, this swelling behavior is also crucial for an appropriate diffusion of nutrients and cells [167].

PVA/CS+PF membranes showed slightly higher swelling degree than PVA/CS+PK membranes (Figures 3.2A and 3.2B). Since the average pore diameter and porosities of PVA/CS+PK membranes is slightly higher than for PVA/CS+PF membranes (please see Table 3.1), the higher water uptake ability of PVA/CS+PF membranes may be explained by the different characteristics presented by the two types of stabilizers used. Both stabilizers (or lubricants) belong to perfluoropolyether (PFPE) class of compounds, that have a general chemical structure $CF_3O(CF_2OCF_2CF_2O)_nCF_3$ with low water affinity. However, Fluorolink C is a functionalized PFPE with the functional group $–CONHC_{18}H_{37}$, that improves the water solubility of the stabilizer and probably the PGDMA carrier during the processing step, despite the removal of the stabilizer afterwards during the washing with fresh CO_2 [284, 285]. Such fact, leads to a superior swelling degree and, consequently, to a quicker drug release profile from PVA/CS+PF membranes (Figure 3.5B), as more solution is uptaken into the particle matrix, facilitating the drug release.

PVA/CS+β-CDs membranes presented water uptake ability similar to membranes with PF (Figures 3.2B and 3.2C), a consequence of the hydrophilic external surface of β-CDs [286]. These membranes presented higher pore diameter and large dense sections, resulting in less porosity than membranes containing PGDMA carriers.

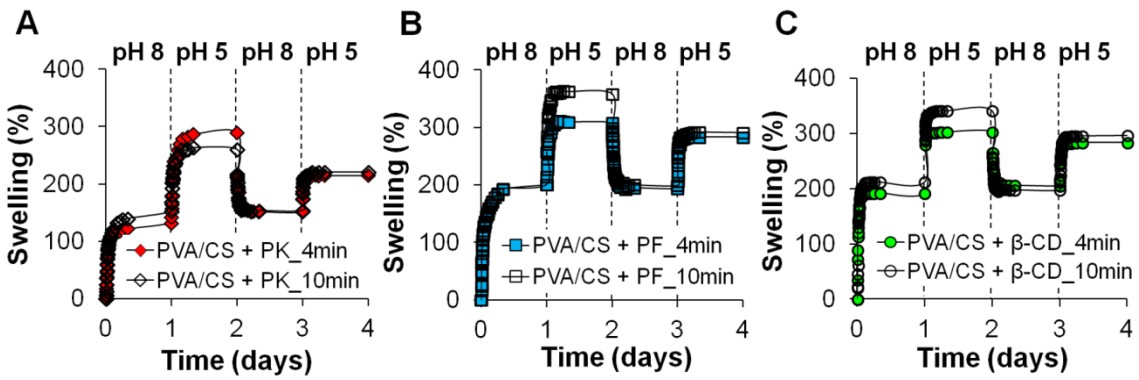

Figure 3.2. Swelling behavior of (**A**) PVA/CS+PK_4min (♦) and PVA/CS+PK_10min (◊); (**B**) PVA/CS+PF_4min (■) and PVA/CS+PF_10min (□); (**C**) PVA/CS+β-CD_4min (●) and PVA/CS+β-CD_10min (○) membranes at different pHs.

Table 3.1. Average membranes' pore diameter and porosity determined by mercury intrusion porosimetry.

Membranes	Average pore diameter (μm)	Porosity (%)
PVA/CS + PK_4min	0.47	51.6
PVA/CS + PK_10min	0.58	56.2
PVA/CS + PF_4min	0.45	46.2
PVA/CS + PF_10min	0.51	56.0
PVA/CS + β-CD_4min	0.65	31.0
PVA/CS + β-CD_10min	0.77	37.1

3.4.3. Water vapor permeability

Besides the characterization of the swelling behavior, the evaluation of the WVTR through the dressing is extremely important in order to ensure a suitable moist environment at the wound: an exorbitant vapor permeability can lead to wound dehydration and dressing adhesion, while a low permeation can cause the maceration of surrounding healthy tissue caused by exudate retention [171].

Comparing the results herein obtained with the previous PVA/CS membranes developed (please see Table 3.2), it is possible to say that the incorporation of nano and microcarriers into the membranes enhanced the water vapor diffusion through the dressings. Indeed, the several dressings developed, independently of the imposed driving force, present higher vapor permeation values than PVA/CS_4min and PVA/CS_10min membranes, which in part could be also an effect of the absence of an asymmetrical structure. Once more, the decrease of the RH also promotes a decrease of WVP, WVTR and permeance on the several membranes produced. However, these properties did not present a statistically significant difference ($p<0.05$) for the RH% tested. The results showed that the difference on membranes' inner structure does not have a large effect on the WVP of the membranes. In addition, it is common to obtain a high coefficient of water vapor sorption, when RH is high [211], as it was also observed.

In the literature, it is often mentioned that wound dressings with WVTRs within the range of (20-25) x 10^2 g/m^2 day would provide suitable moisture and avoid exudate accumulation [287]. Nonetheless the dressings herein developed as well as other commercially available wound dressings are not in conformity with this range, as already mentioned on Chapter 1 and 2. The WVTR depends on the chemical characteristics of the polymers from the dressing is made, the thickness and porosity of the dressing, and RH and temperature imposed which, ultimately,

determines the water vapor pressure which is the driving force for water vapor transfer across the dressing [103, 166, 171-174, 222]. Despite the WVTR of the produced membranes being far away from the ideal range, their high swelling degree offsets the obtained results. In addition, PVA/CS+PF and PVA/CS+β-CDs membranes revealed to be the best systems to be used as wound dressings due to the higher WVTR and water uptake ability, enabling the absorption of wound exudate while keeping a moisturized environment, thanks to the gel-like properties of the membranes at wet state.

Table 3.2. Water vapor permeation of the different developed membranes.

Wound Dressing	RH (%)	WVTR ($x10^2$ g/m^2 day)	WVP ($x10^{-13}$ g/m s Pa)	Permeance ($x10^{-10}$ g/m^2 s Pa)
PVA/CS + PF_4min	81 – 22	4 ± 2	2.0 ± 0.9	1.2 ± 0.5
PVA/CS + PF_10min	81 – 22	10 ± 2	6 ± 2	2.8 ± 0.7
PVA/CS + PK_4min	81 – 22	3.7 ± 0.3	1.4 ± 0.1	1 ± 0.1
PVA/CS + PK_10min	81 – 22	3.7 ± 0.3	1.3 ± 0.1	1 ± 0.1
PVA/CS + β-CD_4min	81 – 22	3.7 ± 0.5	0.9 ± 0.2	1 ± 0.1
PVA/CS + β-CD_10min	81 – 22	5.15 ± 0.05	1.7 ± 0.2	1.30 ± 0.01
PVA/CS + PF_4min	65 – 22	3.8 ± 0.8	1.1 ± 0.2	1.3 ± 0.2
PVA/CS + PF_10min	65 – 22	6.9 ± 0.5	3.0 ± 0.2	2.3 ± 0.2
PVA/CS + PK_4min	65 – 22	1.6 ± 0.2	0.9 ± 0.2	0.6 ± 0.1
PVA/CS + PK_10min	65 – 22	1.8 ± 0.2	0.70 ± 0.02	0.60 ± 0.04
PVA/CS + β-CD_4min	65 – 22	2.6 ± 0.5	0.70 ± 0.04	0.9 ± 0.2
PVA/CS + β-CD_10min	65 – 22	4.1 ± 0.5	1.2 ± 0.1	1.5 ± 0.1
PVA/CS_4min [103]	81 – 22	2.0 ± 0.2	5.3 ± 0.9	9.4 ± 0.8
Asymmetric PVA/CS_10min [103]	81 – 22	2.1 ± 0.2	5.6 ± 0.8	9.9 ± 0.8
PVA/CS_4min [103]	65 – 22	1.1 ± 0.1	3.7 ± 0.3	6.6 ± 0.8
Asymmetric PVA/CS_10min [103]	65 – 22	1.2 ± 0.3	4.9 ± 0.9	7 ± 2

3.4.4. Oxygen permeability

The permeability of oxygen across the membrane is another important property for the wound healing process. O_2 is an essential nutrient for cell metabolism, especially for energy production and for reparative processes like cell proliferation and collagen synthesis [176, 178]. As stated

on Chapter 1, an excellent wound healing is attained for O_2 diffusion flux from 456-1840 L/m^2 day, which is far away from the values obtained for the membranes herein studied as shown on Table 3.3 (just the ones depressurized in 10 min presenting higher pore sizes). Despite the produced membranes present pore size higher than the kinetic diameter of O_2 (~0.343 nm) [180], the relatively low porosity could be the reason of low O_2 permeability. For instance, the CS asymmetrical membranes developed by Mi *et al.* [49] presented a sponge-like inner layer with 74% of posority with pore sizes of about 10-100 µm, which have lead to a suitable O_2 diffusion flux of about 644 L/m^2 per day. Other dressings present the so called finger-like voids, that allow oxygen transportation across the membrane, without demanding gas exchange between or through the pores available in the membrane [184]. However, we believe that due to the hydrogel-based like properties of the membranes upon contact with the wound exudate, the more open pores and the gelled matrix will favour the gas permeability through the dressings.

Table 3.3. Comparison of the oxygen permeability of the different developed membranes.

Wound Dressing	O_2 Permeability (x10^{-5} cm^3 cm/cm^2 s atm)	Diffusion Flux (x10^{-4} L/m^2 day)
PVA/CS + PF_10min	57.5 ± 14.2	31.5 ± 8.7
PVA/CS + PK_10min	2.98 ± 0.37	1.76 ± 0.22
PVA/CS + β-CD_10min	2.90 ± 0.15	2.20 ± 0.11
Asymmetrical PVA/CS	20.4 ± 11.6	11.6 ± 0.66

3.4.5. Biodegradability and tensile properties

In Figure 3.3 it is possible to observe the membranes' weight loss over the 21 days at different pHs. This procedure aimed to mimic the pH variation that occurs during the wound healing process [220]. As observed, the weight loss (40-70%) was more noticeable during the first 7 days, at basic pH, for all types of membranes and then, the weight of membranes stabilizes. The asymmetrical PVA/CS dressings previously developed presented the maximum weight loss of 5-10% [103]. The results show that the incorporation of the carriers within the polymeric matrix increases the rate of degradation, due to the looser interactions between the PVA and CS, which could be also the reason for the absence of membranes with asymmetrical structures. This will not prevent the final applicability of these membranes. In general, the biodegradability of a material is a requirement for wound treatment, otherwise it will induce the formation of new lesions and increase the pain felt by the patient when the dressing is changed [288, 289].

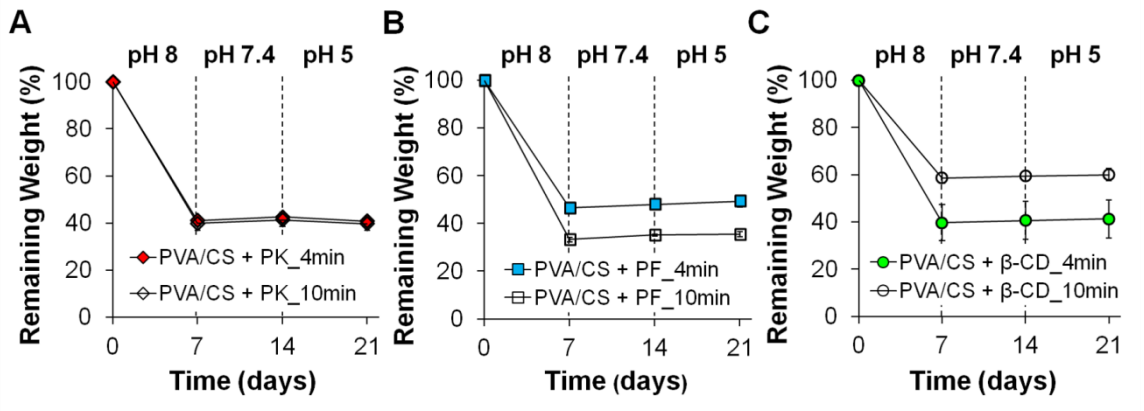

Figure 3.3. Evaluation of the structural stability of (**A**) PVA/CS+PK_4min (♦) and PVA/CS+PK_10min (◊); (**B**) PVA/CS+PF_4min (■) and PVA/CS+PF_10min (□); (**C**) PVA/CS+β-CD_4min (●) and PVA/CS+β-CD_10min (○) membranes at different pHs, over 21 days.

The tensile tests of the various types of membranes produced were performed in dry and wet state, during 21 days, at three pH values that were interchanged every 7 days, following the same procedure used for the biodegradability assays. The results obtained revealed that wet membranes have a higher elasticity (lower Young's modulus) than the dry ones (Figure 3.4). Furthermore, dry membranes produced with a depressurization period of 10 min were more elastic than those depressurized only in 4 min, independently of the carrier loaded. This may explain the higher surface density and lower porosity for the second type of membranes. Among the membranes produced, the PVA/CS ones containing β-CDs were the most elastic, displaying an elongation at break of about 600% (for more information regarding the maximal tensile strain (%) and tensile strength (MPa) of dry and wet membranes please see Figures S3.1 and S3.2 on supplementary information). Such results may be related with the higher pores size shown by PVA/CS+β-CDs membranes in comparison with the other systems developed.

In Figure 3.4 it is also possible to observe the pH influence on Young's modulus of the membranes. The elasticity decreased when the pH was changed from 8 to 7.4 but at pH 5 the elasticity increased, owing to the higher water uptake ability of membranes at pH 5 (Figure 3.2). Nevertheless, the elongation at break of wet membranes (about 300-350%) was smaller than of the dry ones due to the loss of structural integrity, as shown by the biodegradability studies (Figure 3.3). The Young's modulus of dry and wet membranes obtained was lower than that presented by native skin, which varies between 4.6 and 20 MPa for the extension tests [185]. However, all the dressings herein developed presented higher elasticity and elongation at break than other wound dressings, currently in use in the clinic, allowing a suitable handling during their application as wound bandages [48, 171, 223].

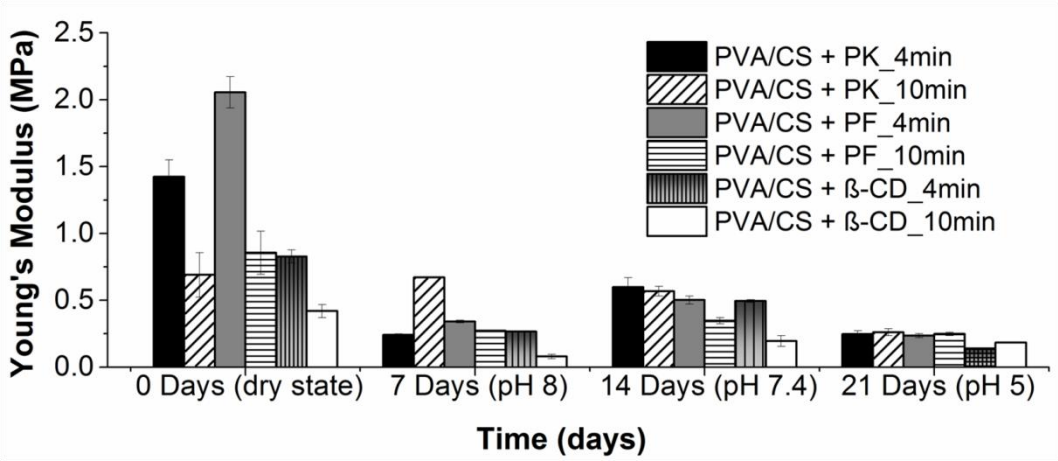

Figure 3.4. Young's modulus analysis of PVA/CS_4min and PVA/CS_10min membranes containing the different carriers in dry and wet state.

3.4.6. *In vitro* drug release studies

As previously described, notwithstanding their suitable physicochemical characteristics, the quantity of drug loaded into hydrogels is restricted and rapidly released, limiting their applicability as drug delivery systems. In order to overcome such drawback, drug-loaded microsystems have been incorporated within the polymeric matrices of the membranes produced. This strategy is commonly used to protect unstable biologics from degradation and also to control the sustained release of either small drugs or biological active compounds. In these systems, the loaded bioactive molecules have to overcome two barriers before reaching the surrounding environment: first the carriers (microparticles) and later, the membrane's matrix [251, 290].

Following the work developed by Restani *et al.* [215], PGDMA microbeads were synthesized by radical polymerization of GDMA in $scCO_2$ conditions using krytox and fluorolink as stabilizers. The amount of the stabilizers used was chosen based on the results of IBP cumulative release (%) obtained on that work. PGDMA microparticles with 10% of krytox (PK) and PGDMA microparticles with 30% of fluorolink (PF) presented the most suitable release profile for the drug used.

In the present work, the drug release studies were performed at a basic pH (pH=8) taking into account the skin pH variations during wound healing process in burn patients as explained before and well described by Osti [220]. Furthermore, being ibuprofen a non-steroidal anti-inflammatory drug, its high effect would be essential during the inflammatory phase of the healing process (in which the skin pH is basic) with the main purpose of avoiding an acute wound inflammation. Accordingly to Qui *et al.* [231], the saturation solubility of IBP at pH 7.4 is documented to be 6.14 mg/mL, becoming much higher for pH > 7.4. In this study, the total

amount of IBP loaded into the several membranes using supercritical CO_2 technology was about 10 mg per gram of membrane (working below IBP saturation), providing perfect sink conditions during drug release.

Figure 3.5 (A, B and C) shows the drug release profile of the several drug delivery systems. The IBP release profiles obtained for PVA/CS dressings containing the PF microparticles (Figure 3.5B) revealed that drug release occurs abruptly, promoting a complete release after 8 h, independently of the depressurizing time used in membranes production. As stated above on the swelling studies (Figure 3.2), those membranes presenting higher water uptake capacity, display a faster drug release profile. When PK microbeads were used (Figure 3.5A) different results were observed: i) for PVA/CS+PK membranes depressurized in 4 min a burst release of IBP (80%) occurred during the first 2 h and then a controlled release of the drug was noticed until its complete liberation after 24 h; ii) the PVA/CS+PK membranes depressurized in 10 min displayed a controlled release of the drug during the first 8 h of the experiment, when its complete liberation occurred.

As β-CDs were incorporated within membranes, a more controlled drug release profile was obtained (Figure 3.5C). Indeed, after 12 h (a period that is coincident with the peak of the inflammatory phase) about 80% of the drug was released and the complete release of IBP was only attained after 3 days, independently of the depressurization rate used for membranes production.

The diffusion mechanism of drug release profiles were further evaluated by fitting the experimental data into the Korsmeyer-Peppas model (Equation 3.6) as shown in Figure 3.5 (A1, B1 and C1), only valid for the first 60% of drug released. This model was applied considering drug diffusion from the microcarriers with a geometric spherical shape. It is already known from the previous work that IBP release from the PVA/CS hydrogel-based systems is purely swelling dependent leading to a complete drug release in few minutes [103]. We can now consider that the membranes act as a support for the carriers (not forgetting the protection of the wound) and the IBP release from the carriers will depend on the interactions between drug-carrier and on the solvent uptake ability of the carriers which *per si* is dependent on the amount of water that membranes (the supports) can absorb.

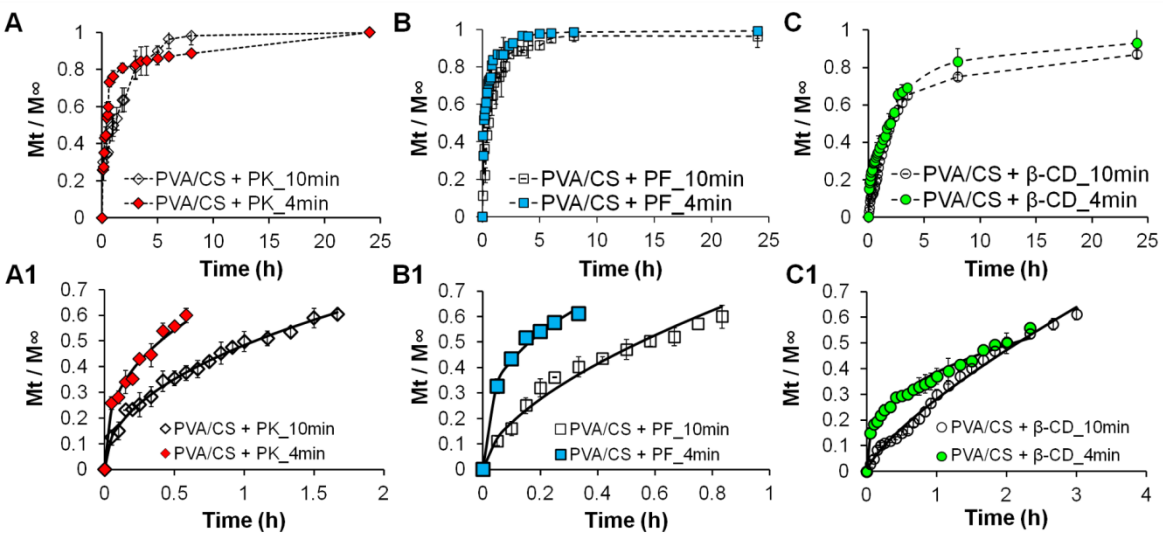

Figure 3.5. *In vitro* drug release studies of IBP loaded into the several drug delivery systems at pH 8 and 35 ºC (**A, B, C**) and IBP release profile fitted through Korsmeyer-Peppas mathematical model for the first 60% of release (**A1, B1, C1**): (**A, A1**) PVA/CS+PK_4min (♦) and PVA/CS+PK_10min (◊); (**B, B1**) PVA/CS+PF_4min (■) and PVA/CS+PF_10min (□); (**C, C1**) PVA/CS+β-CD_4min (●) and PVA/CS+β-CD_10min (○).

As shown in Table 3.4 (that summarizes modeling data), IBP release from microcarriers loaded into membranes depressurized in 4 min, follows a Fickian diffusion mechanism (with *n* values of about 0.3), in which the solvent transport rate or diffusion is much greater than the process of polymeric chain relaxation. On the other hand, IBP release mechanism from microcarriers loaded into membranes depressurized in 10 min is anomalous (with *n* values greater than 0.43) predicting the superposition of diffusion, swelling, dissolution and/or erosion phenomena [291, 292]. Figure S3.3 shows the fitting to the experimental drug release data. As stated before, the solvent uptake ability of the carriers is dependent on the amount of water that can be entrapped within membranes' matrix. Furthermore, the higher swelling degree of membranes, the greater the distance the drug should travel between particles and the membrane's surface exposed to the release medium. As a result, a lower drug amount is released at each period of time, which is in accordance with the results herein obtained. Regarding those results, the incorporation of IBP-loaded microcarriers into the membranes effectively promotes an extended release profile of the drug from 40 min (the drug release period obtained in the previous asymmetrical membranes developed [103]) to some hours and even days as can be observed in Figure 3.5.

Table 3.4. Modeling of IBP release from carriers using the Korsmeyer-Peppas equation.

Drug delivery systems	Korsmeyer-Peppas			Drug release mechanism	$t_{60\%}$ (h)	IBP released (mg/g_{memb} at $t_{60\%}$; Mean ± SD
	$R^{2\,a}$	k^b	n^c			
PVA/CS + PK_4min	0.9536	0.7015	0.3685	Fickian diffusion	0.58	6.78 ± 0.03
PVA/CS + PK_10min	0.9889	0.4840	0.4586	Anomalous transport	1.67	4.41 ± 0.06
PVA/CS + PF_4min	0.9754	0.9172	0.3340	Fickian diffusion	0.33	6.40 ± 0.07
PVA/CS + PF_10min	0.9693	0.7118	0.5885	Anomalous transport	0.83	4.34 ± 0.08
PVA/CS + β-CD_4min	0.9834	0.3794	0.3365	Fickian diffusion	2.33	4.42 ± 0.09
PVA/CS + β-CD_10min	0.9871	0.2812	0.7471	Anomalous transport	3	2.93 ± 0.02

[a] Correlation coefficient.
[b] Diffusion coefficient that reflects the structural and geometric characteristics of the system.
[c] Release exponent which might give an insight on the specific transport mechanism.

In order to evaluate the interactions between the drug and the polymeric matrix an ATR-FTIR was employed. The ATR-FTIR spectrum for pure IBP shows all the characteristic bands of the drug, including the carbonyl stretching at 1707 cm^{-1}. As previously described by Restani *et al.* [215], IBP establishes a double H-bond with the carbonyl and the hydroxyl groups of the PGDMA network. Examining the ATR-FTIR spectrum (Figures S3.4 and S3.5), a shift of the band of hydroxyl group for lower energy states (3447 cm^{-1} from PK and 3419 cm^{-1} from PF) was identified when IBP was loaded, indicating the formation of hydrogen bonding interactions. When β-CDs (Figure S3.6) were incorporated, the C=O stretching was completely absent. This fact has been already described as an evidence of the inclusion of IBP inside β-cyclodextrin cavity [268, 270, 293], which explains the more extended release profile of the IBP observed for β-CDs. Nonetheless, when the carriers with and without IBP are incorporated inside PVA/CS membranes it was not possible to visualize their characteristic bands (Figures S3.7 and S3.8).

Taking into account the overall data herein presented, it may be concluded that the membranes depressurized in 10 min presented the most suitable properties for being used as wound dressings. Specifically those membranes present a more porous structure, leading to higher water uptake capacity and WVTR which is compatible with the maintenance of a controlled moisturized environment at the wound site. In addition, they present better mechanical properties that allow their handling during the healing process. Thus, the membranes depressurized in 10 min were chosen to further evaluate their suitability for the treatment of burn wounds through *in vitro* and *in vivo* assays.

3.4.7. Dressings biocompatibility

The cytocompatibility of PVA/CS membranes loaded with the different carriers containing or not IBP was evaluated through *in vitro* studies. NHDF cells adhered and grew in the presence of the different systems (Figures S3.9 and S3.10), and in the negative control (cells seeded without materials), highlighting the membranes biocompatibility. To further characterize the biocompatibility of membranes an MTS assay was also performed. As observed in Figure 3.6, cells remained viable in contact with membrane specimens after 1, 3 and 7 days of incubation. The results obtained reveal that these systems do not affect cellular viability, which is a crucial property for their application in wound regeneration.

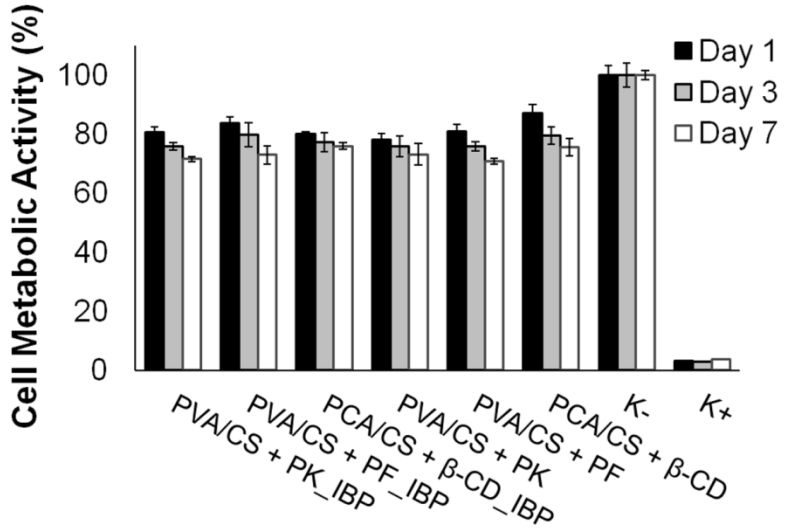

Figure 3.6. Evaluation of cellular activity in contact with the different dressings with and without IBP through an MTS assay after 1, 3 and 7 days. (K^-) live cells; (K^+) dead cells.

3.4.8. Evaluation of membranes performance during the wound healing process

The local and systemic histocompatibility of the different dressings was evaluated *in vivo*, through the induction of a full-thickness dermal wound in Wistar rats. The animals were initially separated into 9 groups, as already reported in Section 3.3.12. Groups 1-3 were set as controls. Animals of group 1 had their wounds only treated with PBS and were used as control to screen the wound healing process without the application of any dressing. The application of PVA/CS-based hydrogel (group 2) was used to check if this system had any adverse effect on the healing. In group 3, a 1 mg/mL IBP solution was applied to verify the impact of the drug direct application in the progression of the wound healing process. All other groups were used as test samples where different carriers loaded with or without IBP and encapsulated within membranes were experienced to check their suitability for the envisioned biomedical

application. IBP-loaded PVA/CS hydrogel was not set as a study group taking into account the fast drug release profile reported in previous work [103]. Along the study the animals exhibit a general good health condition, as confirmed by their weight gain.

Wound closure was assessed by macroscopic observation and histological analysis of the wounded area. In Figure S3.11A is possible to observe the wound beds after burn induction and the different treatments applied. The qualitative assessment (Figure S3.11A), the wound size evaluation (Figure 3.7A and Figures S3.11C and D) and the histological analysis (Figure 3.7B and Figure S3.11B) show that PVA/CS+β-CD_IBP are promising wound dressings, since the wound closed significantly more rapidly during the treatment, in comparison to the control assays and the other tested groups.

PVA is a very attractive synthetic polymer for producing membranes due to its good biocompatibility, thermal and chemical stability, adequate mechanical resistance and biodegradability. Conversely, CS is a natural polysaccharide commonly investigated for the treatment of skin wounds attributable to its antimicrobial properties, biocompatibility, biodegradability and hemostatic activity. Furthermore, its hydrophilic surface advances cell adhesion, growth and differentiation, events that are crucial for stimulating the healing process [96, 147, 165, 207]. However, and based on the histological studies, the groups treated with PBS and neat IBP lead to scab formation during the wound closure, which is one of the main problems affecting wound-management [294]. On the other hand, the wound size of animals treated with IBP-loaded carriers showed an evident decrease in the wound area during the first days, compared to those where no IBP was administered (Figure 3.7A and Figures S3.11C and D). The results stress not only the significance of an initial covering of the damaged area with hydrogel-based systems but also the incorporation of IBP in these systems to avoid an acute inflammatory phase in the early stages of healing. As stated before, due to its anti-inflammatory properties, IBP can minimize the complications associated with the wound healing process such as maceration, infection and pain, by enhancing wound contraction and, consequently, the healing course. Yuan *et al*. [242] also described the anti-inflammatory effect of ibuprofen-loaded electrospun PLLA fibrous scaffolds and the promotion of muscle healing through *in vivo* studies.

A detailed histological analysis of skin specimens was carried out after 10 and 21 days to characterize the wound healing progression for all groups (Figure 3.7B and Figure S3.11B). At 10 days post-injury, the data collected showed the formation of necrotic tissue (scab) in control groups (groups 1 and 3), while in other assays where wound dressings were applied, no scab formation was observed. This fact emphasizes, once more, the importance of covering the wound to avoid scab formation and wound contamination. In a previous study, it was stated that the use of elastomeric biodegradable hydrogel-based structures can reduce the scab formation, allowing a suitable wound contraction [295].

After 21 days, all the skin lesions exhibited a complete epithelization and wound dressing degradation, except the animals treated with PK membranes (membranes that have a low water uptake capacity and WVTR).

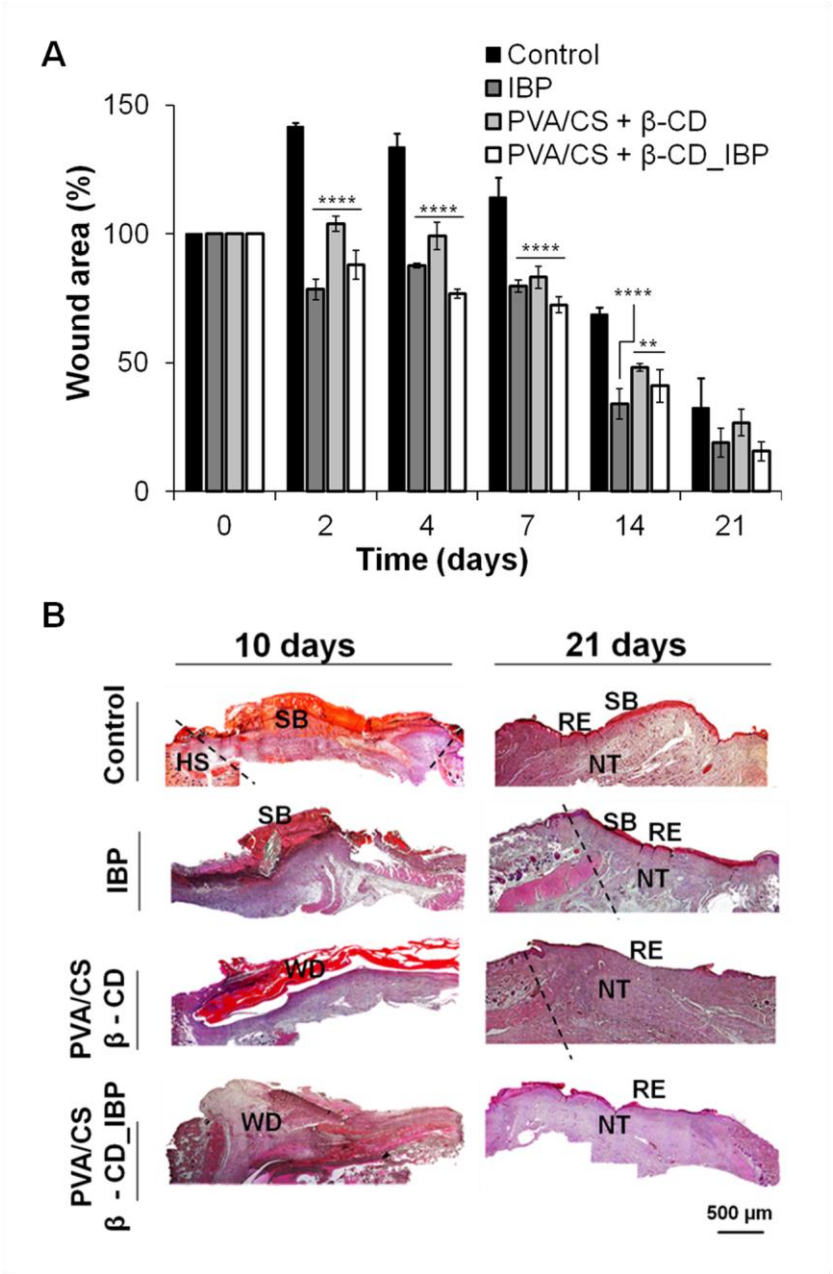

Figure 3.7. Characterization of the wound healing process under *in vivo* conditions. (**A**) Representation of the percentage of wound closure showing the faster healing for the group treated with PVA/CS+β-CD_IBP. (**B**) Histological analysis of skin samples obtained after 10 and 21 days, highlighting the wound healing progression along the time frame chosen. HS: healthy skin; SB: scab; RE: re-epithelization; NT: neo-tissue; and WD: wound dressing. Wound margins were delineated.

Figure 3.8 shows magnified images of the histological skin samples of animals group displaying the best results. Inflammatory cells were noticed in all groups 10 days post-injury. At day 21, no signs of inflammation or the presence of reactive granulomas were noticed in the group treated with PVA/CS+β-CD_IBP dressing, although, it was possible to identify granulocytes,

macrophages and neutrophils at the injured site for the control assay (treated with PBS). All the wound dressings tested were completely degraded and new tissue (epidermal and dermal layer) was visualized in skin samples obtained from test groups. For some experimental assays, inflammatory cells were also present despite the use of IBP. It is reported that the presence of some inflammatory cells such as macrophages are required for the wound healing, once they are involved in the secretion of growth factors responsible for cell growth, proliferation and protein synthesis. These cells can influence proteases and their inhibitors production, determining ECM synthesis or remodeling, and contribute to biomaterials' degradation [277, 296].

The absence of an inflammatory reaction in damaged skin areas treated with different membranes and the nonattendance of pathological features in the organs obtained by necropsy (data not shown) revealed the local and systemic histocompatibility of the biomaterials.
In addition, the increase in thickness of the epithelial layer and the complete epithelization observed in the treated skin wounds, suggest that the produced membranes can be used to re-establish tissue architecture, supporting their future application in skin wound regeneration.

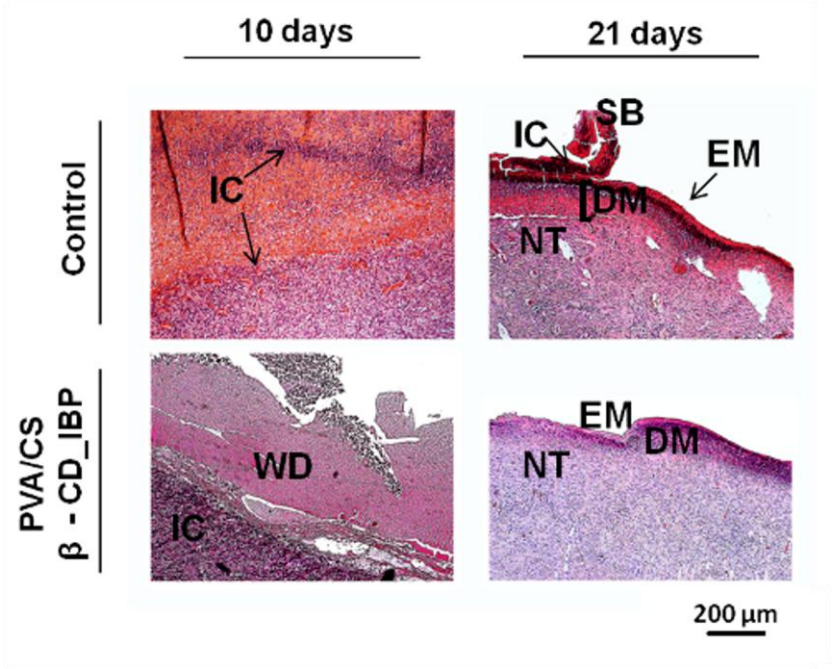

Figure 3.8. Magnified images of H&E-stained histological sections of the test groups after 10 and 21 days post-injury. IC: inflammatory cells; EM: epidermis; DM: dermis; NT: neo-tissue and WD: wound dressing.

The Masson's trichrome analysis (Figure 3.9 and Figure S3.12) identified the presence of collagen type III in the neo-dermis in all tested groups, 21 days post-injury, which was produced by fibroblast cells. The synthesized collagen promoted the migration of fibroblast to the wounded area, which is fundamental for the formation of neo-tissue. As described in literature [297, 298], over the healing process, the collagen type III will be replaced by collagen type I.

Collagen type I plays a crucial role in skin formation and repair, as well as, in the maintenance of skin tensility and elasticity.

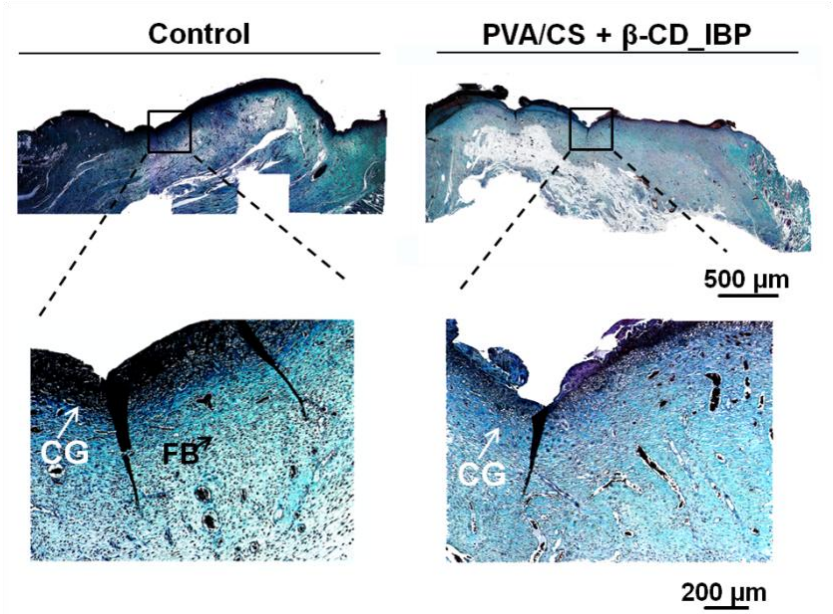

Figure 3.9. Representative images of Masson's Trichrome analysis of stained explants of the control and PVA/CS+β-CD_IBP groups. Images with higher magnification show the presence of collagen type III (CG) in the dermal matrix.

3.5. Conclusions

In this study, the use of ibuprofen-controlled release carriers was the key strategy to make practicable the use of hydrogel based dressings with relevant properties for wound healing. The dressings were made from a blend of chitosan, a natural polymer, and PVA encapsulating the controlled IBP release systems in order to develop macroporous networks with adequate morphological and mechanical characteristics for the envisioned biomedical application. Sustainable, solvent free and green approaches were used to develop the IBP loaded carriers as well as the assembled wound dressings. β-CDs and previously synthesized PGDMA microbeads were loaded with IBP using $scCO_2$ impregnation. The incorporation of loaded IBP-delivery systems into the hydrogel matrix, by $scCO_2$-induced phase inversion, endowed the mediation of the anti-inflammatory drug delivery throughout the wound healing process. β-CDs revealed to be the most promising drug delivery systems where the complete release of the drug occurred only after 3 days unlike the 1 day observed for PGDMA microbeads, which can be explained by the inclusion of IBP in the hydrophobic cavity of the carrier. The sustained IBP release profile was also studied through *in vivo* assays. The wound size of animals treated with PVA/CS+β-CD_IBP decreased over time, while for the other tested groups treated with PVA/CS+PF_IBP and PVA/CS+PK_IBP an increase of the wound size was observed between 2 and 7 days post injury. In addition, IBP displayed an anti-inflammatory effect during the wound healing and did not impair skin regeneration. The histological analysis also emphasizes the

importance to cover the wounded area in order to avoid scab formation and its microbial contamination, for which the presence of the dressings was crucial.

Taking into account all the results obtained, the developed membranes provide suitable wound-healing environment accomplishing the required criteria set forth for an ideal wound dressing. Particularly, PVA/CS+β-CD_IBP systems revealed to be those with the best characteristics for treating full-thickness wounds, since it is able to perform exudate absorption and vapor permeation compatible with a faster wound healing process, without scarring and also re-establishing all the functional and structural features of native skin. Moreover, the presence of IBP was crucial to prevent an excessive inflammatory phase during the first stages of healing and, consequently, to promote faster tissue repair. Based on the results obtained, we believe that the use of ibuprofen will be considered in skin regeneration and that the IBP-carriers herein reported can be easily extended as prototypes for sustained-release of other types of drugs.

Acknowledgments

The authors would like to thank the financial support from Fundação para a Ciência e Tecnologia (FCT - Lisbon) and FEDER funds through POCI-COMPETE 2020 contracts UID/Multi/00709/2013, UID/QUI/50006/2013, POCI-01-0145-FEDER-007265, POCI-01-0145-FEDER-007491 and SFRH/BD/80648/2011 (P.M.). The authors also thank Professor Isabel Coelhoso and her Ph.D. Student A. Rita Ferreira (Biochemical and Process Engineering Group, FCT-NOVA) for the help and scientific advice with the water vapor permeability measurements, Professor Teresa Casimiro and Dr. Vasco Bonifácio for the fruitful discussions, the Department of Materials Sciences (FCT-NOVA) to provide the equipment for mechanical measurements, and to Dr. Catarina Ferreira (FCS-UBI) for her technical support in the preparation of histological samples.

CHAPTER 4. *Conclusions and future prospects*

4. Conclusions and future prospects

4.1. Conclusions

The continuous search for an ideal wound dressing has resulted in the development of 3D constructs with different morphologies and topographies, made of synthetic and/or natural polymers, and loaded with/without cells or bioactive agents. Currently there are several commercially available tissue-engineered skin constructs, although none of them is able to fully reproduce the native structure and functions of skin.

One of the main purposes of this Ph.D. dissertation was to highlight the potential of asymmetrical membranes to be used as wound dressings. Indeed, they can be a feasible alternative to epidermal/dermal substitutes commercially available which require the use of silicone or bandages to mimic the top thin layer protecting the wound from physical damage and microorganisms penetration. These adhesive systems can cause tissue trauma once removed, leading to the increase of wound size, exacerbate wound pain and delay healing. Furthermore, the adhesives used can cause cutaneous allergy and do not allow cells adhesion and tissue proliferation. These factors can adversely affect patient's quality of life and have cost implications for healthcare providers. The use of an integral asymmetrical membrane can avoid such drawbacks through the use of biocompatible and biodegradable polymers, while mimicking the structure of a healthy skin.

Asymmetrical membranes were successfully produced through wet- and dry/wet-phase inversion techniques, presenting the suitable structure (thickness and porosity) to have the desired values of water uptake and vapor and gas permeation in order to promote a perfect wound healing process. However, those methods are time-consuming (the full process takes, usually, more than 24 h) and require the use of toxic solvents, which need to be removed by additional post-treatments. Furthermore, the studies reported so far only describe the use of two polymers, PU and CS, for the production of asymmetrical membranes using conventional methods due to the non-solvent used on the coagulation bath (usually NaOH-Na_2CO_3). Naturally, wound-management and care should not be restricted to two polymers, and to methods with high production costs.

To overcome such limitations, this work led to the implementation of greener, easier, clean and faster synthetic route to the production of asymmetrical membranes with hydrogel-like properties and drug delivery systems for skin wound healing. In fact, comparing the synthesis, it can be concluded that following $scCO_2$-assisted phase inversion method, instead of the conventional ones, a more sustainable protocol can be achieved with a clear reduction of purification steps and time and with by using safer and less toxic solvents (please see Table 4.1).

Table 4.1. Comparison between conventional and $scCO_2$ – assisted phase inversion methods on asymmetrical membranes development from a green chemistry point of view [48, 49, 88, 103, 224, 299].

Parameter	Conventional methods	$scCO_2$ synthesis	Green chemistry principles
Solvents used	2 (NaOH-Na_2CO_3 + distilled water)	2 ($scCO_2$ + ethanol)	Safer solvents Less hazardous synthesis
Purification steps	2	0	Design for separation
Time consumption (h)	24.17 - 25	4	Time efficiency
Temperatures (ºC)	50-70	45	Energy efficiency

To cope with this demand and realize the use of green approaches on wound management, asymmetrical dressings made of PVA/CS were developed using supercritical fluids technologies. The membranes presented a skin top layer of about 15 µm and a porous inner layer able to absorb a highly amount of exudate (350-450%). Interestingly, the dressings can gel upon contact with biological fluids forming a stable and durable (with low biodegradability) hydrogel-like sheets, able to maintain a humidified atmosphere at the wound and with suitable mechanical properties for handling.

However, as a property of hydrogel-like dressings all the drug cargo that is entrapped into the gel is usually released in a too short period of time, thus not suitable for wound healing. Indeed, such result was observed when IBP was loaded into the PVA/CS asymmetrical membranes developed: after 40 minutes all the drug cargo was release, which from the wound healing process point of view is really fast. As a non-steroidal anti-inflammatory drug it should be released at least 12 h post-injury which corresponds to the peak of the inflammatory phase [103, 224, 300]. To overcome such handicap and to turn sustainable the application of the PVA/CS membranes and to explore the effect of IBP in the treatment of full-thickness wounds (the two other main goals of this Ph.D. dissertation), PGDMA microbeads (synthesized in $scCO_2$ conditions) and β-CDs loaded with the drug were introduced into the hydrogel matrices modulating the release of the anti-inflammatory drug according to the demands of a good wound healing process. As observed on Figure 4.1, which correlates the wound healing phases with the percentage (M_t/M_∞) of IBP released and the percentage of wound healed over time by using the several dressings, the membranes containing the carriers enabled a more sustained drug release until the inflammatory phase. β-CDs revealed to be the best carrier releasing 79% of the drug cargo 12 h post-injury (corresponding to the peak of the inflammatory phase), while at the same time period almost 100% of IBP was released from PVA/CS+PK_IBP and

PVA/CS+PF_IBP systems. The sustained drug release from PVA/CS+β-CD_IBP led to faster skin regeneration as observed. In the groups treated with PVA/CS+PK_IBP and PVA/CS+PF_IBP an increase of the wound size was verified at days 4 and 7, which could be explained by the faster drug release from these systems that do not reached the time range of the inflammatory phase.

In addition, the *in vivo* studies emphasized that a simple and non-expensive (in comparison with several growth factors and other active agents) NSAID was crucial to prevent an excessive inflammatory phase at the early stage and to promote the tissue repair at the later stage of healing process. Moreover, the presence of the several dressings developed avoided scab formation.

Overall, the strategy presented in this work highlight the benefits of a simple NSAID for skin wound regeneration and opens new opportunities for the production of easy to use well-designed membranes to be handled as wound dressings that can act also as controlled drug release systems in a faster, clean, economic, non-time-consuming and non-labor intensive way.

Figure 4.1. Schematic representation of the effect of a sustained IBP release on skin wound regeneration taking into account the healing phases.

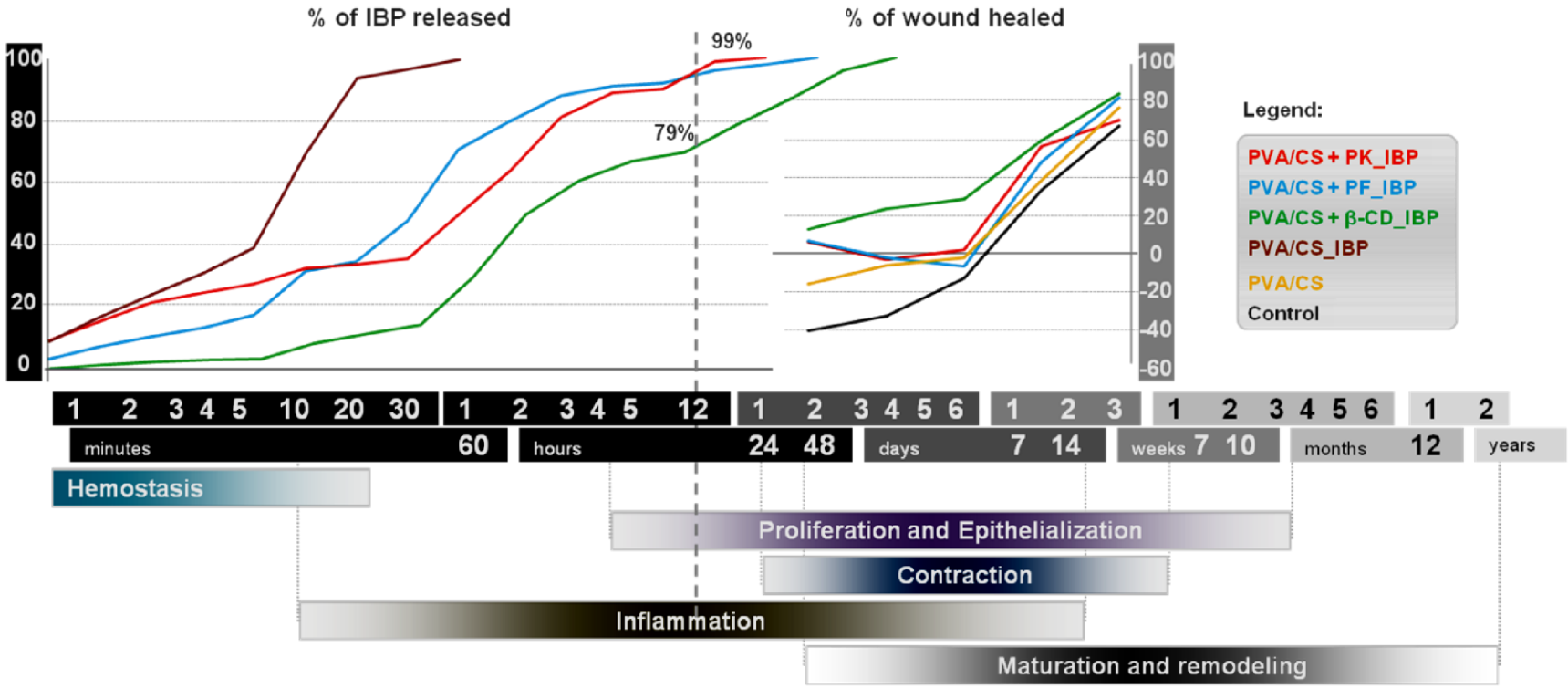

4.2. Future prospects

Since the $scCO_2$-assisted phase inversion method is a relatively new technique and was only applied recently for the production of asymmetrical dressings, the desired properties of an ideal wound dressing were not yet obtained, as can be concluded from data summarized in Table 4.2.

Table 4.2. Comparison of the properties of the different membranes developed taking into account the desired values of an ideal wound dressing.

Parameters	Desired values	PVA/CS	PVA/CS+PK	PVA/CS+PF	PVA/CS+β-CD
Thickness of the dense skin top layer (μm)	5-10	15	30	Not present (n.p.)	n.p.
Porosity (%) **Average pore diameter** (μm)	60-90 10-100	40 0.0995	56.2 0.58	56 0.51	37.1 0.77
Water uptake ability (%)	100-900	350-450	150-300	200-350	200-350
WVTR (x 10^2 g/m^2 day) **O_2 permeation** (L/m^2 day)	(20 - 25) 456 – 1840	1.2-2.1 11.6 x 10^{-4}	1.8 – 3.7 1.76 x 10^{-4}	6.9 – 10 31.5 x 10^{-4}	4.1 – 5.15 2.20 x 10^{-4}
Young's modulus (MPa)	4.6 - 20	0.96 – 7.4	0.26 – 0.69	0.25 – 0.86	0.18 – 0.42

A plethora of studies should be performed, opening new frontiers to develop better systems. The developed asymmetrical membranes produced by $scCO_2$-phase inversion technique made of PVA/CS present some limitations: the thickness of the top dense skin layer is high (~15 μm) and the porosity of the sponge-like inner layer (~40%) is low for a suitable balance between WVTR and gas flux permeation. As described previously, the membranes should present a dense skin top layer with a thickness of 5-10 μm and a porosity in the range of 60-90%. In addition, the pore diameter of the all membranes developed is too small which can also difficult the passage of the water vapor and oxygen molecules. The characteristics of the developed membranes could be improved by testing other pressures, temperatures, depressurization rates, other co-solvents and polymers or by using a stainless steel cap (the disk where the polymer solution is loaded) with lower height. Nonetheless, we believe that the high water uptake ability of the membranes developed through $scCO_2$-assisted phase inversion technique contrabalances the low water vapor and gaseous exchange improving the wound dressings' performance.

Additionally, it should be interesting to understand why the introduction of carriers avoided the formation of an asymmetrical structure on PVA/CS+PF and PVA/CS+β-CD membranes. From the biodegradability assays it seemed that the incorporation of the carriers within the polymeric

matrix increases the rate of degradation, due to the looser interactions between the PVA and CS, which *per si*, could also affect the inner structure of the membranes. However, more membranes should be developed and their inner structure evaluated. The interactions between IBP and β-CDs, the best drug delivery system reported, could be also an extremely interesting study to be performed.

Other type of polymers and carriers could also be tested. For example, dextran, a bacterial polysaccharide, has been extensively used in the treatment of burned skin wounds and as a carrier for a variety of therapeutic agents [164, 301-303]. Additionally, gelatin- and alginate-based microspheres have received a lot of attention as growth factor delivery systems for wound healing for decades. In addition to proteins, DNA-based chains have appeared as suitable alternatives with reduced productions costs and toxicity [261, 304-306].

As described, the use of green technologies for the production of asymmetrical membranes is just taking off, and therefore there is here a great opportunity for dreamer scientists to discover the long-awaited ideal dressing. Furthermore, the world economic status demands for inexpensive, non-time-consuming and non-labor intensive procedures. Considering an industrial application, the processes can be easily scaled-up and are only limited to the dimensions of the $scCO_2$ apparatus. However, it is crucial to unite multidisciplinary researchers, specially, clinicians, pharmacologists, chemists and engineers to continue to work together to meet this challenge.

BIBLIOGRAPHY

References

[1] M. Balasubramani, T.R. Kumar, M. Babu, Skin substitutes: a review, Burns, 27 (2001) 534-544.

[2] A.D. Metcalfe, M.W.J. Ferguson, Bioengineering skin using mechanisms of regeneration and repair, Biomaterials, 28 (2007) 5100-5113.

[3] L. Yildirimer, N.T. Thanh, A.M. Seifalian, Skin regeneration scaffolds: a multimodal bottom-up approach, Trends Biotechnol., 30 (2012) 638-648.

[4] S. Böttcher-Haberzeth, T. Biedermann, E. Reichmann, Tissue engineering of skin, Burns, 36 (2010) 450-460.

[5] R.A. Clark, K. Ghosh, M.G. Tonnesen, Tissue engineering for cutaneous wounds, J. Investig. Dermatol., 127 (2007) 1018-1029.

[6] D. Sachs, J. Voorhees, Age-Reversing Drugs and Devices in Dermatology, Clin. Pharmacol. Ther., 89 (2011) 34-43.

[7] R.V. Shevchenko, S.L. James, S.E. James, A review of tissue-engineered skin bioconstructs available for skin reconstruction, J. Roy. Soc. Interface, 7 (2010) 229-258.

[8] N. Dai, M. Williamson, N. Khammo, E. Adams, A. Coombes, Composite cell support membranes based on collagen and polycaprolactone for tissue engineering of skin, Biomaterials, 25 (2004) 4263-4271.

[9] A.P. Rodrigues, E.M. Saraiva Sanchez, A.C. da Costa, Â.M. Moraes, The influence of preparation conditions on the characteristics of chitosan-alginate dressings for skin lesions, J. Appl. Polym. Sci., 109 (2008) 2703-2710.

[10] J.M. Wong, D.O. Nyachieo, N.A. Benzekri, L. Cosmas, D. Ondari, S. Yekta, J.M. Montgomery, J.M. Williamson, R.F. Breiman, Sustained high incidence of injuries from burns in a densely populated urban slum in Kenya: An emerging public health priority, Burns, 40 (2014) 1194-1200.

[11] S.N. Forjuoh, Burns in low-and middle-income countries: a review of available literature on descriptive epidemiology, risk factors, treatment, and prevention, Burns, 32 (2006) 529-537.

[12] M.D. Peck, Epidemiology of burns throughout the world. Part I: Distribution and risk factors, Burns, 37 (2011) 1087-1100.

[13] Mock C., Peck M., Peden M., K. E., A World Health Organization plan for burn prevention and care, World Health Organization, Geneva, 2008.

[14] C.-C. Liao, A.M. Rossignol, Landmarks in burn prevention, Burns, 26 (2000) 422-434.

[15] C. Alemdaroglu, Z. Degim, N. Çelebi, F. Zor, S. Oztürk, D. Erdogan, An investigation on burn wound healing in rats with chitosan gel formulation containing epidermal growth factor, Burns, 32 (2006) 319-327.

[16] J. Boateng, K. Matthews, H. Stevens, G. Eccleston, Wound healing dressings and drug delivery systems: A review, J. Pharm. Sci., 97 (2008) 2892-2923.

[17] G.S. Lazarus, D.M. Cooper, D.R. Knighton, D.J. Margolis, R.E. Percoraro, G. Rodeheaver, M.C. Robson, Definitions and guidelines for assessment of wounds and evaluation of healing, Wound Repair Reg., 2 (1994) 165-170.

[18] D. Heimbach, L. Engrav, B. Grube, J. Marvin, Burn depth: a review, World J. Surg., 16 (1992) 10-15.

[19] S. Monstrey, H. Hoeksema, J. Verbelen, A. Pirayesh, P. Blondeel, Assessment of burn depth and burn wound healing potential, Burns, 34 (2008) 761-769.

[20] F. Sjöberg, Pre-hospital, fluid and early management, burn wound evaluation, Springer-Verlag/Wien, Handbook of burns, 2012.

[21] W. Paul, C. Sharma, Chitosan and alginate wound dressings: A short review, Trends Biomater. Artif. Organs, 18 (2004) 18-23.

[22] R. Shevchenko, S. James, S. James, A review of tissue-engineered skin bioconstructs available for skin reconstruction, J. Roy. Soc. Interface, 7 (2010) 229-258.

[23] S. MacNeil, Progress and opportunities for tissue-engineered skin, Nature, 445 (2007) 874-880.

[24] D.J. Wong, H.Y. Chang, Skin tissue engineering, The Stem Cell Research Community, StemBook, 126 (2009) 858-868.

[25] G. Gurtner, S. Werner, Y. Barrandon, M. Longaker, Wound repair and regeneration, Nature, 453 (2008) 314-321.

[26] K.S. Midwood, L.V. Williams, J.E. Schwarzbauer, Tissue repair and the dynamics of the extracellular matrix, Int. J. Biochem. Cell. B., 36 (2004) 1031-1037.

[27] S.A. Eming, T. Krieg, J.M. Davidson, Inflammation in wound repair: molecular and cellular mechanisms, J. Invest. Dermatol., 127 (2007) 514-525.

[28] L. Branski, C. Pereira, D. Herndon, M. Jeschke, Gene therapy in wound healing: present status and future directions, Gene Ther., 14 (2007) 1-10.

[29] F. Strodtbeck, Physiology of wound healing, Newborn Infant Nurs. Rev., 1 (2001) 43-52.

[30] F. Auger, D. Lacroix, L. Germain, Skin substitutes and wound healing, Skin Pharmacol. Physi., 22 (2009) 94-102.

[31] K. Ousey, C. McIntosh, Physiology of Wound Healing, Lower Extremity Wounds, Chapter 2 (2007) 25-46.

[32] A.K. Tsirogianni, N.M. Moutsopoulos, H.M. Moutsopoulos, Wound healing: immunological aspects, Injury, 37 (2006) S5-S12.

[33] T.J. Shaw, P. Martin, Wound repair at a glance, J. Cell Sci., 122 (2009) 3209-3213.

[34] S. Enoch, D.J. Leaper, Basic science of wound healing, Surgery, 26 (2008) 31-37.

[35] H. Meng, L. Chen, Z. Ye, S. Wang, X. Zhao, The effect of a self-assembling peptide nanofiber scaffold (peptide) when used as a wound dressing for the treatment of deep second degree burns in rats, J. Biomed. Mater. Res. B, 89 (2009) 379-391.

[36] B.S. Atiyeh, S.N. Hayek, S.W. Gunn, New technologies for burn wound closure and healing—review of the literature, Burns, 31 (2005) 944-956.

[37] E. Catalano, A. Cochis, E. Varoni, L. Rimondini, B. Azzimonti, Tissue-engineered skin substitutes: an overview, J. Art. Org., 16 (2013) 397-403.

[38] A.C. Brown, S.E. Stabenfeldt, B. Ahn, R.T. Hannan, K.S. Dhada, E.S. Herman, V. Stefanelli, N. Guzzetta, A. Alexeev, W.A. Lam, Ultrasoft microgels displaying emergent platelet-like behaviours, Nat. Mater., 13 (2014) 1108-1114.

[39] T.T. Nyame, H.A. Chiang, D.P. Orgill, Clinical Applications of Skin Substitutes, Surg. Clin. N. Am., 94 (2014) 839-850.

[40] F. Groeber, M. Holeiter, M. Hampel, S. Hinderer, K. Schenke-Layland, Skin tissue engineering - *In vivo* and *in vitro* applications, Adv. Drug Deliv. Rev., 63 (2011) 352-366.

[41] R.F. Pereira, C.C. Barrias, P.L. Granja, P.J. Bartolo, Advanced biofabrication strategies for skin regeneration and repair, Nanomedicine, 8 (2013) 603-621.

[42] S. Shahrokhi, A. Arno, M.G. Jeschke, The use of dermal substitutes in burn surgery: acute phase, Wound Repair Reg., 22 (2014) 14-22.

[43] S. Huang, X. Fu, Tissue-engineered skin: bottleneck or breakthrough, Int. J. Burn Trauma, 1 (2011) 1.

[44] G.G. Gauglitz, M.G. Jeschke, Combined gene and stem cell therapy for cutaneous wound healing, Mol. Pharm., 8 (2011) 1471-1479.

[45] S. Kobsa, N.J. Kristofik, A.J. Sawyer, A.L. Bothwell, T.R. Kyriakides, W.M. Saltzman, An electrospun scaffold integrating nucleic acid delivery for treatment of full-thickness wounds, Biomaterials, 34 (2013) 3891-3901.

[46] Y. Chen, L. Yan, T. Yuan, Q. Zhang, H. Fan, Asymmetric polyurethane membrane with *in situ* generated nano-TiO_2 as wound dressing, J. Appl. Polym. Sci., 119 (2011) 1532-1541.

[47] W. Hinrichs, E. Lommen, C.R. Wildevuur, J. Feijen, Fabrication and characterization of an asymmetric polyurethane membrane for use as a wound dressing, J. Appl. Biomater., 3 (1992) 287-303.

[48] L. Liu, D. Hu, G. Xu, L. Shou, J. Yao, Fabrication and evaluation of polyurethane-based asymmetric membranes, J. Mater. Sci. , 48 (2013) 1902-1910.

[49] F.-L. Mi, S.-S. Shyu, Y.-B. Wu, S.-T. Lee, J.-Y. Shyong, R.-N. Huang, Fabrication and characterization of a sponge-like asymmetric chitosan membrane as a wound dressing, Biomaterials, 22 (2001) 165-173.

[50] G.G. Gallico III, N.E. O'Connor, C.C. Compton, O. Kehinde, H. Green, Permanent coverage of large burn wounds with autologous cultured human epithelium, New England Journal of Medicine, 311 (1984) 448-451.

[51] A.K. Tausche, M. Skaria, L. Böhlen, K. Liebold, J. Hafner, H. Friedlein, M. Meurer, R.J. Goedkoop, U. Wollina, D. Salomon, An autologous epidermal equivalent tissue-engineered from follicular outer root sheath keratinocytes is as effective as split-thickness skin autograft in recalcitrant vascular leg ulcers, Wound Repair Reg., 11 (2003) 248-252.

[52] P. Lam, E. Chan, E. To, C. Lau, S. Yen, W. King, Development and evaluation of a new composite Laserskin graft, J. Traum., 47 (1999) 918-922.

[53] S. Johnsen, T. Ermuth, E. Tanczos, H. Bannasch, R. Horch, I. Zschocke, M. Peschen, E. Schöpf, W. Vanscheidt, M. Augustin, Treatment of therapy-refractive ulcera cruris of various origins with autologous keratinocytes in fibrin sealant, Vasa, 34 (2005) 25-29.

[54] Z. Ruszczak, Effect of collagen matrices on dermal wound healing, Adv. Drug Deliver. Rev., 55 (2003) 1595-1611.

[55] M. Moustafa, C. Simpson, M. Glover, R.A. Dawson, S. Tesfaye, F. Creagh, D. Haddow, R. Short, S. Heller, S. MacNeil, A new autologous keratinocyte dressing treatment for non-healing diabetic neuropathic foot ulcers, Diabetic Med., 21 (2004) 786-789.

[56] C. Zweifel, C. Contaldo, C. Köhler, A. Jandali, W. Künzi, P. Giovanoli, Initial experiences using non-cultured autologous keratinocyte suspension for burn wound closure, J. Plast. Recontr. Aes., 61 (2008) e1-e4.

[57] C. Dennis, Spray-on skin: Hard graft, Nature, 436 (2005) 166-167.

[58] J. Noordenbos, C. Doré, J.F. Hansbrough, Safety and Efficacy of TransCyte for the Treatment of Partial-Thickness Burns, J. Burn Care Res., 20 (1999) 275-281.

[59] W.A. Marston, J. Hanft, P. Norwood, R. Pollak, The Efficacy and Safety of Dermagraft in Improving the Healing of Chronic Diabetic Foot Ulcers Results of a prospective randomized trial, Diabetes Care, 26 (2003) 1701-1705.

[60] D. Wainwright, Use of an acellular allograft dermal matrix (AlloDerm) in the management of full-thickness burns, Burns, 21 (1995) 243-248.

[61] J.M. Still Jr, EZ DERM™ A Porcine Heterograft Material, Am J Clin Dermatol, 3 (2002) 507-508.

[62] C. Healy, J. Boorman, Comparison of EZ Derm and Jelonet dressings for partial skin thickness burns, Burns, 15 (1989) 52-54.

[63] A.P. Sclafani, T. Romo, A.A. Jacono, Rejuvenation of the aging lip with an injectable acellular dermal graft (Cymetra), Arch. Facial Plast. S., 4 (2002) 252-257.

[64] D. Levy, M.R. Banta, C.A. Charles, W.H. Eaglstein, R.S. Kirsner, Cymetra: a treatment option for refractory ulcers, Wounds, 16 (2004) 359-363.

[65] M. Tavis, J. Thornton, R. Bartlett, J. Roth, E. Woodroof, A new composite skin prosthesis, Burns, 7 (1980) 123-130.

[66] D. Giuggioli, M. Sebastiani, M. Cazzato, A. Piaggesi, G. Abatangelo, C. Ferri, Autologous skin grafting in the treatment of severe scleroderma cutaneous ulcers: a case report, Rheumatology, 42 (2003) 694-696.

[67] W. Haslik, L.-P. Kamolz, G. Nathschläger, H. Andel, G. Meissl, M. Frey, First experiences with the collagen-elastin matrix Matriderm® as a dermal substitute in severe burn injuries of the hand, Burns, 33 (2007) 364-368.

[68] N.S. Moiemen, E. Vlachou, J.J. Staiano, Y. Thawy, J.D. Frame, Reconstructive surgery with Integra dermal regeneration template: histologic study, clinical evaluation, and current practice, Plast. Reconstr. Surg., 117 (2006) 160S-174S.

[69] M. Eisenberg, D. Llewelyn, Surgical management of hands in children with recessive dystrophic epidermolysis bullosa: use of allogeneic composite cultured skin grafts, Brit. J. Plast. Surg., 51 (1998) 608-613.

[70] Y. Bello, A. Falabella, The role of graftskin (Apligraf) in difficult-to-heal venous leg ulcers, J. Wound Care, 11 (2002) 182-183.

[71] L. Uccioli, Clinical results related to the use of the TissueTech Autograft System in the treatment of diabetic foot ulceration, Wounds, 15 (2003) 279-288.

[72] S. Loeb, S. Sourirajan, Sea Water Demineralization by Means of an Osmotic Membrane, Adv Chem Ser, 38 (1963) 117-132.

[73] L. Sidney, The Loeb-Sourirajan Membrane: How It Came About, in: Synthetic Membranes:, American Chemical Society, 1981, pp. 1-9.

[74] T. Mohammadi, E. Saljoughi, Effect of production conditions on morphology and permeability of asymmetric cellulose acetate membranes, Desalination, 243 (2009) 1-7.

[75] F. Liu, N.A. Hashim, Y. Liu, M.M. Abed, K. Li, Progress in the production and modification of PVDF membranes, J. Membrane Sci., 375 (2011) 1-27.

[76] M.F.A. Wahab, A.F. Ismail, S.J. Shilton, Studies on gas permeation performance of asymmetric polysulfone hollow fiber mixed matrix membranes using nanosized fumed silica as fillers, Sep. Purif. Technol., 86 (2012) 41-48.

[77] N. Peng, N. Widjojo, P. Sukitpaneenit, M.M. Teoh, G.G. Lipscomb, T.-S. Chung, J.-Y. Lai, Evolution of polymeric hollow fibers as sustainable technologies: past, present, and future, Prog. Polym. Sci., 37 (2012) 1401-1424.

[78] S. Baumann, W. Meulenberg, H. Buchkremer, Manufacturing strategies for asymmetric ceramic membranes for efficient separation of oxygen from air, J. Eur. Ceram. Soc., 33 (2013) 1251-1261.

[79] H. Hachisuka, T. Ohara, K. Ikeda, New type asymmetric membranes having almost defect free hyper-thin skin layer and sponge-like porous matrix, J. Membrane Sci., 116 (1996) 265-272.

[80] M. Ikeguchi, K. Ishii, Y. Sekine, E. Kikuchi, M. Matsukata, Improving oxygen permeability in $SrFeCo_{0.5}O_x$ asymmetric membranes by modifying support-layer porous structure, Mater. Lett., 59 (2005) 1356-1360.

[81] K. Watenabe, M. Yuasa, T. Kida, Y. Teraoka, N. Yamazoe, K. Shimanoe, HighPerformance OxygenPermeable Membranes with an Asymmetric Structure Using Ba0. 95La0. 05FeO3− δ Perovskite-Type Oxide, Adv. Mater., 22 (2010) 2367-2370.

[82] Z. Zhu, W. Sun, L. Yan, W. Liu, W. Liu, Synthesis and hydrogen permeation of Ni–Ba (Zr 0.1 Ce 0.7 Y 0.2) O 3− δ metal–ceramic asymmetric membranes, Int. J. Hydrogen Energ., 36 (2011) 6337-6342.

[83] K.P. Lee, T.C. Arnot, D. Mattia, A review of reverse osmosis membrane materials for desalination - Development to date and future potential, J. Membrane Sci., 370 (2011) 1-22.

[84] Y. Dai, J. Johnson, O. Karvan, D.S. Sholl, W. Koros, Ultem®/ZIF-8 mixed matrix hollow fiber membranes for CO_2/N_2 separations, J. Membrane Sci., 401 (2012) 76-82.

[85] J. Gurauskis, Ø.F. Lohne, K. Wiik, $La_{0.2}Sr_{0.8}Fe_{0.8}Ta_{0.2}O_3$− δ based thin film membranes with surface modification for oxygen production, Solid State Ionics, 225 (2012) 703-706.

[86] R. Jayakumar, M. Prabaharan, P.S. Kumar, S. Nair, H. Tamura, Biomaterials based on chitin and chitosan in wound dressing applications, Biotechnol. Adv., 29 (2011) 322-337.

[87] Y. Xing, S. Baumann, S. Uhlenbruck, M. Rüttinger, A. Venskutonis, W. Meulenberg, D. Stöver, Development of a metallic/ceramic composite for the deposition of thin-film oxygen transport membrane, J. Eur. Ceram. Soc., 33 (2013) 287-296.

[88] F.-L. Mi, Y.-B. Wu, S.-S. Shyu, A.-C. Chao, J.-Y. Lai, C.-C. Su, Asymmetric chitosan membranes prepared by dry/wet phase separation: a new type of wound dressing for controlled antibacterial release, J. Membr. Sci., 212 (2003) 237-254.

[89] F.I. Broekema, W. van Oeveren, J. Zuidema, S.H. Visscher, R.R. Bos, *In vitro* analysis of polyurethane foam as a topical hemostatic agent, J. Mater. Sci.-Mater.M., 22 (2011) 1081-1086.

[90] K.-Y. Chen, W.-J. Liao, S.-M. Kuo, F.-J. Tsai, Y.-S. Chen, C.-Y. Huang, C.-H. Yao, Asymmetric chitosan membrane containing collagen I nanospheres for skin tissue engineering, Biomacromolecules, 10 (2009) 1642-1649.

[91] A. Busilacchi, A. Gigante, M. Mattioli-Belmonte, S. Manzotti, R.A. Muzzarelli, Chitosan stabilizes platelet growth factors and modulates stem cell differentiation toward tissue regeneration, Carbohyd. Polym., 98 (2013) 665-676.

[92] E. Lih, J.S. Lee, K.M. Park, K.D. Park, Rapidly curable chitosan–PEG hydrogels as tissue adhesives for hemostasis and wound healing, Acta Biomater., 8 (2012) 3261-3269.

[93] N.R. Kunio, G.M. Riha, K.M. Watson, J.A. Differding, M.A. Schreiber, J.M. Watters, Chitosan based advanced hemostatic dressing is associated with decreased blood loss in a swine uncontrolled hemorrhage model, Am. J. Surg., 205 (2013) 505-510.

[94] F.L. Mi, Y.B. Wu, S.S. Shyu, J.Y. Schoung, Y.B. Huang, Y.H. Tsai, J.Y. Hao, Control of wound infections using a bilayer chitosan wound dressing with sustainable antibiotic delivery, J. Biomed. Mater. Res., 59 (2002) 438-449.

[95] L.D. Tijing, A. Amarjargal, Z. Jiang, M.T.G. Ruelo, C.-H. Park, H.R. Pant, D.-W. Kim, D.H. Lee, C.S. Kim, Antibacterial tourmaline nanoparticles/polyurethane hybrid mat decorated with silver nanoparticles prepared by electrospinning and UV photoreduction, Curr. Appl. Phys., 13 (2013) 205-210.

[96] N. Wang, K. Burugapalli, W. Song, J. Halls, F. Moussy, Y. Zheng, Y. Ma, Z. Wu, K. Li, Tailored fibro-porous structure of electrospun polyurethane membranes, their size-dependent properties and trans-membrane glucose diffusion, J. Membrane Sci. , 427 (2013) 207-217.

[97] O. Ihata, Y. Kayaki, T. Ikariya, Synthesis of Thermoresponsive Polyurethane from 2-Methylaziridine and Supercritical Carbon Dioxide, Angew. Chem. Int. Edit., 43 (2004) 717-719.

[98] A.A. Nada, R. James, N.B. Shelke, M.D. Harmon, H.M. Awad, R.K. Nagarale, S.G. Kumbar, A smart methodology to fabricate electrospun chitosan nanofiber matrices for regenerative engineering applications, Polym. Adv. Technol., 25 (2014) 507-515.

[99] M. Temtem, L.M. Silva, P.Z. Andrade, F. dos Santos, C.L. da Silva, J.M. Cabral, M.M. Abecasis, A. Aguiar-Ricardo, Supercritical CO2 generating chitosan devices with controlled morphology. Potential application for drug delivery and mesenchymal stem cell culture, J. Supercrit. Fluid., 48 (2009) 269-277.

[100] A.R.C. Duarte, J. Mano, R. Reis, Supercritical fluids in biomedical and tissue engineering applications: a review, Int. Mater. Rev., 54 (2009) 214-222.

[101] G. Yan, J. Yu, Y. Qiu, X. Yi, J. Lu, X. Zhou, X. Bai, Self-assembly of electrospun polymer nanofibers: a general phenomenon generating honeycomb-patterned nanofibrous structures, Langmuir, 27 (2011) 4285-4289.

[102] B. Sun, Y.-Z. Long, F. Yu, M.-M. Li, H.-D. Zhang, W.-J. Li, T.-X. Xu, Self-assembly of a three-dimensional fibrous polymer sponge by electrospinning, Nanoscale, 4 (2012) 2134-2137.

[103] P.I. Morgado, P.F. Lisboa, M.P. Ribeiro, S.P. Miguel, P.C. Simões, I.J. Correia, A. Aguiar-Ricardo, Poly (vinyl alcohol)/chitosan asymmetrical membranes: Highly controlled morphology toward the ideal wound dressing, J. Membrane Sci., 469 (2014) 262-271.

[104] M. Khayet, C. Cojocaru, M.d.C. García-Payo, Experimental design and optimization of asymmetric flat-sheet membranes prepared for direct contact membrane distillation, J. Membrane Sci., 351 (2010) 234-245.

[105] J. Jansen, M. Buonomenna, A. Figoli, E. Drioli, Ultra-thin asymmetric gas separation membranes of modified PEEK prepared by the dry–wet phase inversion technique, Desalination, 193 (2006) 58-65.

[106] I. Pinnau, W.J. Koros, Influence of quench medium on the structures and gas permeation properties of polysulfone membranes made by wet and dry/wet phase inversion, J. Membrane Sci., 71 (1992) 81-96.

[107] I. Pinnau, W.J. Koros, A qualitative skin layer formation mechanism for membranes made by dry/wet phase inversion, J. Polym. Sci. B, 31 (1993) 419-427.

[108] H.-J. Cantow, R. Mülhaupt, Hermann Staudinger and Polymer Research in Freiburg, in: A.P. Sci. (Ed.) Hierarchical Macromolecular Structures: 60 Years after the Staudinger Nobel Prize I, Springer, 2013, pp. 21-37.

[109] S.P. Nalawade, F. Picchioni, L. Janssen, Supercritical carbon dioxide as a green solvent for processing polymer melts: Processing aspects and applications, Prog. Polym. Sci., 31 (2006) 19-43.

[110] Ž. Knez, E. Markočič, M. Leitgeb, M. Primožič, M.K. Hrnčič, M. Škerget, Industrial applications of supercritical fluids: A review, Energy, 77 (2014) 235-243.

[111] P.G. Jessop, W. Leitner, Chemical Synthesis Using Supercritical Fluids, in, Wiley Online Library, New York, 1999.

[112] E. Reverchon, R. Adami, R. Campardelli, G. Della Porta, I. De Marco, M. Scognamiglio, Supercritical fluids based techniques to process pharmaceutical products difficult to micronize: Palmitoylethanolamide, J. Supercrit. Fluid., 102 (2015) 24-31.

[113] R.C. Reid, J.M. Prausnitz, B.E. Poling, The properties of gases and liquids, McGraw Hill Book Co.,New York, NY, (1987).

[114] W. Leitner, Supercritical carbon dioxide as a green reaction medium for catalysis, Accounts Chem. Res., 35 (2002) 746-756.

[115] X. Han, M. Poliakoff, Continuous reactions in supercritical carbon dioxide: problems, solutions and possible ways forward, Chem. Soc. Rev., 41 (2012) 1428-1436.

[116] J.M. DeSimone, Practical approaches to green solvents, Science, 297 (2002) 799-803.

[117] M. Perrut, Supercritical fluid applications: industrial developments and economic issues, Ind. Eng. Chem. Res., 39 (2000) 4531-4535.

[118] R. Marr, T. Gamse, Use of supercritical fluids for different processes including new developments-a review, Chem. Eng. Process., 39 (2000) 19-28.

[119] W.-J. Kim, J.-D. Kim, J. Kim, S.-G. Oh, Y.-W. Lee, Selective caffeine removal from green tea using supercritical carbon dioxide extraction, J. Food Eng., 89 (2008) 303-309.

[120] H. Peker, M. Srinivasan, J. Smith, B.J. McCoy, Caffeine extraction rates from coffee beans with supercritical carbon dioxide, AICHE J., 38 (1992) 761-770.

[121] Y. Yonei, H. Ōhinata, R. Yoshida, Y. Shimizu, C. Yokoyama, Extraction of ginger flavor with liquid or supercritical carbon dioxide, J. Supercrit. Fluid., 8 (1995) 156-161.

[122] H. Daood, V. Illés, M. Gnayfeed, B. Mészáros, G. Horváth, P. Biacs, Extraction of pungent spice paprika by supercritical carbon dioxide and subcritical propane, J. Supercrit. Fluid., 23 (2002) 143-152.

[123] E. Reverchon, G.D. Porta, F. Senatore, Supercritical CO_2 extraction and fractionation of lavender essential oil and waxes, J. Agr. Food Chem., 43 (1995) 1654-1658.

[124] P.C. Simões, P.J. Carmelo, P.J. Pereira, J.A. Lopes, M.N. da Ponte, G. Brunner, Quality assessment of refined olive oils by gas extraction, J. Supercrit. Fluid., 13 (1998) 337-341.

[125] M. Sousa, M.J. Melo, T. Casimiro, A. Aguiar-Ricardo, The art of CO_2 for art conservation: a green approach to antique textile cleaning, Green Chem., 9 (2007) 943-947.

[126] G. Brunner, Applications of supercritical fluids, Annu. Rev. Chem. Biom. Eng., 1 (2010) 321-342.

[127] P. Christian, M.R. Giles, R.M. Griffiths, D.J. Irvine, R.C. Major, S.M. Howdle, Free radical polymerization of methyl methacrylate in supercritical carbon dioxide using a pseudo-graft

stabilizer: effect of monomer, initiator, and stabilizer concentrations, Macromolecules, 33 (2000) 9222-9227.

[128] A.I. Cooper, Porous materials and supercritical fluids, Adv. Mater., 15 (2003) 1049-1059.

[129] J. Barry, H. Gidda, C. Scotchford, S. Howdle, Porous methacrylate scaffolds: supercritical fluid fabrication and in vitro chondrocyte responses, Biomaterials, 25 (2004) 3559-3568.

[130] J. Jung, M. Perrut, Particle design using supercritical fluids: literature and patent survey, J. Supercrit. Fluid., 20 (2001) 179-219.

[131] A.R.C. Duarte, T. Casimiro, A. Aguiar-Ricardo, A.L. Simplício, C.M. Duarte, Supercritical fluid polymerisation and impregnation of molecularly imprinted polymers for drug delivery, J. Supercrit. Fluid., 39 (2006) 102-106.

[132] M.S. da Silva, R. Viveiros, P.I. Morgado, A. Aguiar-Ricardo, I.J. Correia, T. Casimiro, Development of 2-(dimethylamino) ethyl methacrylate-based molecular recognition devices for controlled drug delivery using supercritical fluid technology, Int. J. Pharm., 416 (2011) 61-68.

[133] P.X. Ma, Scaffolds for tissue fabrication, Mater. Today, 7 (2004) 30-40.

[134] X. Liu, P.X. Ma, Polymeric scaffolds for bone tissue engineering, Ann. Biomed. Eng., 32 (2004) 477-486.

[135] E. Reverchon, S. Cardea, Supercritical fluids in 3D tissue engineering, J. Supercrit. Fluid., 69 (2012) 97-107.

[136] M. Temtem, T. Casimiro, A. Aguiar-Ricardo, Solvent power and depressurization rate effects in the formation of polysulfone membranes with CO_2-assisted phase inversion method, J. Membrane Sci., 283 (2006) 244-252.

[137] S. Cardea, P. Pisanti, E. Reverchon, Generation of chitosan nanoporous structures for tissue engineering applications using a supercritical fluid assisted process, J. Supercrit. Fluid. , 54 (2010) 290-295.

[138] P. Van de Witte, P. Dijkstra, J. Van den Berg, J. Feijen, Phase separation processes in polymer solutions in relation to membrane formation, J. Membrane Sci., 117 (1996) 1-31.

[139] E. Drioli, L. Giorno, Comprehensive membrane science and engineering, Elsevier Science, Amsterdam, 2010.

[140] M. Temtem, D. Pompeu, G. Jaraquemada, E. Cabrita, T. Casimiro, A. Aguiar-Ricardo, Development of PMMA membranes functionalized with hydroxypropyl-β-cyclodextrins for controlled drug delivery using a supercritical CO_2-assisted technology, Int. J. Pharm., 376 (2009) 110-115.

[141] A.R.C. Duarte, V.E. Santo, A. Alves, S.S. Silva, J. Moreira-Silva, T.H. Silva, A.P. Marques, R.A. Sousa, M.E. Gomes, J.F. Mano, Unleashing the potential of supercritical fluids for polymer processing in tissue engineering and regenerative medicine, J. Supercrit.Fluids, 79 (2013) 177-185.

[142] S. Cardea, M. Sessa, E. Reverchon, Supercritical phase inversion to form drug-loaded poly(vinylidene fluoride-co-hexafluoropropylene) membranes, Ind. Eng. Chem. Res., 49 (2010) 2783-2789.

[143] C. Ji, N. Annabi, A. Khademhosseini, F. Dehghani, Fabrication of porous chitosan scaffolds for soft tissue engineering using dense gas CO_2, Acta Biomater., 7 (2011) 1653-1664.

[144] M. Temtem, T. Casimiro, J.F. Mano, A. Aguiar-Ricardo, Preparation of membranes with polysulfone/polycaprolactone blends using a high pressure cell specially designed for a CO_2-assisted phase inversion, J. Supercrit. Fluid., 43 (2008) 542-548.

[145] H. Tompa, Polymer solutions, London: Butterworths Scientific Publications 1956.

[146] H. Strathmann, P. Scheible, R. Baker, A rationale for the preparation of Loeb-Sourirajan-type cellulose acetate membranes, J. Appl. Polym. Sci., 15 (1971) 811-828.

[147] E. Reverchon, S. Cardea, C. Rapuano, Formation of poly-vinyl-alcohol structures by supercritical CO_2, J. Appl. Polym. Sci. , 104 (2007) 3151-3160.

[148] H. Matsuyama, H. Yano, T. Maki, M. Teramoto, K. Mishima, K. Matsuyama, Formation of porous flat membrane by phase separation with supercritical CO_2, J. Membrane Sci., 194 (2001) 157-163.

[149] H. Matsuyama, A. Yamamoto, H. Yano, T. Maki, M. Teramoto, K. Mishima, K. Matsuyama, Effect of organic solvents on membrane formation by phase separation with supercritical CO_2, J. Membrane Sci., 204 (2002) 81-87.

[150] E. Vatankhah, M.P. Prabhakaran, G. Jin, L.G. Mobarakeh, S. Ramakrishna, Development of nanofibrous cellulose acetate/gelatin skin substitutes for variety wound treatment applications, J. Biomater. Appl., 28 (2014) 909-921.

[151] W. Zhong, M.M. Xing, H.I. Maibach, Nanofibrous materials for wound care, Cutan. Ocul. Toxicol., 29 (2010) 143-152.

[152] L. Wu, H. Li, S. Li, X. Li, X. Yuan, X. Li, Y. Zhang, Composite fibrous membranes of PLGA and chitosan prepared by coelectrospinning and coaxial electrospinning, J. Biomed. Mater. Res. A, 92 (2010) 563-574.

[153] V. Leung, R. Hartwell, S.S. Elizei, H. Yang, A. Ghahary, F. Ko, Postelectrospinning modifications for alginate nanofiber-based wound dressings, J. Biomed. Mater.Res. B, 102 (2014) 508-515.

[154] R. Ng, R. Zang, K.K. Yang, N. Liu, S.-T. Yang, Three-dimensional fibrous scaffolds with microstructures and nanotextures for tissue engineering, RSC Advances, 2 (2012) 10110-10124.

[155] D. Nisbet, J. Forsythe, W. Shen, D. Finkelstein, M. Horne, Review paper: a review of the cellular response on electrospun nanofibers for tissue engineering, J. Biomater. Appl., 24 (2008) 7-29.

[156] B. Sun, Y. Long, H. Zhang, M. Li, J. Duvail, X. Jiang, H. Yin, Advances in three-dimensional nanofibrous macrostructures via electrospinning, Progress in Polymer Science, 39 (2014) 862-890.

[157] J.M. Holzwarth, P.X. Ma, 3D nanofibrous scaffolds for tissue engineering, J. Mater. Chem., 21 (2011) 10243-10251.

[158] N.J. Jenness, Y. Wu, R.L. Clark, Fabrication of three-dimensional electrospun microstructures using phase modulated femtosecond laser pulses, Mater. Lett., 66 (2012) 360-363.

[159] Q. Cheng, B.L.-P. Lee, K. Komvopoulos, S. Li, Engineering the microstructure of electrospun fibrous scaffolds by microtopography, Biomacromolecules, 14 (2013) 1349-1360.

[160] T.C. Reis, I.J. Correia, A. Aguiar-Ricardo, Electrodynamic tailoring of self-assembled three-dimensional electrospun constructs, Nanoscale, 5 (2013) 7528-7536.

[161] T.C. Reis, S. Castleberry, A.M. Rego, A. Aguiar-Ricardo, P.T. Hammond, Three-dimensional multilayered fibrous constructs for wound healing applications, Biomater. Sci., (2016).

[162] M. Serrano, R. Pagani, M. Vallet-Regı, J. Pena, A. Ramila, I. Izquierdo, M. Portolés, *In vitro* biocompatibility assessment of poly (ε-caprolactone) films using L929 mouse fibroblasts, Biomaterials, 25 (2004) 5603-5611.

[163] N. Faucheux, R. Schweiss, K. Lützow, C. Werner, T. Groth, Self-assembled monolayers with different terminating groups as model substrates for cell adhesion studies, Biomaterials, 25 (2004) 2721-2730.

[164] M. Ribeiro, P. Morgado, S. Miguel, P. Coutinho, I. Correia, Dextran-based hydrogel containing chitosan microparticles loaded with growth factors to be used in wound healing, Mater. Sci. Eng., 33 (2013) 2958-2966.

[165] M.P. Ribeiro, A. Espiga, D. Silva, P. Baptista, J. Henriques, C. Ferreira, J.C. Silva, J.P. Borges, E. Pires, P. Chaves, Development of a new chitosan hydrogel for wound dressing, Wound Repair Regen., 17 (2009) 817-824.

[166] M. Dias, P. Fernandes, J. Guedes, S. Hollister, Permeability analysis of scaffolds for bone tissue engineering, J. Biomech. , 45 (2012) 938-944.

[167] S.P. Miguel, M.P. Ribeiro, H. Brancal, P. Coutinho, I.J. Correia, Thermoresponsive chitosan-agarose hydrogel for skin regeneration, Carbohyd. Polym., 111 (2014) 366-373.

[168] Y. Yuan, T.R. Lee, Contact angle and wetting properties, in: Surface science techniques, Springer, 2013, pp. 3-34.

[169] A. Toncheva, M. Spasova, D. Paneva, N. Manolova, I. Rashkov, Polylactide (PLA)-based electrospun fibrous materials containing ionic drugs as wound dressing materials: A review, Int. J. Polym. Mater. , 63 (2014) 657-671.

[170] R. Augustine, E.A. Dominic, I. Reju, B. Kaimal, N. Kalarikkal, S. Thomas, Electrospun poly (ε-caprolactone)-based skin substitutes: *In vivo* evaluation of wound healing and the mechanism of cell proliferation, J. Biomed. Mater. Res. B, (2014).

[171] J.J. Elsner, M. Zilberman, Novel antibiotic-eluting wound dressings: An *in vitro* study and engineering aspects in the dressing's design, J. Tissue Viab., 19 (2010) 54-66.

[172] L.-O. Lamke, G. Nilsson, H. Reithner, The evaporative water loss from burns and the water-vapour permeability of grafts and artificial membranes used in the treatment of burns, Burns, 3 (1977) 159-165.

[173] D. Queen, J. Gaylor, J. Evans, J. Courtney, W. Reid, The preclinical evaluation of the water vapour transmission rate through burn wound dressings, Biomaterials, 8 (1987) 367-371.

[174] M.F. Jonkman, I. Molenaar, P. Nieuwenhuis, P. Bruin, A.J. Pennings, New method to assess the water vapour permeance of wound coverings, Biomaterials, 9 (1988) 263-267.

[175] A. Dias, M. Braga, I. Seabra, P. Ferreira, M. Gil, H. De Sousa, Development of natural-based wound dressings impregnated with bioactive compounds and using supercritical carbon dioxide, Int. J. Pharm., 408 (2011) 9-19.

[176] G.M. Gordillo, C.K. Sen, Revisiting the essential role of oxygen in wound healing, Am. J. Surg., 186 (2003) 259-263.

[177] A.A. Tandara, T.A. Mustoe, Oxygen in wound healing - more than a nutrient, World J. Surg., 28 (2004) 294-300.

[178] A. Bishop, Role of oxygen in wound healing, J. Wound Care, 17 (2008) 399-402.

[179] H. Xu, J. Chang, Y. Chen, H. Fan, B. Shi, Asymmetric polyurethane membrane with inflammation-responsive antibacterial activity for potential wound dressing application, J. Mater. Sci., 48 (2013) 6625-6639.

[180] D.M. D'Alessandro, B. Smit, J.R. Long, Carbon dioxide capture: prospects for new materials, Angew. Chem. Int. Edit., 49 (2010) 6058-6082.

[181] R.H. Swenson, R. Windgassen, Compositions expressing a pressure of carbon dioxide for improved healing of wounds, in, US6113922 A, 2000.

[182] S. Thomas, Surgical dressings and wound management, Medetec Publications, Cardiff, South Wales, 2010.

[183] H.B.T. Jeazet, C. Staudt, C. Janiak, Metal–organic frameworks in mixed-matrix membranes for gas separation, Dalton T., 41 (2012) 14003-14027.

[184] M. Szycher, S.J. Lee, Modern wound dressings: a systematic approach to wound healing, J. Biomater. Appl., 7 (1992) 142-213.

[185] H. Zahouani, C. Pailler-Mattei, B. Sohm, R. Vargiolu, V. Cenizo, R. Debret, Characterization of the mechanical properties of a dermal equivalent compared with human skin *in vivo* by indentation and static friction tests, Skin Res. Technol. , 15 (2009) 68-76.

[186] S.-Y. Ong, J. Wu, S.M. Moochhala, M.-H. Tan, J. Lu, Development of a chitosan-based wound dressing with improved hemostatic and antimicrobial properties, Biomaterials, 29 (2008) 4323-4332.

[187] B. Boekema, L. Pool, M. Ulrich, The effect of a honey based gel and silver sulphadiazine on bacterial infections of in vitro burn wounds, Burns, 39 (2012) 754-759.

[188] P.G. Bowler, S. Welsby, V. Towers, R. Booth, A. Hogarth, V. Rowlands, A. Joseph, S.A. Jones, Multidrug-resistant organisms, wounds and topical antimicrobial protection, Int. Wound J., 9 (2012) 387-396.

[189] S. Chusri, N. Chaicoch, W. Thongza-ard, S. Limsuwan, S.P. Voravuthikunchai, *In vitro* antibacterial activity of ethanol extracts of nine herbal formulas and its plant components used for skin infections in Southern Thailand, J. Med. Plants Res., 6 (2012) 1021-1027.

[190] A.J. Sawyer, D. Wesolowski, N. Gandotra, A. Stojadinovic, M. Izadjoo, S. Altman, T.R. Kyriakides, A peptide-morpholino oligomer conjugate targeting Staphylococcus aureus gyrA mRNA improves healing in an infected mouse cutaneous wound model, Int. J. Pharm., 453 (2013) 651-655.

[191] Y. Guo, R.I. Ramos, J.S. Cho, N.P. Donegan, A.L. Cheung, L.S. Miller, *In vivo* bioluminescence imaging to evaluate systemic and topical antibiotics against community-acquired methicillin-resistant *Staphylococcus aureus*-infected skin wounds in mice, Antimicrob. Agents Ch., 57 (2013) 855-863.

[192] V.G. Correia, M. Coelho, T. Barroso, V.P. Raje, V.D. Bonifácio, T. Casimiro, M.G. Pinho, A. Aguiar-Ricardo, Anti-biofouling 3D porous systems: the blend effect of oxazoline-based oligomers on chitosan scaffolds, Biofouling, 29 (2013) 273-282.

[193] V.G. Correia, V.D. Bonifácio, V.P. Raje, T. Casimiro, G. Moutinho, C.L. da Silva, M.G. Pinho, A. Aguiar-Ricardo, Oxazoline-Based Antimicrobial Oligomers: Synthesis by CROP Using Supercritical CO_2, Macromol. Biosci., 11 (2011) 1128-1137.

[194] M. Límová, Active wound coverings: bioengineered skin and dermal substitutes, Surg. Clin. N. Am., 90 (2010) 1237-1255.

[195] J. Mann, F. Oakley, F. Akiboye, A. Elsharkawy, A. Thorne, D. Mann, Regulation of myofibroblast transdifferentiation by DNA methylation and MeCP2: implications for wound healing and fibrogenesis, Cell Death Differ., 14 (2006) 275-285.

[196] J.W. Tyrone, J.E. Mogford, L.A. Chandler, C. Ma, Y. Xia, G.F. Pierce, T.A. Mustoe, Collagen-embedded platelet-derived growth factor DNA plasmid promotes wound healing in a dermal ulcer model, J. Surg. Res., 93 (2000) 230-236.

[197] J. Mann, D.A. Mann, Epigenetic regulation of wound healing and fibrosis, Curr. Opin. Rheumatol., 25 (2013) 101-107.

[198] S. Huang, Y. Xu, C. Wu, D. Sha, X. Fu, *In vitro* constitution and *in vivo* implantation of engineered skin constructs with sweat glands, Biomaterials, 31 (2010) 5520-5525.

[199] E.C. Costa, V.M. Gaspar, P. Coutinho, I.J. Correia, Optimization of liquid overlay technique to formulate heterogenic 3D co-cultures models, Biotechnol. Bioeng., 111 (2014) 1672-1685.

[200] M.Y. Bai, T.C. Chou, J.C. Tsai, W.C. Yu, The effect of active ingredient-containing chitosan/polycaprolactone nonwoven mat on wound healing: *In vitro* and *in vivo* studies, J. Biomed. Mater. Res. A, 102 (2014) 2324-2333.

[201] R.V. Shevchenko, M. Eeman, B. Rowshanravan, I.U. Allan, I.N. Savina, M. Illsley, M. Salmon, S.L. James, S.V. Mikhalovsky, S.E. James, The *in vitro* characterization of a gelatin scaffold, prepared by cryogelation and assessed *in vivo* as a dermal replacement in wound repair, Acta Biomater., 10 (2014) 3156-3166.

[202] N.A. Coolen, M. Vlig, A.J. Van Den Bogaerdt, E. Middelkoop, M.M. Ulrich, Development of an *in vitro* burn wound model, Wound Repair Reg., 16 (2008) 559-567.

[203] A. Alves, E.D. Pinho, N.M. Neves, R.A. Sousa, R.L. Reis, Processing ulvan into 2D structures: cross-linked ulvan membranes as new biomaterials for drug delivery applications, Int. J. Pharm., 426 (2012) 76-81.

[204] C. Weller, G. Sussman, Wound dressings update, J. Pharm. Pract. Res., 36 (2006) 318-324.

[205] A.R.C. Duarte, J.F. Mano, R.L. Reis, The role of organic solvent on the preparation of chitosan scaffolds by supercritical assisted phase inversion, J. Supercrit. Fluids, 72 (2012) 326-332.

[206] Q. Wang, Z. Dong, Y. Du, J.F. Kennedy, Controlled release of ciprofloxacin hydrochloride from chitosan/polyethylene glycol blend films, Carbohydr. Polym., 69 (2007) 336-343.

[207] Q. Wang, Y.m. Du, L.h. Fan, Properties of chitosan/poly(vinyl alcohol) films for drug-controlled release, J. Appl. Polym. Sci. , 96 (2005) 808-813.

[208] T. Dai, M. Tanaka, Y.-Y. Huang, M.R. Hamblin, Chitosan preparations for wounds and burns: antimicrobial and wound-healing effects, Expert Rev. Anti Infect. Ther., 9 (2011) 857-879.

[209] V.G. Correia, A.M. Ferraria, M.G. Pinho, A. Aguiar-Ricardo, Antimicrobial contact-active oligo(2-oxazoline)s-grafted surfaces for fast water disinfection at the point-of-use, Biomacromolecules, (2015).

[210] J. Siepmann, F. Siepmann, Mathematical modeling of drug delivery, Int. J. Pharm., 364 (2008) 328-343.

[211] V.D. Alves, A.R. Ferreira, N. Costa, F. Freitas, M.A. Reis, I.M. Coelhoso, Characterization of biodegradable films from the extracellular polysaccharide produced by Pseudomonas oleovorans grown on glycerol byproduct, Carbohyd. Polym., 83 (2011) 1582-1590.

[212] T.R. Correia, B.P. Antunes, P.H. Castilho, J.C. Nunes, M.T.P. de Amorim, I.C. Escobar, J.A. Queiroz, I.J. Correia, A.M. Morão, A bi-layer electrospun nanofiber membrane for plasmid DNA recovery from fermentation broths, Sep. Purif. Technol., 112 (2013) 20-25.

[213] R. Gonzalez, J. Tarloff, Evaluation of hepatic subcellular fractions for Alamar blue and MTT reductase activity, Toxicol. in vitro, 15 (2001) 257-259.

[214] A. Palmeira-de-Oliveira, M. Ribeiro, R. Palmeira-de-Oliveira, C. Gaspar, S. Costa-de-Oliveira, I. Correia, C. Pina Vaz, J. Martinez-de-Oliveira, J. Queiroz, A. Rodrigues, Anti-Candida activity of a chitosan hydrogel: mechanism of action and cytotoxicity profile, Gynecol. Obstet. Inves. , 70 (2010) 322-327.

[215] R.B. Restani, V.G. Correia, V.D. Bonifácio, A. Aguiar-Ricardo, Development of functional mesoporous microparticles for controlled drug delivery, J. Supercrit. Fluid., 55 (2010) 333-339.

[216] H.G. Landau, Heat conduction in a melting solid, Quart. Appl. Math, 8 (1950) 81-94.

[217] H. Fujita, Diffusion in polymer-diluent systems, Fortschritte der Hochpolymeren-Forschung, Springer, Berlin (1961) 1-47.

[218] R. Jarvis, C. Pantelides, DASOLV: a differential-algebraic equation solver, Center for Process Systems Engineering, Imperial College of Science, Technology, and Medicine, London, Version, 1 (1992).

[219] Gproms3.6, Model validation guide, London.

[220] E. Osti, Skin pH variations from the acute phase to re-epithelialization in burn patients treated with new materials (Burnshield®, Semipermeable Adhesive Film, Dermasilk®, and Hyalomatrix®). Non-Invasive Preliminary Experimental Clinical Trial, Ann. Burns Fire Disasters 21 (2008) 73-77.

[221] W.-W. Hu, Y.-J. Chen, R.-C. Ruaan, W.-Y. Chen, Y.-C. Cheng, C.-C. Chien, The regulation of DNA adsorption and release through chitosan multilayers, Carbohyd. Polym. , 99 (2014) 394-402.

[222] P. Wu, A. Fisher, P. Foo, D. Queen, J. Gaylor, *In vitro* assessment of water vapour transmission of synthetic wound dressings, Biomaterials, 16 (1995) 171-175.

[223] J. Lee, G. Tae, Y.H. Kim, I.S. Park, S.-H. Kim, S.H. Kim, The effect of gelatin incorporation into electrospun poly (l-lactide-co-ε-caprolactone) fibers on mechanical properties and cytocompatibility, Biomaterials, 29 (2008) 1872-1879.

[224] P.I. Morgado, A. Aguiar-Ricardo, I.J. Correia, Asymmetric membranes as ideal wound dressings: An overview on production methods, structure, properties and performance relationship, J. Membrane Sci., 490 (2015) 139-151.

[225] S. Silver, L.T. Phung, G. Silver, Silver as biocides in burn and wound dressings and bacterial resistance to silver compounds, J. Ind. Microbiol. Biot., 33 (2006) 627-634.

[226] B.S. Atiyeh, M. Costagliola, S.N. Hayek, S.A. Dibo, Effect of silver on burn wound infection control and healing: review of the literature, Burns, 33 (2007) 139-148.

[227] G. Sandri, M.C. Bonferoni, F. Ferrari, S. Rossi, C. Aguzzi, M. Mori, P. Grisoli, P. Cerezo, M. Tenci, C. Viseras, Montmorillonite–chitosan–silver sulfadiazine nanocomposites for topical treatment of chronic skin lesions: *in vitro* biocompatibility, antibacterial efficacy and gap closure cell motility properties, Carbohyd. Polym., 102 (2014) 970-977.

[228] K. Ito, A. Saito, T. Fujie, K. Nishiwaki, H. Miyazaki, M. Kinoshita, D. Saitoh, S. Ohtsubo, S. Takeoka, Sustainable antimicrobial effect of silver sulfadiazine-loaded nanosheets on infection in a mouse model of partial-thickness burn injury, Acta Biomater., 24 (2015) 87-95.

[229] L. Juan, Z. Zhimin, M. Anchun, L. Lei, Z. Jingchao, Deposition of silver nanoparticles on titanium surface for antibacterial effect, Int. J. Nanomed., 5 (2010) 261.

[230] A.K. Ekenseair, F.K. Kasper, A.G. Mikos, Perspectives on the interface of drug delivery and tissue engineering, Adv. Drug Deliv. Rev., 65 (2013) 89-92.

[231] X. Qiu, S. Leporatti, E. Donath, H. Möhwald, Studies on the drug release properties of polysaccharide multilayers encapsulated ibuprofen microparticles, Langmuir, 17 (2001) 5375-5380.

[232] G. Sun, X. Zhang, Y.-I. Shen, R. Sebastian, L.E. Dickinson, K. Fox-Talbot, M. Reinblatt, C. Steenbergen, J.W. Harmon, S. Gerecht, Dextran hydrogel scaffolds enhance angiogenic responses and promote complete skin regeneration during burn wound healing, P. Natl. A. Sci., 108 (2011) 20976-20981.

[233] W.K. Stadelmann, A.G. Digenis, G.R. Tobin, Impediments to wound healing, Am. J. Surg., 176 (1998) 39S-47S.

[234] R.G. Sibbald, H. Orsted, G.S. Schultz, P. Coutts, D. Keast, Preparing the wound bed 2003: focus on infection and inflammation, Ostomy Wound Manag., 49 (2003) 24-51.

[235] C.K. Sen, G.M. Gordillo, S. Roy, R. Kirsner, L. Lambert, T.K. Hunt, F. Gottrup, G.C. Gurtner, M.T. Longaker, Human skin wounds: a major and snowballing threat to public health and the economy, Wound Repair Regen. , 17 (2009) 763-771.

[236] T.C. Santos, B. Höring, K. Reise, A.P. Marques, S.S. Silva, J.M. Oliveira, J.F. Mano, A.G. Castro, R.L. Reis, M. van Griensven, *In vivo* performance of chitosan/soy-based membranes as wound-dressing devices for acute skin wounds, Tissue Eng. Pt. A, 19 (2013) 860-869.

[237] L. McNichol, C. Lund, T. Rosen, M. Gray, Medical adhesives and patient safety: state of the science: consensus statements for the assessment, prevention, and treatment of adhesive-related skin injuries, J. Dermatol. Nurse. Assoc., 5 (2013) 323-338.

[238] Y.-J. Park, R. Kwon, Q.Z. Quan, D.H. Oh, J.O. Kim, M.R. Hwang, Y.B. Koo, J.S. Woo, C.S. Yong, H.-G. Choi, Development of novel ibuprofen-loaded solid dispersion with improved bioavailability using aqueous solution, Arch. Pharm. Res., 32 (2009) 767-772.

[239] K. Müller-Decker, W. Hirschner, F. Marks, G. Fürstenberger, The Effects of Cyclooxygenase Isozyme Inhibition onIncisional Wound Healing in Mouse Skin, J. Invest. Dermatol., 119 (2002) 1189-1195.

[240] L.M. Coussens, Z. Werb, Inflammation and cancer, Nature, 420 (2002) 860-867.

[241] M. Milani, P. Iacobelli, Vaginal use of Ibuprofen isobutanolammonium (ginenorm): efficacy, tolerability, and pharmacokinetic data: a review of available data, ISRN Obstetrics Gynecol., 2012 (2012).

[242] Z. Yuan, J. Zhao, W. Zhu, Z. Yang, B. Li, H. Yang, Q. Zheng, W. Cui, Ibuprofen-loaded electrospun fibrous scaffold doped with sodium bicarbonate for responsively inhibiting inflammation and promoting muscle wound healing *in vivo*, Biomater. Sci., 2 (2014) 502-511.

[243] S. Heilmann, S. Küchler, C. Wischke, A. Lendlein, C. Stein, M. Schäfer-Korting, A thermosensitive morphine-containing hydrogel for the treatment of large-scale skin wounds, Int. J. Pharm., 444 (2013) 96-102.

[244] H.-E. Thu, M.H. Zulfakar, S.-F. Ng, Alginate based bilayer hydrocolloid films as potential slow-release modern wound dressing, Int. J. Pharm., 434 (2012) 375-383.

[245] B. Steffansen, S.P. Herping, Novel wound models for characterizing ibuprofen release from foam dressings, Int. J. Pharm., 364 (2008) 150-155.

[246] B. Jørgensen, G.J. Friis, F. Gottrup, Pain and quality of life for patients with venous leg ulcers: proof of concept of the efficacy of Biatain®-Ibu, a new pain reducing wound dressing, Wound Repair Regen., 14 (2006) 233-239.

[247] M. Temtem, D. Pompeu, T. Barroso, J. Fernandes, P.C. Simões, T. Casimiro, A.M.B. do Rego, A. Aguiar-Ricardo, Development and characterization of a thermoresponsive polysulfone membrane using an environmental friendly technology, Green Chem., 11 (2009) 638-645.

[248] T. Barroso, M. Temtem, T. Casimiro, A. Aguiar-Ricardo, Development of pH-responsive poly(methylmethacrylate-co-methacrylic acid) membranes using $scCO_2$ technology. Application to protein permeation., J. Supercrit. Fluid., 51 (2009) 57-66.

[249] M.S. Da Silva, R. Viveiros, M.B. Coelho, A. Aguiar-Ricardo, T. Casimiro, Supercritical CO_2-assisted preparation of a PMMA composite membrane for bisphenol A recognition in aqueous environment, Chem. Eng. Sci., 68 (2012) 94-100.

[250] T. Barroso, M. Temtem, T. Casimiro, A. Aguiar-Ricardo, Antifouling performance of poly(acrylonitrile)-based membranes: from green synthesis to application, J. Supercrit. Fluid., 56 (2011) 312-321.

[251] T. Hoare, D. Kohane, Hydrogels in drug delivery: Progress and challenges, Polymer, 49 (2008) 1993-2007.

[252] M. Kokabi, M. Sirousazar, Z.M. Hassan, PVA–clay nanocomposite hydrogels for wound dressing, Eur. Polym. J., 43 (2007) 773-781.

[253] M. Hamidi, A. Azadi, P. Rafiei, Hydrogel nanoparticles in drug delivery, Adv. Drug Deliver. Rev., 60 (2008) 1638-1649.

[254] S.S. Anumolu, A.R. Menjoge, M. Deshmukh, D. Gerecke, S. Stein, J. Laskin, P.J. Sinko, Doxycycline hydrogels with reversible disulfide crosslinks for dermal wound healing of mustard injuries, Biomaterials, 32 (2011) 1204-1217.

[255] H.J. Yoo, H.D. Kim, Synthesis and properties of waterborne polyurethane hydrogels for wound healing dressings, J. Biomed. Mater. Res. B, 85 (2008) 326-333.

[256] J.O. Kim, J.K. Park, J.H. Kim, S.G. Jin, C.S. Yong, D.X. Li, J.Y. Choi, J.S. Woo, B.K. Yoo, W.S. Lyoo, Development of polyvinyl alcohol–sodium alginate gel-matrix-based wound dressing system containing nitrofurazone, Int. J. Pharm., 359 (2008) 79-86.

[257] T. Coviello, P. Matricardi, C. Marianecci, F. Alhaique, Polysaccharide hydrogels for modified release formulations, J. Control. Release, 119 (2007) 5-24.

[258] F. Brandl, F. Kastner, R.M. Gschwind, T. Blunk, J. Teßmar, A. Göpferich, Hydrogel-based drug delivery systems: comparison of drug diffusivity and release kinetics, J. Control. Release, 142 (2010) 221-228.

[259] S. Koutsopoulos, S. Zhang, Two-layered injectable self-assembling peptide scaffold hydrogels for long-term sustained release of human antibodies, J. Control. Release, 160 (2012) 451-458.

[260] C.J. Park, S.G. Clark, C.A. Lichtensteiger, R.D. Jamison, A.J.W. Johnson, Accelerated wound closure of pressure ulcers in aged mice by chitosan scaffolds with and without bFGF, Acta Biomater., 5 (2009) 1926-1936.

[261] F. Gu, B. Amsden, R. Neufeld, Sustained delivery of vascular endothelial growth factor with alginate beads, J. Control. Release, 96 (2004) 463-472.

[262] T.W. Prow, J.E. Grice, L.L. Lin, R. Faye, M. Butler, W. Becker, E.M. Wurm, C. Yoong, T.A. Robertson, H.P. Soyer, Nanoparticles and microparticles for skin drug delivery, Adv. Drug Deliver. Rev., 63 (2011) 470-491.

[263] L. Mei, D. Hu, J. Ma, X. Wang, Y. Yang, J. Liu, Preparation, characterization and evaluation of chitosan macroporous for potential application in skin tissue engineering, Int. J. Biol. Macromol., 51 (2012) 992-997.

[264] C. Guse, S. Koennings, F. Kreye, F. Siepmann, A. Göpferich, J. Siepmann, Drug release from lipid-based implants: elucidation of the underlying mass transport mechanisms, Int. J. Pharm., 314 (2006) 137-144.

[265] D. Limón, E. Amirthalingam, M. Rodrigues, L. Halbaut, B. Andrade, M.L. Garduño-Ramírez, D.B. Amabilino, L. Pérez-García, A.C. Calpena, Novel nanostructured supramolecular hydrogels for the topical delivery of anionic drugs, Eur. J. Pharm. Biopharm., 96 (2015) 421-436.

[266] M. Gimeno, P. Pinczowski, M. Pérez, A. Giorello, M.Á. Martínez, J. Santamaría, M. Arruebo, L. Luján, A controlled antibiotic release system to prevent orthopedic-implant associated infections: An *in vitro* study, Eur. J. Pharm. Biopharm., 96 (2015) 264-271.

[267] S. Junco, T. Casimiro, N. Ribeiro, M.N. Da Ponte, H.C. Marques, A comparative study of naproxen–beta cyclodextrin complexes prepared by conventional methods and using supercritical carbon dioxide, J. Incl. Phenom. Macro., 44 (2002) 117-121.

[268] K. Hussein, M. Türk, M.A. Wahl, Comparative evaluation of ibuprofen/β-cyclodextrin complexes obtained by supercritical carbon dioxide and other conventional methods, Pharm. Res., 24 (2007) 585-592.

[269] A. Vyas, S. Saraf, S. Saraf, Cyclodextrin based novel drug delivery systems, J. Incl. Phenom. Macro., 62 (2008) 23-42.

[270] M. Di Cagno, P.C. Stein, N. Skalko-Basnet, M. Brandl, A. Bauer-Brandl, Solubilization of ibuprofen with β-cyclodextrin derivatives: Energetic and structural studies, J. Pharmaceut. Biomed., 55 (2011) 446-451.

[271] S. Rawat, S.K. Jain, Solubility enhancement of celecoxib using β-cyclodextrin inclusion complexes, Eur. J. Pharm. Biopharm., 57 (2004) 263-267.

[272] A. Löber, A. Verch, B. Schlemmer, S. Höfer, B. Frerich, M.R. Buchmeiser, Monolithic polymers for cell cultivation, differentiation, and tissue engineering, Angew. Chem. Int. Edit. , 47 (2008) 9138-9141.

[273] L.A. Neves, J.G. Crespo, I.M. Coelhoso, Gas permeation studies in supported ionic liquid membranes, J. Membrane Sci., 357 (2010) 160-170.

[274] P.L. Ritger, N.A. Peppas, A simple equation for description of solute release II. Fickian and anomalous release from swellable devices, J. Control. Release, 5 (1987) 37-42.

[275] P.L. Ritger, N.A. Peppas, A simple equation for description of solute release I. Fickian and non-Fickian release from non-swellable devices in the form of slabs, spheres, cylinders or discs, J. Control. Release, 5 (1987) 23-36.

[276] J.G. Marques, V.M. Gaspar, E. Costa, C.M. Paquete, I.J. Correia, Synthesis and characterization of micelles as carriers of non-steroidal anti-inflammatory drugs (NSAID) for application in breast cancer therapy, Colloid. Surface. B 113 (2014) 375-383.

[277] A. Zonari, T.M. Martins, A.C.C. Paula, J.N. Boleoni, S. Novikoff, A.P. Marques, V.M. Correlo, R.L. Reis, A.M. Goes, Polyhydroxybutyrate-co-hydroxyvalerate structures loaded with adipose stem cells promote skin healing with reduced scarring, Acta Biomater. , (2015).

[278] W. Hennink, C.F. Van Nostrum, Novel crosslinking methods to design hydrogels, Adv. Drug Deliv. Rev., 64 (2012) 223-236.

[279] I. Gibas, H. Janik, Review: synthetic polymer hydrogels for biomedical applications, Chem. Chem. Technol., 4 (2010).

[280] S.J. Buwalda, K.W. Boere, P.J. Dijkstra, J. Feijen, T. Vermonden, W.E. Hennink, Hydrogels in a historical perspective: from simple networks to smart materials, J. Control. Release 190 (2014) 254-273.

[281] E. Reverchon, S. Cardea, E.S. Rappo, Production of loaded PMMA structures using the supercritical CO_2 phase inversion process, J. Membrane Sci., 273 (2006) 97-105.

[282] E. Reverchon, S. Cardea, C. Rapuano, A new supercritical fluid-based process to produce scaffolds for tissue replacement, J. Supercrit. Fluid., 45 (2008) 365-373.

[283] Y. Houdas, E. Ring, Human body temperature, Springer Science & Business Media, 1982.

[284] V.G. Sakhrani, C. Tomasino, Method for treating a hydrophilic surface, in, US8084103 B2, 2011.

[285] F. Loeker, P.C. Marr, S.M. Howdle, FTIR analysis of water in supercritical carbon dioxide microemulsions using monofunctional perfluoropolyether surfactants, Colloid. Surface. A, 214 (2003) 143-150.

[286] A.K. Chatjigakis, C. Donze, A.W. Coleman, P. Cardot, Solubility behavior of beta-cyclodextrin in water/cosolvent mixtures, Anal. Chem. , 64 (1992) 1632-1634.

[287] P. Wong, MSc Thesis, University of Strathclyde, (1980).

[288] S. Meaume, L. Teot, I. Lazareth, J. Martini, S. Bohbot, Importance of pain reduction through dressing selection in routine wound management: the MAPP study, J. Wound Care 13 (2004) 409-414.

[289] L. Khalid, O. Stojadinovic, M. Tomic-Canic, Post-operative Wound Care and Dressings, in: Handbook of Lasers in Dermatology, Springer, 2014, pp. 425-435.

[290] N. Arya, S. Chakraborty, N. Dube, D.S. Katti, Electrospraying: A facile technique for synthesis of chitosan-based micro/nanospheres for drug delivery applications, J. Biomed. Mater. Res. B 88 (2009) 17-31.

[291] J. Siepmann, N. Peppas, Modeling of drug release from delivery systems based on hydroxypropyl methylcellulose (HPMC), Adv. Drug Deliver. Rev., 64 (2012) 163-174.

[292] M.L. Bruschi, Strategies to Modify the Drug Release from Pharmaceutical Systems, Woodhead publishing series in biomedicine. Elsevier, (2015).

[293] R. Challa, A. Ahuja, J. Ali, R. Khar, Cyclodextrins in drug delivery: an updated review, Aaps Pharmscitech, 6 (2005) E329-E357.

[294] I.V. Yannas, Emerging rules for inducing organ regeneration, Biomaterials, 34 (2013) 321-330.

[295] E.R. Lorden, K.J. Miller, L. Bashirov, M.M. Ibrahim, E. Hammett, Y. Jung, M.A. Medina, A. Rastegarpour, M.A. Selim, K.W. Leong, Mitigation of hypertrophic scar contraction via an elastomeric biodegradable scaffold, Biomaterials, 43 (2015) 61-70.

[296] T.J. Koh, L.A. DiPietro, Inflammation and wound healing: the role of the macrophage, Expert Rev. Mol. Med., 13 (2011) e23.

[297] W. Cheng, R. Yan-hua, N. Fang-gang, Z. Guo-an, The content and ratio of type I and III collagen in skin differ with age and injury, Afr. J. Biotechnol. , 10 (2013) 2524-2529.

[298] A. Nyström, D. Velati, V.R. Mittapalli, A. Fritsch, J.S. Kern, L. Bruckner-Tuderman, Collagen VII plays a dual role in wound healing, J. Clin. Invest. , 123 (2013) 3498–3509.

[299] A. Aguiar-Ricardo, V.D. Bonifácio, T. Casimiro, V.G. Correia, Supercritical carbon dioxide design strategies: from drug carriers to soft killers, Phil. Trans. R. Soc. A, 373 (2015) 20150009.

[300] J. Li, J. Chen, R. Kirsner, Pathophysiology of acute wound healing, Clin. Dermatol., 25 (2007) 9-18.

[301] G. Sun, X. Zhang, Y.-I. Shen, R. Sebastian, L.E. Dickinson, K. Fox-Talbot, M. Reinblatt, C. Steenbergen, J.W. Harmon, S. Gerecht, Dextran hydrogel scaffolds enhance angiogenic responses and promote complete skin regeneration during burn wound healing, P. Natl. Acad. Sci. USA, 108 (2011) 20976-20981.

[302] A.R. Unnithan, N.A. Barakat, P.T. Pichiah, G. Gnanasekaran, R. Nirmala, Y.-S. Cha, C.-H. Jung, M. El-Newehy, H.Y. Kim, Wound-dressing materials with antibacterial activity from electrospun polyurethane–dextran nanofiber mats containing ciprofloxacin HCl, Carbohyd. Polym., 90 (2012) 1786-1793.

[303] M.-R. Hwang, J.O. Kim, J.H. Lee, Y.I. Kim, J.H. Kim, S.W. Chang, S.G. Jin, J.A. Kim, W.S. Lyoo, S.S. Han, Gentamicin-loaded wound dressing with poly(vinyl alcohol)/dextran hydrogel: gel characterization and *in vivo* healing evaluation, Aaps Pharmscitech, 11 (2010) 1092-1103.

[304] T.A. Holland, Y. Tabata, A.G. Mikos, *In vitro* release of transforming growth factor-β1 from gelatin microparticles encapsulated in biodegradable, injectable oligo (poly (ethylene glycol) fumarate) hydrogels, J. Control. Release, 91 (2003) 299-313.

[305] J. Panyam, V. Labhasetwar, Biodegradable nanoparticles for drug and gene delivery to cells and tissue, Adv. Drug Deliver. Rev., 55 (2003) 329-347.

[306] S. Huang, X. Fu, Naturally derived materials-based cell and drug delivery systems in skin regeneration, J. Control. Release, 142 (2010) 149-159.

SUPPLEMENTARY INFORMATION

Supplementary information

Chapter 2. *Poly(vinyl alcohol)/chitosan asymmetrical membranes: highly controlled morphology toward the ideal wound dressing*

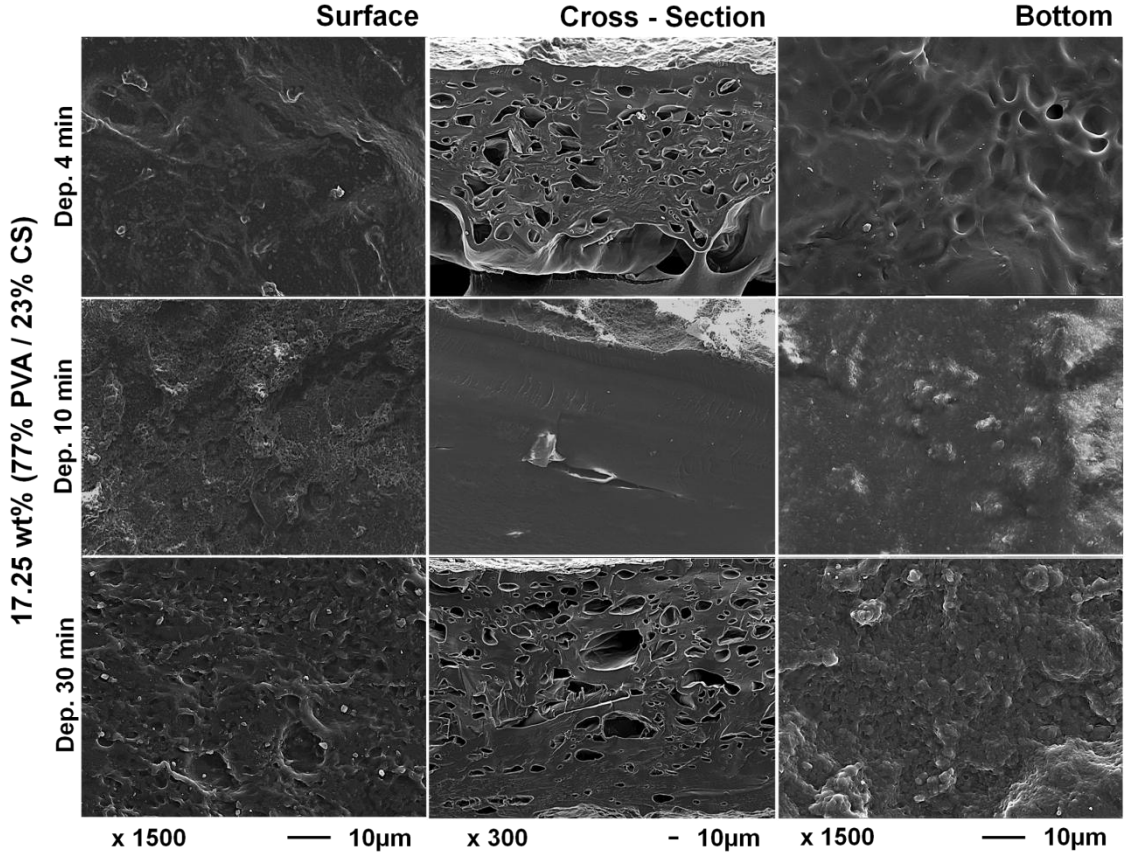

Figure S2.1. Scanning electron micrographs of 17.25 wt% (77% PVA / 23% CS) membranes surface, cross-section and bottom obtained with depressurization rates of 4, 10 and 30 min.

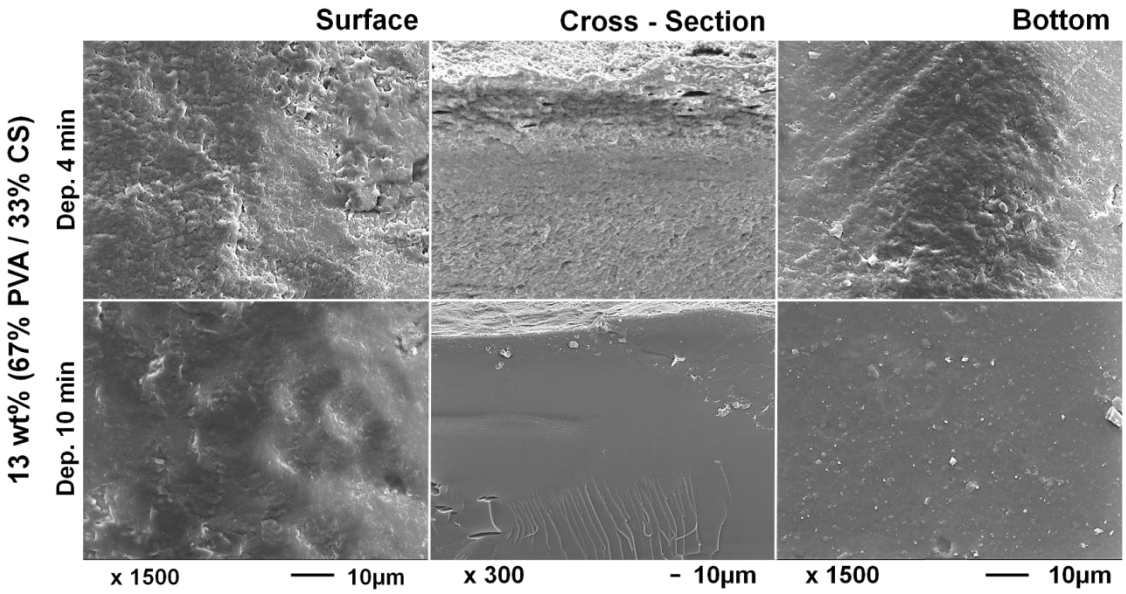

Figure S2.2. Scanning electron micrographs of 13 wt% (67% PVA / 33% CS) membranes surface, cross-section and bottom obtained with depressurization rates of 4 and 10 min.

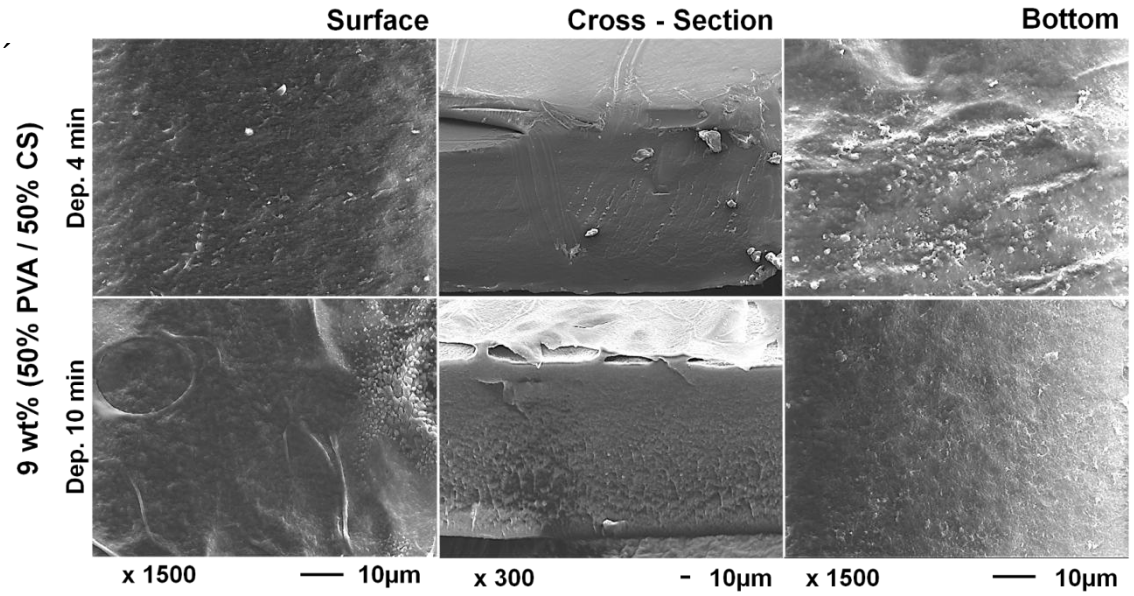

Figure S2.3. Scanning electron micrographs of 9 wt% (50% PVA / 50% CS) membranes surface, cross-section and bottom obtained with depressurization rates of 4 and 10 min.

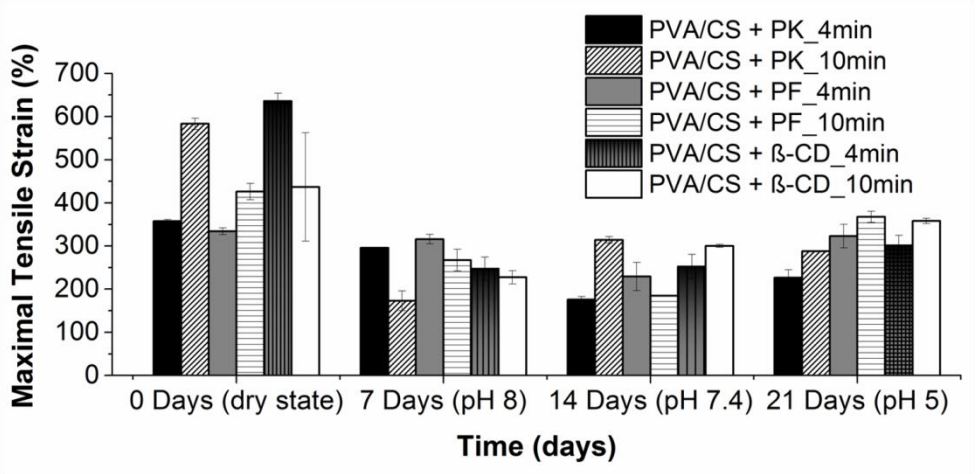

Figure S3.1. Maximal tensile strain (%) analysis of PVA/CS_4min and PVA/CS_10min membranes with the different carriers at dry and wet state.

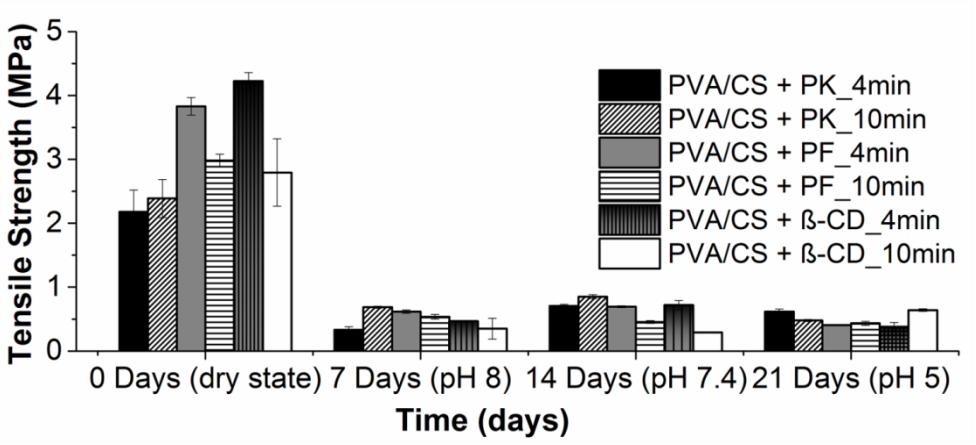

Figure S3.2. Tensile strength (MPa) analysis of PVA/CS_4min and PVA/CS_10min membranes with the different carriers at dry and wet state.

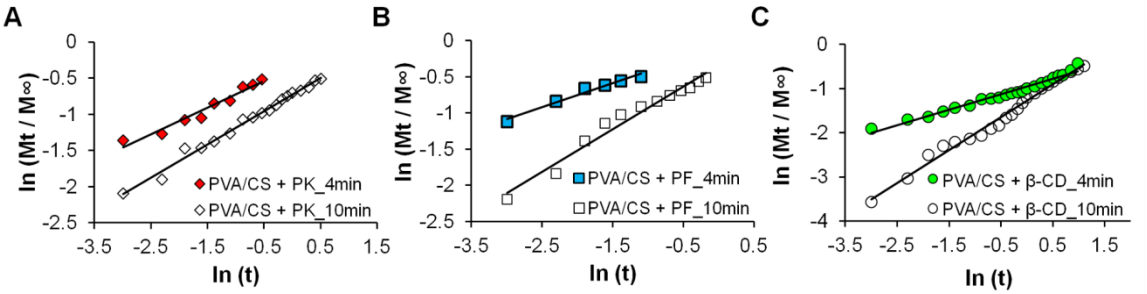

Figure S3.3. Korsmeyer-Peppas Model for mechanism of IBP release from the different drug delivery systems at pH 8 and 35º C: (**A**) PVA/CS+PK_4min (♦) and PVA/CS+PK_10min (◊); (**B**) PVA/CS+PF_4min (■) and PVA/CS+PF_10min (□); (**C**) PVA/CS+β-CD_4min (●) and PVA/CS+β-CD_10min (○) membranes.

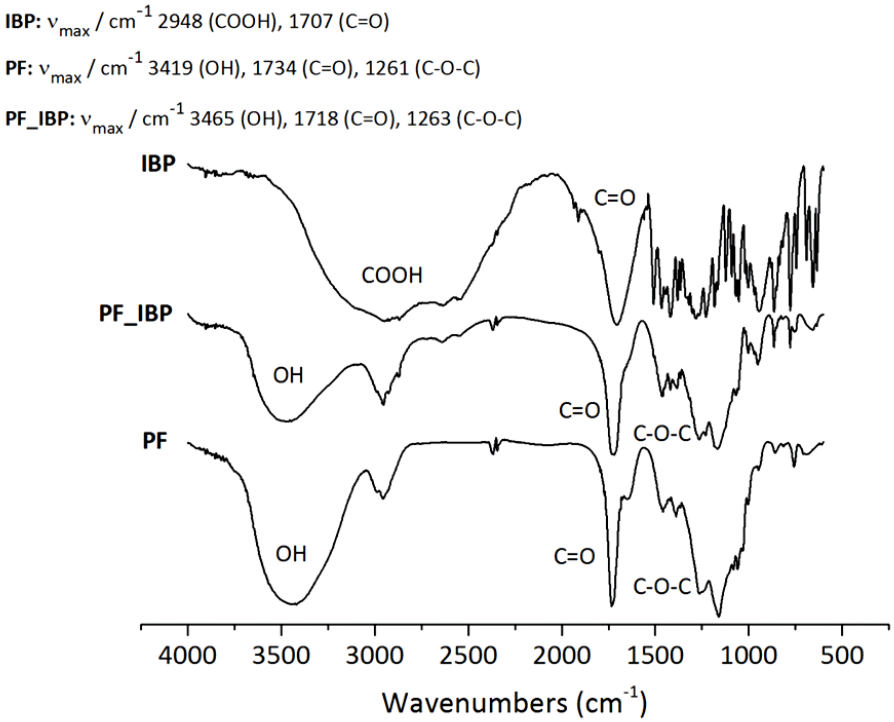

Figure S3.4. ATR-FTIR spectra of pure (*S*)-IBP, PF microbeads loaded with IBP (PF_IBP) and PF microbeads.

IBP: ν_{max} / cm^{-1} 2948 (COOH), 1707 (C=O)

PK: ν_{max} / cm^{-1} 3447 (OH), 1725 (C=O), 1262 (C-O-C)

PK_IBP: ν_{max} / cm^{-1} 3462 (OH), 1726 (C=O), 1263 (C-O-C)

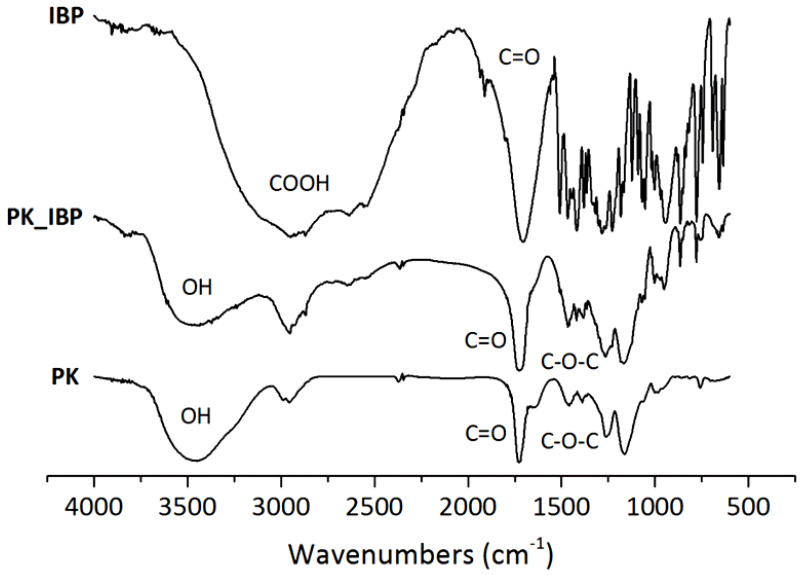

Figure S3.5. ATR-FTIR spectra of pure (*S*)-IBP, PK microbeads loaded with IBP (PK_IBP) and PK microbeads.

IBP: ν_{max} / cm^{-1} 2948 (COOH), 1707 (C=O)

β - CD: ν_{max} / cm^{-1} 2923 (Cyclohexane), 1157 (C-O-C)

β - CD_IBP: ν_{max} / cm^{-1} 2923 (Cyclohexane), 1157 (C-O-C)

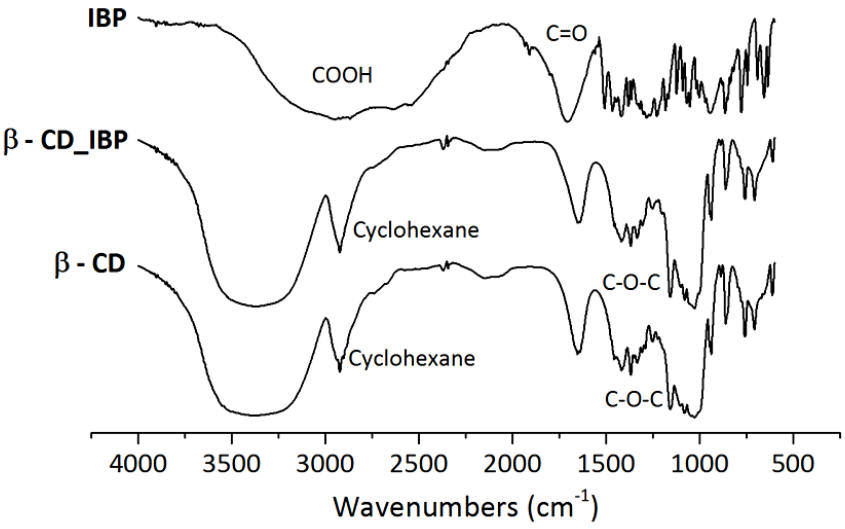

Figure S3.6. ATR-FTIR spectra of pure (*S*)-IBP, β-CD loaded with IBP (β-CD_IBP) and β-CD without IBP.

PVA characteristic bands: ν / cm^{-1} 3200 - 3300 (OH), 2898 - 2935 (CH_2)

CS characteristic bands: ν / cm^{-1} 3200 - 3300 (OH), 1560 (NH_2)

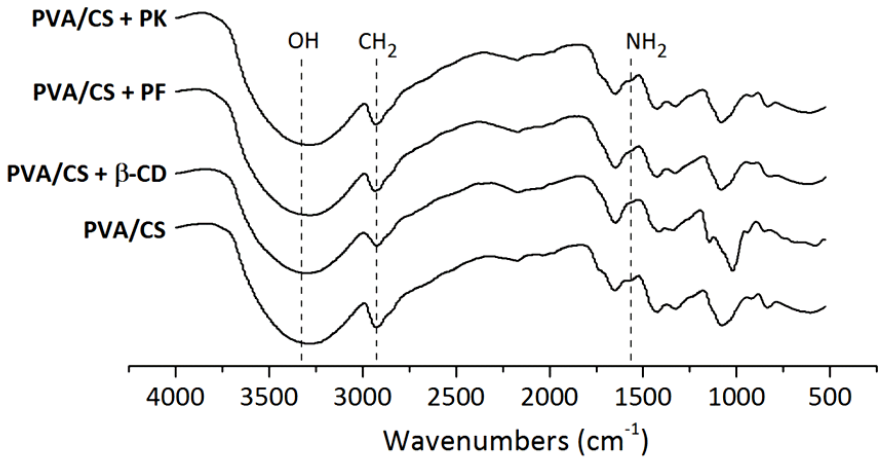

Figure S3.7. ATR-FTIR spectra of PVA/CS+PK membranes, PVA/CS+PF membranes, PVA/CS+β-CD membranes and PVA/CS membranes.

PVA characteristic bands: ν / cm^{-1} 3200 - 3300 (OH), 2898 - 2935 (CH_2)

CS characteristic bands: ν / cm^{-1} 3200 - 3300 (OH), 1560 (NH_2)

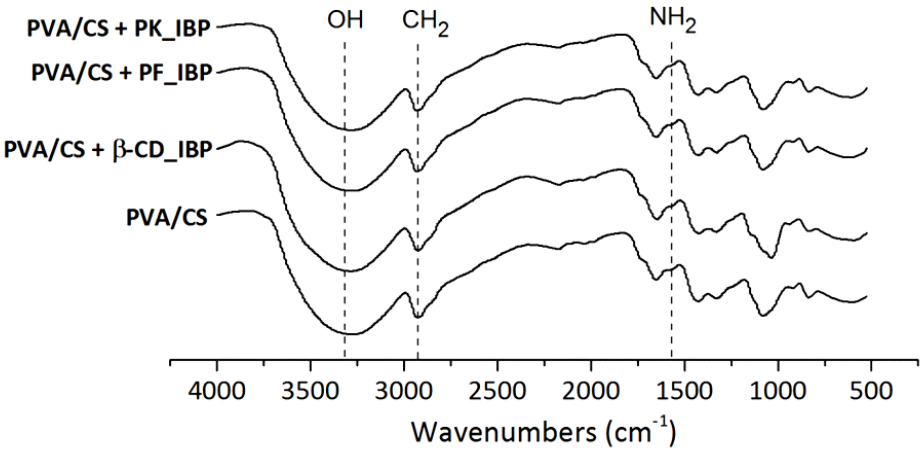

Figure S3.8. ATR-FTIR spectra of PVA/CS+PK membranes loaded with IBP, PVA/CS+PF membranes loaded with IBP, PVA/CS+β-CD membranes loaded with IBP and PVA/CS membranes.

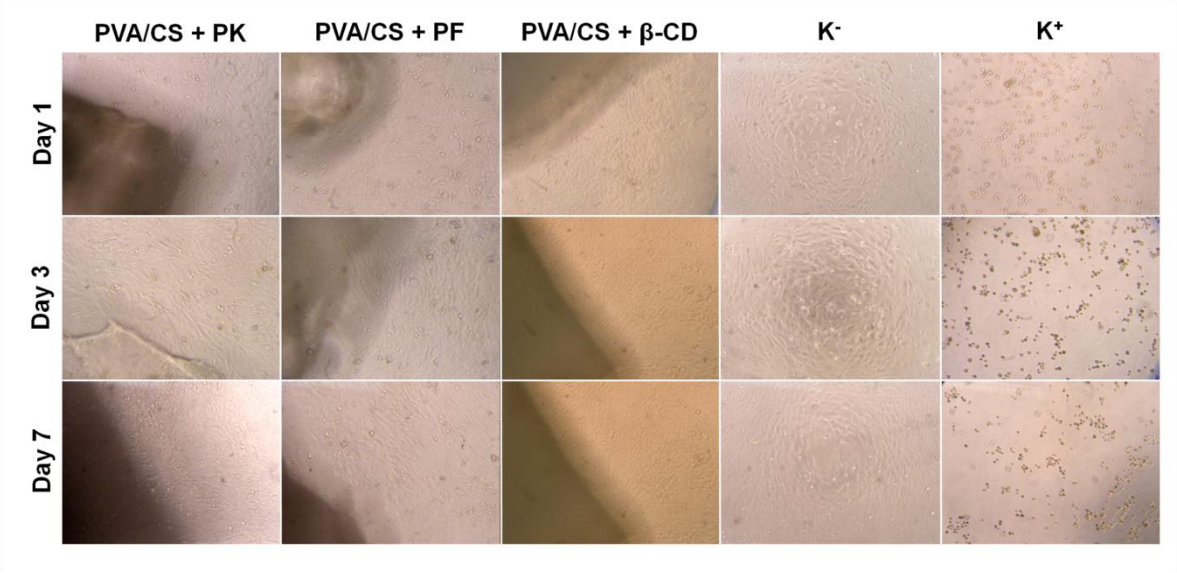

Figure S3.9. Microscopic photographs of human fibroblast cells after being seeded in the presence of the developed membranes with the different carriers during 1, 3 and 7 days. K^- : live cells; K^+ : dead cells. Original magnification 100x.

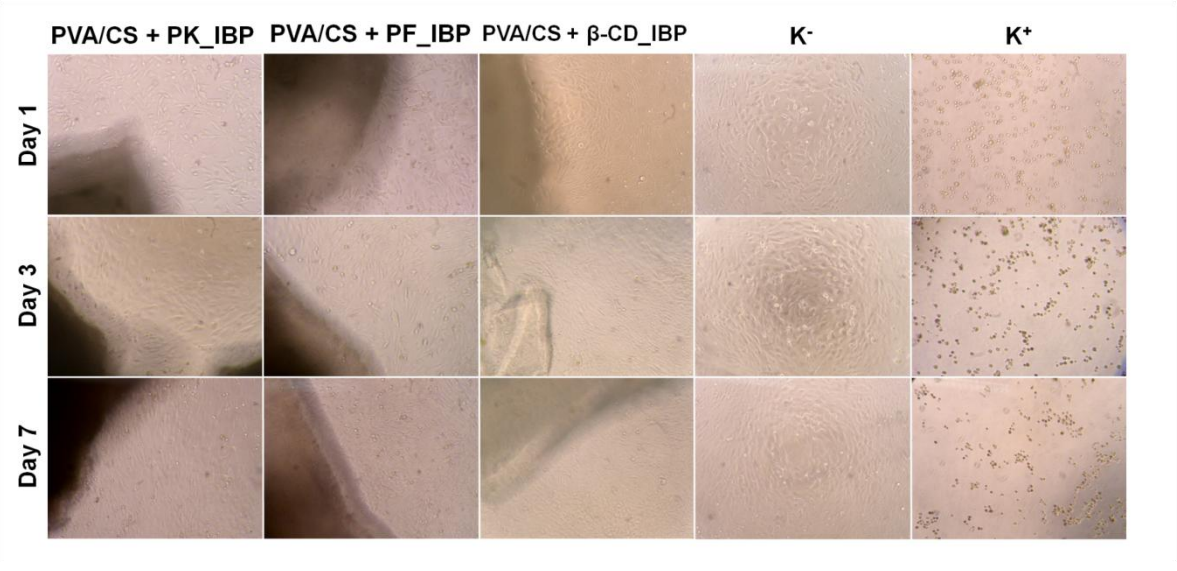

Figure S3.10. Microscopic photographs of human fibroblast cells after being seeded in the presence of the developed membranes with the different carriers loaded with IBP during 1, 3 and 7 days. K^- : live cells; K^+ : dead cells. Original magnification 100x.

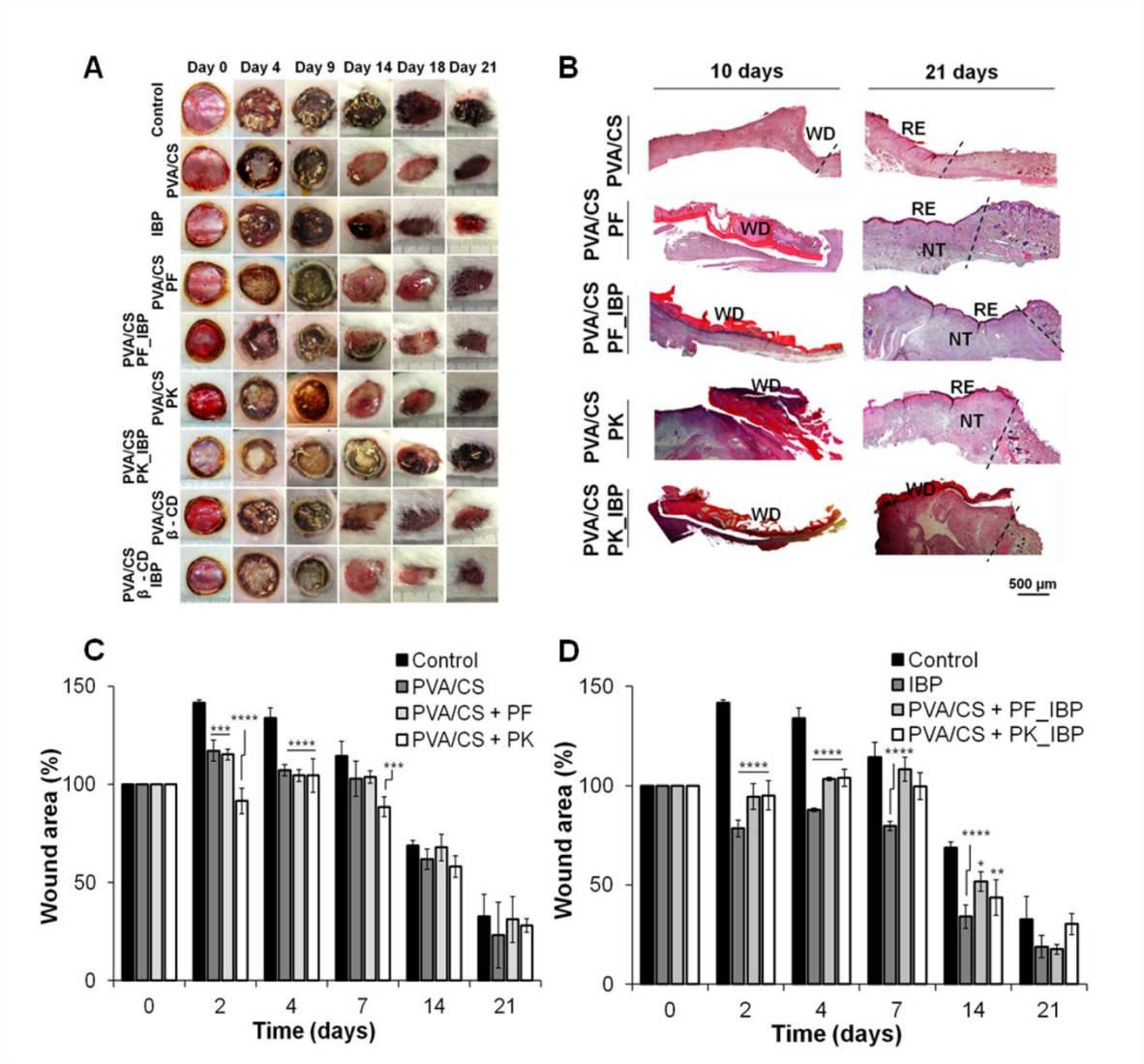

Figure S3.11. Characterization of the wound healing process under *in vivo* conditions. (**A**) Representative macroscopic images of the different wounds induced in animals from the different groups, after 4, 9, 14, 18 and 21 days. (**B**) Histological analysis of skin samples obtained after 10 and 21 days for groups treated with PVA/CS, PVA/CS+PF, PVA/CS+PF_IBP, PVA/CS+PK and PVA/CS+PK_IBP, highlighting the wound healing progression along the time frame chosen. HS: healthy skin; SB: scab; RE: re-epithelization; NT: neo-tissue; and WD: wound dressing. Wound margins were delineated. (**C**) and (**D**) Representation of the percentage of wound closure in tested groups treated with and without IBP, respectively.

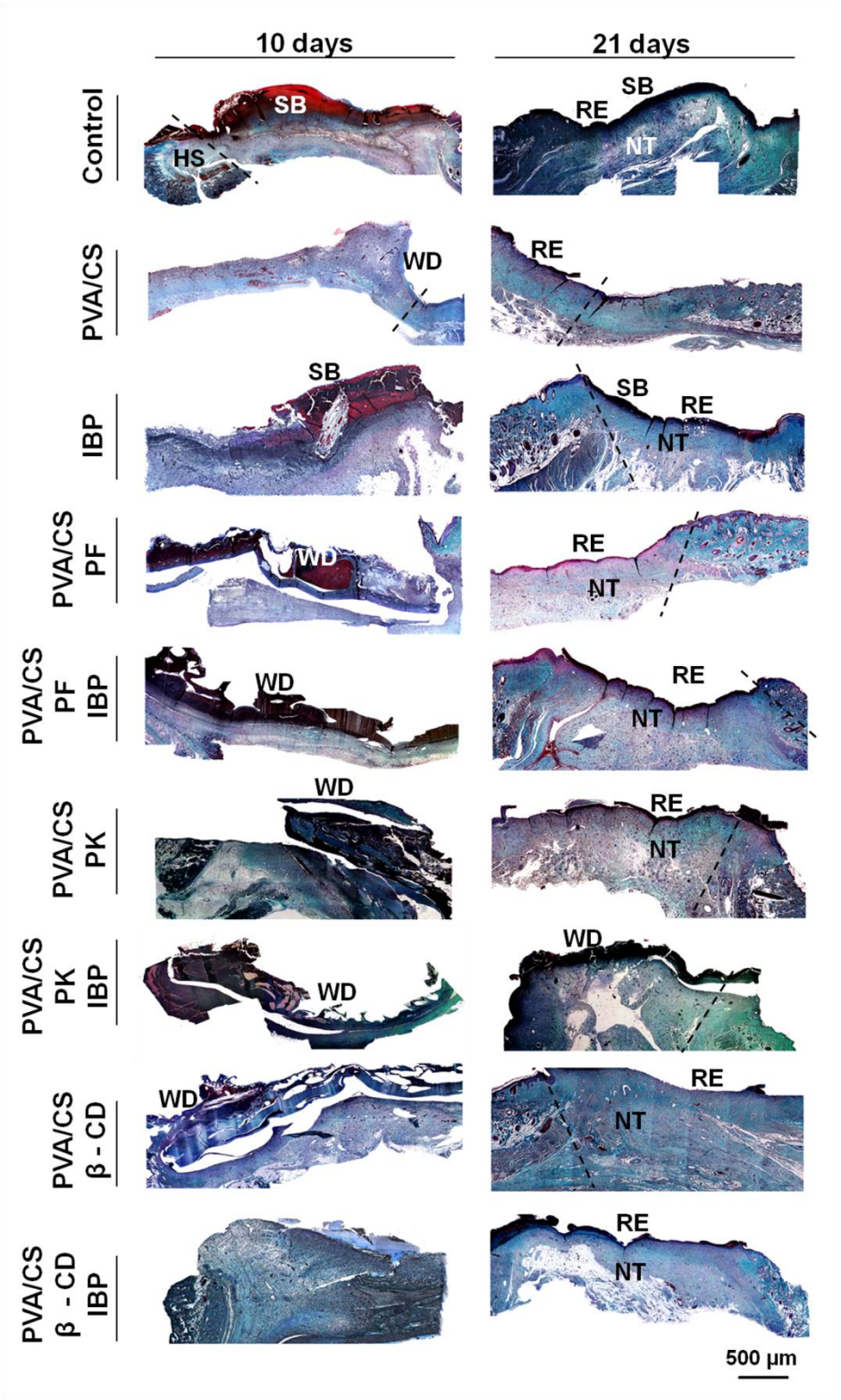

Figure S3.12. Representative images of Masson's trichrome-stained histological sections of explants at day 10 and 21, highlighting the wound healing progression along the time frame chosen. HS: healthy skin; SB: scab; RE: re-epithelization; NT: neo-tissue; and WD: wound dressing. Wound margins were delineated.